

CERN-TH/97-16  
hep-ph/9702287

## HEAVY-QUARK PRODUCTION

**Stefano FRIXIONE<sup>1</sup>**

ETH, Zurich, Switzerland

**Michelangelo L. MANGANO<sup>2</sup> and Paolo NASON<sup>3</sup>**

CERN, TH Division, Geneva, Switzerland

**Giovanni RIDOLFI**

INFN, Genoa, Italy

### Abstract

We review the present theoretical and experimental status of heavy quark production in high-energy collisions. In particular, we cover hadro- and photoproduction at fixed target experiments, at HERA and at the hadron colliders, as well as aspects of heavy quark production in  $e^+e^-$  collisions at the  $Z^0$  peak.

CERN-TH/97-16  
February 1997

---

<sup>1</sup>Supported by the Swiss National Foundation

<sup>2</sup>On leave of absence from INFN, Pisa, Italy

<sup>3</sup>On leave of absence from INFN, Milan, Italy

## CONTENTS

<b>1</b>	<b>Introduction</b>	<b>3</b>
<b>2</b>	<b>Fixed-target production</b>	<b>5</b>
2.1	Total cross sections . . . . .	5
2.2	Single-inclusive distributions . . . . .	10
2.3	Double-differential distributions . . . . .	16
<b>3</b>	<b>Heavy-flavour production at HERA</b>	<b>20</b>
3.1	Photoproduction cross sections . . . . .	20
3.2	Charm photoproduction . . . . .	24
3.3	Bottom photoproduction . . . . .	28
3.4	Deep-inelastic production . . . . .	29
3.5	Future physics . . . . .	31
3.5.1	Determination of $f_g^{(p)}$ . . . . .	31
3.5.2	Polarization asymmetries . . . . .	33
3.5.3	HERA-B . . . . .	35
<b>4</b>	<b>Heavy-quark production at hadron colliders</b>	<b>35</b>
4.1	Inclusive bottom production . . . . .	37
4.1.1	Preliminaries . . . . .	37
4.1.2	The effect of higher-order corrections . . . . .	38
4.1.3	Comparison with experimental results . . . . .	40
4.2	$b\bar{b}$ correlations . . . . .	48
4.3	Heavy-quark jets in perturbative QCD . . . . .	50
4.3.1	Preliminaries . . . . .	50
4.3.2	The structure of heavy-quark jets at the Tevatron . . . . .	51
4.4	Associated production of heavy quarks with $W$ or $\gamma$ . . . . .	57
4.4.1	Photon plus heavy quarks . . . . .	57
4.4.2	$W$ bosons plus heavy quarks . . . . .	59
4.5	Production of top quarks . . . . .	60
4.5.1	Total $t\bar{t}$ production cross sections . . . . .	60
4.5.2	Top kinematical distributions . . . . .	65

<b>5 Higher orders and resummation</b>	<b>69</b>
5.1 What are soft-gluon effects . . . . .	70
5.2 Problems with the $x$ -space resummation formula . . . . .	74
5.3 Phenomenological applications . . . . .	76
<b>6 Heavy-flavour production in <math>e^+e^-</math> collisions</b>	<b>79</b>
6.1 Preliminaries . . . . .	79
6.2 Fragmentation function . . . . .	79
6.3 Heavy-quark production via gluon splitting . . . . .	80
6.4 Correlations . . . . .	82
<b>7 Conclusions and outlook</b>	<b>84</b>

## 1 INTRODUCTION

The theory of heavy-flavour production covers in reality a wide variety of phenomena, which are at times only loosely related from a theoretical point of view. In ref. [Nason92] an ample discussion was given of the next-to-leading order (NLO) correction to the hadroproduction of heavy flavours for the total and single-inclusive cross section and for the double-differential distributions. Both hadroproduction and photoproduction have been considered in the literature, and NLO calculations of heavy-flavour production in deep-inelastic scattering have been available for a long time. Some very special topics, such as the multiplicity of heavy flavours in jets, have also been discussed in the previous volume.

In this chapter we will discuss and review recent progress that took place since the publication of ref. [Nason92]. Many theoretical and experimental issues on heavy-flavour production have been clarified, and new problems have arisen. First of all, the top quark has been observed, and its cross section turns out to have roughly the predicted magnitude. In the future, both at the Tevatron and at the LHC, it will be possible to study more details of the  $t\bar{t}$  production mechanism. From the point of view of perturbative QCD this is a very interesting possibility, since theoretical predictions for the top are very reliable. This is in fact the only case in heavy-flavour production when radiative corrections to the total cross section are indeed small. They are of the order of 15% at the Tevatron energy. The first studies on kinematical distributions of the top have already appeared, showing a qualitative agreement with QCD predictions. We will review in this work the present status of the theoretical calculation of top cross section and distributions. The importance of these studies is twofold. On the one hand one would like to test the underlying strong interaction dynamics, and on the other hand, deviations from QCD predictions may hint at the effects of physics beyond the Standard Model.

## 4 Heavy-Quark Production

The study of bottom production at the Tevatron has undergone a considerable improvement, thanks to the introduction of vertexing techniques. The inclusive transverse-momentum distribution of  $b$  mesons has been a long-standing problem, since the measured cross section used to be several times higher than the theoretical calculation. Experimental refinements of the measurement have reduced the cross section by a considerable amount. Nevertheless, the data still tend to lie on the upper side of the theoretical prediction. Although it is clear by now that the hard QCD production mechanism is basically the correct one, it appears that some details remain to be understood. Vertexing techniques have also allowed additional measurements of correlations between the  $b$  and the  $\bar{b}$  quark, adding evidence for the validity of the hard production mechanism.

Fixed-target studies of heavy-flavour production have provided a wealth of data on charm. Total cross sections, single-inclusive distributions, correlations between the quark and the antiquark have been measured in both hadro- and photoproduction. The theoretical apparatus of perturbative QCD is in this case at its very limit of applicability, because the charm mass is very close to typical hadronic scales. Thus, effects of non-perturbative origin will very likely play an important role. Conversely, it is hoped that these effects may be better understood by studying charm production. Although modern fixed-target experiments have considerably improved the situation, many open problems remain in this field. All experimental results are in qualitative agreement with perturbative QCD calculations, thus supporting the “hard” nature of charm-production phenomena. However, several quantitative deviations from pure QCD are observed. It is interesting to see whether simple models of non-perturbative phenomena, such as fragmentation effects, intrinsic transverse momenta, and dragging effects, may be sufficient to explain these deviations. We will discuss these problems at length. As of now, in our opinion, several different scenarios are possible, and more experimental data may help to discriminate between them.

The electron–proton collider HERA has begun to produce data on charm photoproduction and electroproduction. In this case, thanks to the wide kinematical range potentially available, the possibility exists of performing QCD studies on the proton and photon structure functions.

Bottom and charm production studies at LEP have reached a remarkable stage of precision. Accurate measurements are now available for the  $b$  production rate and for its fragmentation function. Furthermore, measurements of the gluon splitting rate into  $b$  and  $c$  pairs have been performed.

On the theoretical side, new developments have taken place, in relation to the experimental progress that has been achieved. Thus, top cross section calculations have been revisited, and the problem of threshold effects has been re-examined and considerably clarified. The resummation of perturbative effects at large transverse momentum has been investigated, because of its relevance to the interpretation of the CDF and D0 data. With a similar motivation, production of heavy-flavoured jets has been considered. Lastly, the computation of heavy-flavour electroproduction has been extended to next-to-leading order, in view of comparisons with HERA data.

We have limited the scope of the present work to open heavy-flavour production. The problem of quarkonium production is of a rather different nature, not directly related to the topics touched in our review. We have tried to be as complete as possible. However, we have skipped topics that are, in our opinion, less important for the purpose of testing the underlying production dynamics.

## 2 FIXED-TARGET PRODUCTION

Heavy-flavour production has been studied extensively in fixed-target experiments, with both hadron and photon beams. The typical centre-of-mass energy is in the range 10-40 GeV, where the bottom cross section is rather small. Therefore most of the available data are on charmed-hadron production.

In this section we will present a comparison between existing fixed-target data for the hadroproduction and the photoproduction of heavy flavours and NLO QCD predictions. Because of the small value of the charm-quark mass, the perturbative expansion may not be reliable, due to higher-order terms of the perturbative expansion and to non-perturbative effects. We will discuss these problems and the importance of such contributions. More details are given in refs. [Mangano93] and [Frixione94a].

### 2.1 Total cross sections

A list of experimental results on total cross sections for  $D$ -meson hadroproduction is presented in table 1. We used these results to estimate the total charm-pair cross section  $\sigma_{c\bar{c}}$ . In most cases fixed-target experiments give their cross sections with the Feynman- $x$  cut  $x_F > 0$ . The ratio  $\sigma_{c\bar{c}}/\sigma_{c\bar{c}}(x_F^c > 0)$  has been evaluated theoretically [Mangano93] and is approximately equal to 1.6 in pion–nucleon collisions and to 2 in proton–nucleon collisions; it is nearly independent of the heavy-quark mass and beam energy (at least for  $m_c$  between 1.2 and 1.8 GeV, and beam energy  $E_b$  between 100 and 1000 GeV). Therefore, the total  $D\bar{D}$  cross section is obtained from  $\sigma(D/\bar{D}, x_F > 0)$  by dividing by 2 to get the pair cross section from the single-inclusive one, and multiplying by 1.6 (for pion) or 2 (for proton) to account for the partial coverage of the  $x_F$ -range.

The contribution to  $\sigma_{c\bar{c}}$  from  $\Lambda_c$  and  $D_s$  production must also be included. We use (see ref. [Aoki92] and references therein)

$$\frac{\sigma(D_s)}{\sigma(D^0 + D^+)} \simeq 0.2, \quad (2.1)$$

$$\frac{\sigma(\Lambda_c)}{\sigma(D^0 + D^+)} \simeq 0.3 \quad (2.2)$$

(here particle means also antiparticle). Measurements of the cross sections for  $D_s$  and  $\Lambda_c$  have recently been presented by the E769 [Alves96] and WA92 [Adamovich96] collaborations, and values consistent with eqs. (2.1) and (2.2) have been found. Therefore, to obtain  $\sigma_{c\bar{c}}$  from the total cross section for  $D\bar{D}$  production, we have to multiply by a factor of 1.5.

The WA75 collaboration [Aoki92] does not present single-inclusive cross sections for  $D$  mesons, but quotes directly the  $c\bar{c}$  cross section

$$\sigma_{c\bar{c}} = 23.1 \pm 1.3^{+4.0}_{-3.3} \mu\text{b}, \quad (2.3)$$

## 6 Heavy-Quark Production

	$E_b$ (GeV)	$\sigma$ (total) or $\sigma_+$ ( $x_F > 0$ ) ( $\mu\text{b}$ )	$\sigma_{D\bar{D}}$ ( $\mu\text{b}$ )	$D^+/D^0$
$pN$ [Kodama91]	800	$\sigma(D^0/\bar{D}^0) = 38 \pm 3 \pm 13$ $\sigma(D^+/D^-) = 38 \pm 9 \pm 14$	$38 \pm 10$	$1.0 \pm 0.6$
$pN$ [Barlag88]	200	$\sigma_+(D/\bar{D}) = 1.5 \pm 0.7 \pm 0.1$	$1.5 \pm 0.7$	—
$pp$ [Ammar88]	800	$\sigma(D^0/\bar{D}^0) = 22^{+9}_{-7} \pm 5$ $\sigma(D^+/D^-) = 26 \pm 4 \pm 6$	$24 \pm 6$	$1.2 \pm 0.6$
$pp$ [Aguilar88]	400	$\sigma(D^0/\bar{D}^0) = 18.3 \pm 2.5$ $\sigma(D^+/D^-) = 11.9 \pm 1.5$	$15.1 \pm 1.5$	$0.7 \pm 0.1$
$pN$ [Alves96]	250	$\sigma_+(D^0/\bar{D}^0) = 5.6 \pm 1.3 \pm 1.5$ $\sigma_+(D^+/D^-) = 3.2 \pm 0.4 \pm 0.3$	$8.8 \pm 1.5$	$0.57 \pm 0.22$
$\pi^- p$ [Aguilar85a]	360	$\sigma_+(D^0/\bar{D}^0) = 10.1 \pm 2.2$ $\sigma_+(D^+/D^-) = 5.7 \pm 1.6$	$12.6 \pm 2.2$	$0.6 \pm 0.2$
$\pi^- N$ [Barlag91]	230	$\sigma_+(D^0/\bar{D}^0) = 6.3 \pm 0.3 \pm 1.2$ $\sigma_+(D^+/D^-) = 3.2 \pm 0.2 \pm 0.7$	$7.6 \pm 1.1$	$0.5 \pm 0.2$
$\pi^- N$ [Barlag88]	200	$\sigma_+(D^0/\bar{D}^0) = 3.4^{+0.5}_{-0.4} \pm 0.3$ $\sigma_+(D^+/D^-) = 1.7^{+0.4}_{-0.3} \pm 0.1$	$4.1^{+0.6}_{-0.5}$	$0.5 \pm 0.1$
$\pi^- N$ [Kodama92]	600	$\sigma_+(D^0/\bar{D}^0) = 22.05 \pm 1.37 \pm 4.82$ $\sigma_+(D^+/D^-) = 8.66 \pm 0.46 \pm 1.96$	$24.6 \pm 4.3$	$0.4 \pm 0.1$
$\pi^- N$ [Alves96]	210	$\sigma_+(D^0/\bar{D}^0) = 6.3 \pm 0.9 \pm 0.3$ $\sigma_+(D^+/D^-) = 1.7 \pm 0.3 \pm 0.1$	$6.4 \pm 0.8$	$0.27 \pm 0.06$
$\pi^- N$ [Alves96]	250	$\sigma_+(D^0/\bar{D}^0) = 8.2 \pm 0.7 \pm 0.5$ $\sigma_+(D^+/D^-) = 3.6 \pm 0.2 \pm 0.2$	$9.4 \pm 0.7$	$0.44 \pm 0.06$
$\pi^+ N$ [Alves96]	250	$\sigma_+(D^0/\bar{D}^0) = 5.7 \pm 0.8 \pm 0.4$ $\sigma_+(D^+/D^-) = 2.6 \pm 0.3 \pm 0.2$	$6.6 \pm 0.8$	$0.46 \pm 0.09$
$\pi^- N$ [Adamovich96]	350	$\sigma_+(D^0/\bar{D}^0) = 7.78 \pm 0.14 \pm 0.52$ $\sigma_+(D^+/D^-) = 3.28 \pm 0.08 \pm 0.29$	$8.8 \pm 0.5$	$0.42 \pm 0.05$

Table 1: *Experimental results on total cross sections for charm production. The notation  $\sigma_+$  represents the inclusive cross section for positive rapidity. The pair cross section  $\sigma_{D\bar{D}}$  includes our corrections for possible  $x_F$  cuts, as discussed in the text.*

for a 350 GeV  $\pi^-$  beam on emulsion, assuming an atomic mass dependence  $A^{0.87}$  (this result was not inserted in table 1). The E789 collaboration [Leitch94], using an 800 GeV proton beam colliding on a Be or Au target, studied the nuclear dependence of the  $D$ -meson cross section, finding an  $A^\alpha$  behaviour, with  $\alpha = 1.02 \pm 0.03 \pm 0.02$ . As a by-product, they obtain

$$\sigma(D^0/\bar{D}^0) = 17.7 \pm 0.9 \pm 3.4 \mu\text{b}. \quad (2.4)$$

An analogous measurement for the charged- $D$  cross section is not expected<sup>4</sup>.

From table 1 we see that most of the experimental collaborations report separately the total cross sections for charged and neutral  $D$ -meson production. In the last column of table 1 we show the ratio  $R$  between these two values. For pion–nucleon collisions, the agreement between various collaborations is fairly good (except for the result of ref. [Alves96] obtained with a beam energy of 210 GeV), and the errors on  $R$  are moderate; the  $D^0$  cross section is found to be about twice as large as the  $D^+$  cross section. A simple model for estimating the charged-to-neutral  $D$  cross section ratio is the following. One assumes isospin invariance in the  $c \rightarrow D$  and  $c \rightarrow D^*$  transition. Furthermore, one assumes that the  $D$  cross section is one third of the  $D^*$  cross section, due to the counting of polarization states. Using then the published values of the  $D^* \rightarrow D$  branching ratios [Barnett96], the result is roughly

$$R \equiv \frac{\sigma(D^+)}{\sigma(D^0)} \simeq 0.32. \quad (2.5)$$

Observe that this number has changed with respect to the value of 0.43 quoted in ref. [Frixione94], because of changes in the measured branching ratios. This number is compatible with the values reported in table 1 for  $\pi N$  collisions, especially for the most recent data. For  $pN$  collisions, the same simple argument should hold. Experimental measurements do not give a unique indication; some results seem to give comparable total cross sections for charged and neutral  $D$ . We do not find any reasonable explanation of this fact. For example, the HERWIG Monte Carlo program [Marchesini88, Marchesini92] gives roughly the same  $R$  value for the proton and for the pion beams. On the other hand, the experimental data for the proton beam are much less clear than in the case of  $\pi^- N$  collisions, the uncertainty on  $R$  being quite large. The two  $R$  values with the smallest uncertainty, namely those reported in ref. [Aguilar88] and in ref. [Alves96], indicate a behaviour similar to the one observed in  $\pi^- N$  collisions.

In fig. 1 we plot the  $c\bar{c}$  and  $b\bar{b}$  cross sections, computed in QCD at NLO, as functions of the beam energy, for  $\pi^- N$  collisions. The same quantities are shown in fig. 2 for a proton beam. The cross sections are calculated using the parton distribution sets of ref. [Martin95a] for the nucleon, and the central set SMRS2 [Sutton92] for the pion. The default values of the charm and bottom masses are 1.5 and 4.75 GeV respectively,

---

<sup>4</sup>M. Schub, private communication.

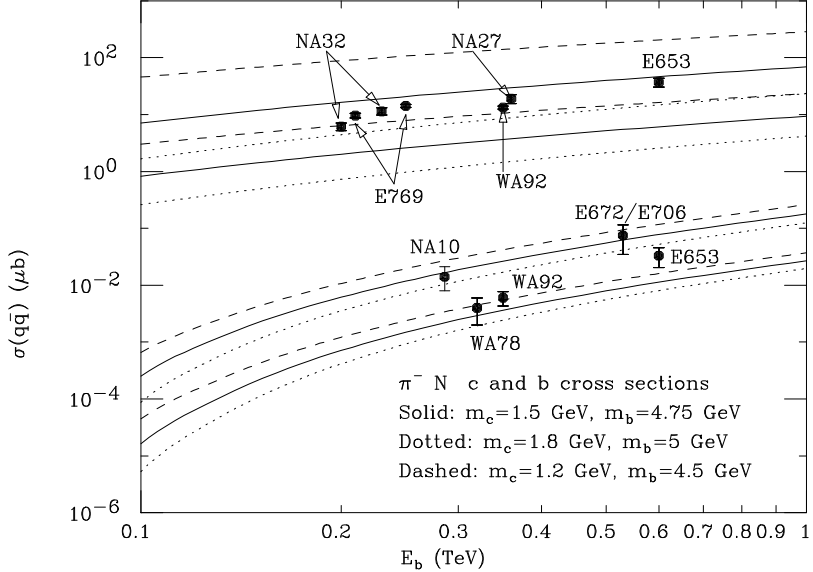


Figure 1: *Pair cross sections for b and c production in  $\pi^-N$  collisions versus experimental results.*

and the default choices for the factorization scale  $\mu_F$  and the renormalization scale  $\mu_R$  are

$$\mu_F = 2m_c, \quad \mu_R = m_c \quad (2.6)$$

for charm and

$$\mu_F = \mu_R = m_b \quad (2.7)$$

for bottom.

The bands in the figures are obtained as follows. We varied  $\mu_R$  between half the central value and twice this value. The factorization scale  $\mu_F$  was also varied between  $m_b/2$  and  $2m_b$  in the case of bottom, while it was kept fixed at  $2m_c$  in the case of charm. This is because the adopted parametrizations of parton densities are given for  $Q^2$  larger than 5 GeV $^2$ . The bands shown in the figures are therefore only an underestimate of the uncertainties involved in the computation of charm production cross sections. We verified that considering independent variations for the factorization and renormalization scales does not lead to a wider range in the bottom cross section for the energies shown in the figures. We also show the effect of varying  $m_c$  between 1.2 GeV and 1.8 GeV, and  $m_b$  between 4.5 and 5 GeV.

The proton parton densities of ref. [Martin95a] are available for a wide range of  $\Lambda_{\text{QCD}}$  values, corresponding to  $\alpha_s(m_Z)$  values between 0.105 and 0.130. The bands shown in figs. 1 and 2 for bottom production are obtained by letting  $\Lambda_{\text{QCD}}$  vary in this range. In the case of charm, values of  $\Lambda_{\text{QCD}}$  corresponding to  $\alpha_s(m_Z)$  above 0.115 induce values of  $\alpha_s(m_c)$  too large to be used in a perturbative expansion. For

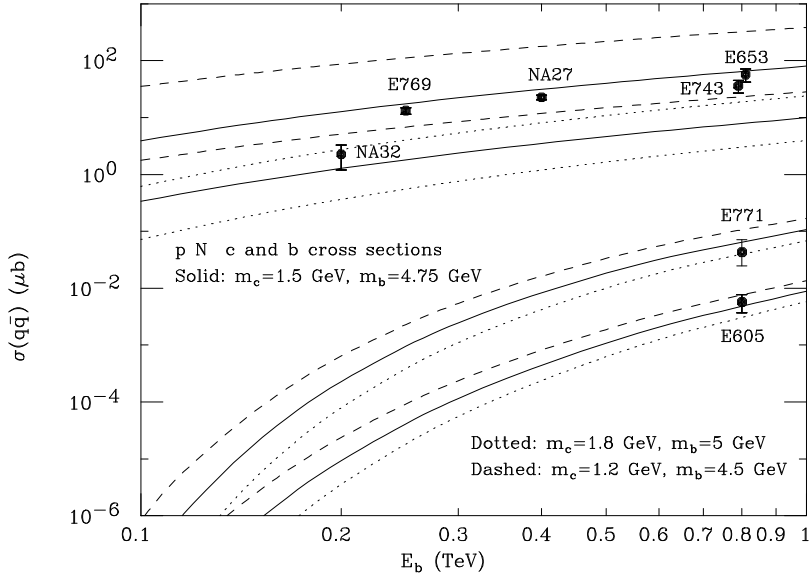


Figure 2: *Pair cross sections for  $b$  and  $c$  production in  $pN$  collisions versus experimental results.*

this reason, the upper bounds on charm production cross sections are obtained with  $\alpha_s(m_z) = 0.115$ . We point out that, by varying  $\Lambda_{\text{QCD}}$ , one is forced to neglect the correlation between  $\Lambda_{\text{QCD}}$  and the pion parton densities, which were fitted in ref. [Sutton92] with  $\Lambda_5^{\overline{\text{MS}}} = 122$  MeV.

Experimental results on bottom production at fixed target have been reported in refs. [Bari91, Basile81, Kodama93, Catanesi89, Bordalo88, Jesik95] for pion–nucleon collisions. Recently, the first measurement of the bottom cross section with a proton beam has become available [Jansen95]. Preliminary results for  $pN$  collisions have also been presented in ref [Spiegel96]. These results are shown in figs. 1 and 2. We made no effort to correct the data in order to get the  $b\bar{b}$ -quark cross section when the  $B$ -hadron cross section was reported.

As can be seen, experimental results on total charm cross sections are in reasonable agreement with theoretical expectations, if the large theoretical uncertainties are taken into proper account. We can see that the hadroproduction data are compatible with a value of 1.5 GeV for the charm-quark mass. In the case of bottom production, the spread of the experimental data is almost as large as that of the theoretical predictions. Both currently available data points lie in the theoretical band.

We remind the reader that many puzzling ISR results in  $pp$  collisions at 62 GeV cannot be currently explained (see the review in ref. [Tavernier87]), in particular the large  $\Lambda_b$  production rates reported in refs. [Bari91, Basile81].

Total cross sections for charm production have also been measured in photoproduction experiments. In fig. 3 the relevant experimental results of refs. [Alvarez93,

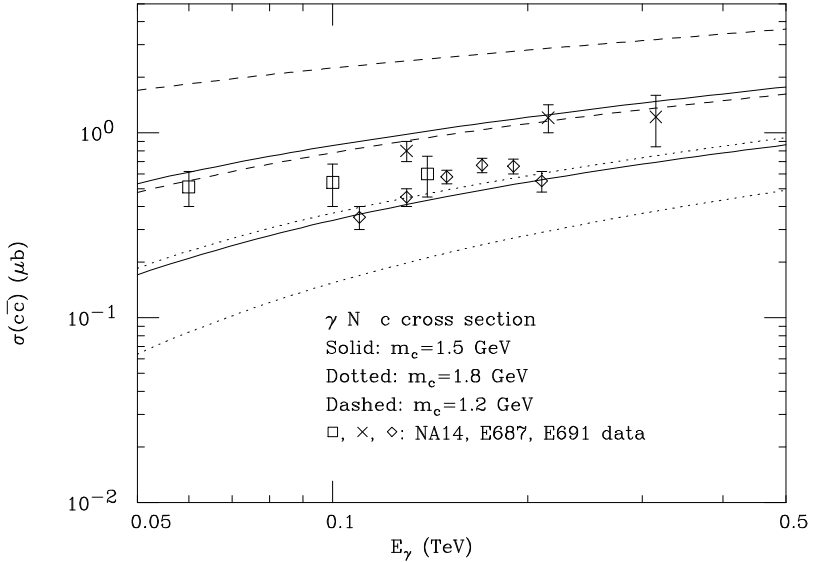


Figure 3: *Pair cross sections for  $c$  production in  $\gamma N$  collisions versus experimental results.*

Anjos89, Anjos90, Bellini94] are shown in comparison with NLO QCD predictions. As can be seen, the theoretical uncertainties are smaller in this case than in the hadroproduction case. Again, a charm mass of 1.5 GeV is compatible with photoproduction data. It should be stressed that some of the experimental results are totally incompatible with one another. Until these discrepancies are resolved, it will not be possible to use the data to constrain physical parameters. For example, while the E687 data are inconsistent with a charm mass of 1.8 GeV, this mass value cannot be excluded because of the E691 data.

## 2.2 Single-inclusive distributions

Many hadroproduction and photoproduction experiments have measured single-inclusive  $x_F$  and  $p_T$  distributions for charmed hadrons in  $\pi N$  collisions [Kodama92, Barlag88, Barlag91, Aguilar85a, Alves92, Adamovich92, Aoki88, Aoki92a] and in  $pN$  collisions [Kodama91, Barlag88, Ammar88, Aguilar88, Adamovich92]. Distributions are expected to be more affected by non-perturbative phenomena than total cross sections. For example, an intrinsic transverse momentum of the incoming partons, and the hadronization of the produced charm quarks, may play an important rôle in this case. We will therefore try to assess the impact of such phenomena by means of simple models.

Recent measurements of single-inclusive differential cross sections have been performed at CERN by the WA92 collaboration [Adamovich96], which uses a  $\pi^-$  beam

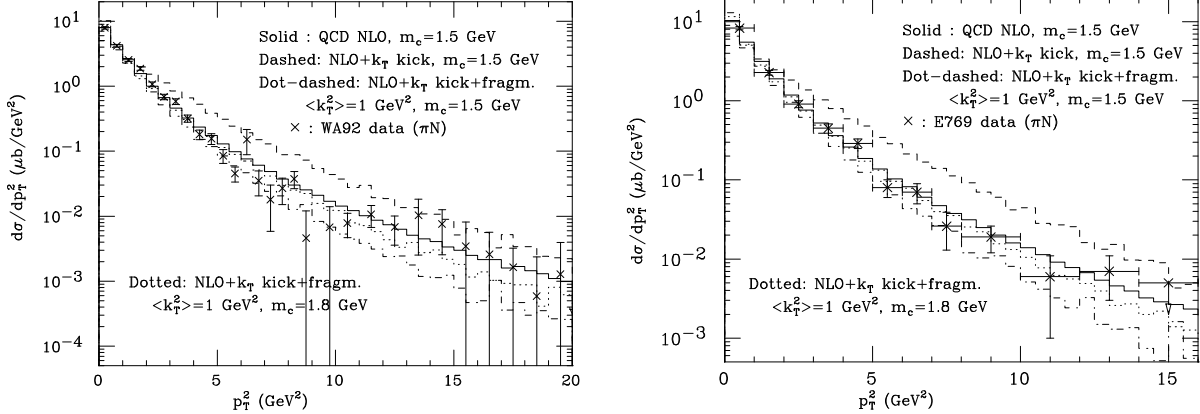


Figure 4: The single-inclusive  $p_T^2$  distribution measured by WA92 (left) and E769 (right), compared to the NLO QCD predictions, with and without the inclusion of non-perturbative effects.

of 350 GeV colliding with isosinglet nuclei, and at FNAL by the E769 collaboration [Alves96a] with pion, proton and kaon beams of 250 GeV on isosinglet targets.

In fig. 4 we show the comparison between the single-inclusive  $p_T^2$  distributions measured by the WA92 and E769 collaborations in  $\pi N$  collisions and the theoretical predictions<sup>5</sup>. The solid curves represent the pure NLO QCD predictions for charm quarks. The dashed curves show the effect of adding to the perturbative results an intrinsic transverse momentum of the incoming partons ( $k_T$  kick). This procedure is, to a large extent, arbitrary. We implemented it in the following way. We call  $\vec{p}_T(Q\bar{Q})$  the total transverse momentum of the pair. For each event, in the longitudinal centre-of-mass frame of the heavy-quark pair, we boost the  $Q\bar{Q}$  system to rest. We then perform a second transverse boost, which gives the pair a transverse momentum equal to  $\vec{p}_T(Q\bar{Q}) + \vec{k}_T(1) + \vec{k}_T(2)$ ;  $\vec{k}_T(1)$  and  $\vec{k}_T(2)$  are the transverse momenta of the incoming partons, which are chosen randomly, with their moduli distributed according to

$$\frac{1}{N} \frac{dN}{dk_T^2} = \frac{1}{\langle k_T^2 \rangle} \exp(-k_T^2/\langle k_T^2 \rangle). \quad (2.8)$$

Alternatively, one may proceed as in the previous case, but giving the additional transverse momentum  $\vec{k}_T(1) + \vec{k}_T(2)$  to the whole final-state system (at the NLO in QCD, this means the  $Q\bar{Q}$  pair plus a light parton), and not to the  $Q\bar{Q}$  pair only. We verified that the two methods give very similar results for  $\langle k_T^2 \rangle$  smaller than about 2  $\text{GeV}^2$ .

Another non-perturbative effect that must be accounted for is the hadronization process. This effect can be described by convoluting the partonic cross section

<sup>5</sup>In this subsection and in the following one, the relative normalization of experimental distributions and theoretical curves has been fixed in order to give the same total rate.

with a fragmentation function, for which we choose the parametrization proposed in ref. [Peterson83]:

$$D(x) = \frac{N}{x [1 - 1/x - \epsilon/(1 - x)]^2}, \quad (2.9)$$

where  $N$  is fixed by the condition  $\int D(x)dx = 1$ . We used  $\epsilon = 0.06$ , which is the central value quoted in ref. [Chrin87] for  $D$  mesons. The fragmentation process degrades the parent charm-quark momentum, and thus softens the  $p_T^2$  distribution.

From fig. 4, we see that the effect of the  $k_T$  kick on the predictions for bare quarks results in a hardening of the  $p_T^2$  spectrum, overshooting the data. On the other hand, by combining the  $k_T$  kick with  $\langle k_T^2 \rangle = 1 \text{ GeV}^2$  and the Peterson fragmentation, the theoretical predictions undershoot the data (dot-dashed curves), although no serious inconsistency can be inferred given the size of the experimental uncertainty. Taking the data at face value, one can notice that larger values for  $\langle k_T^2 \rangle$  and for  $m_c$  would improve the agreement. We have checked that, in order to reproduce the WA92 and E769 data, an average intrinsic transverse momentum  $\langle k_T^2 \rangle = 2 \text{ GeV}^2$  is needed. This value is exceedingly large with respect to the typical hadronic scale of a few hundred MeV. On the other hand, the data are well described (dotted plots) by the theoretical curves including fragmentation and  $k_T$  kick with  $\langle k_T^2 \rangle = 1 \text{ GeV}^2$ , if the larger value of  $m_c = 1.8 \text{ GeV}$  is adopted.

We conclude that, when using the central value of the charm mass,  $m_c = 1.5 \text{ GeV}$ , favoured by the total cross section measurements, the theoretical results for the  $p_T^2$  spectrum can describe the data well, only if a large  $k_T$  kick is applied to the fragmented curve. If a larger value of the charm mass is adopted, a more moderate and physically acceptable  $k_T$  kick is enough to get a good agreement with the measurements. Therefore, there seems to be a potential discrepancy between theory and experiments in the  $p_T^2$  spectrum in charm hadroproduction. From a different point of view, however, the discrepancy may be interpreted as the signal that some of the other theoretical assumptions are not totally sound. For example, the Peterson fragmentation function may not be suitable to describe the hadronization process in hadronic collisions; the data would suggest a function more peaked towards the  $x \simeq 1$  region. Moreover, higher-order perturbative corrections may also play a rôle, especially in the low- $p_T$  region.

We now turn to the  $x_F$  distribution. The experimental measurements of refs. [Kodama92, Barlag88, Barlag91, Aguilar85a, Alves92, Adamovich92, Aoki88, Aoki92a] (for  $\pi N$  collisions) and of refs. [Kodama91, Barlag88, Ammar88, Aguilar88, Adamovich92] (for  $pN$  collisions) find on average a behaviour that is harder than the perturbative QCD result for bare quarks (see ref. [Frixione94] for details). As in the case of the  $p_T^2$  distribution, some description of the hadronization phenomena should be added to the perturbative calculation in order to compare it with the data. This problem was considered in ref. [Mangano93], where the hadronization phenomena were studied using the parton shower Monte Carlo HERWIG. In ref. [Mangano93] the conclusion was reached that the combined effects of perturbative higher orders and non-perturbative (partonic intrinsic transverse momentum and hadronization) contributions eventually

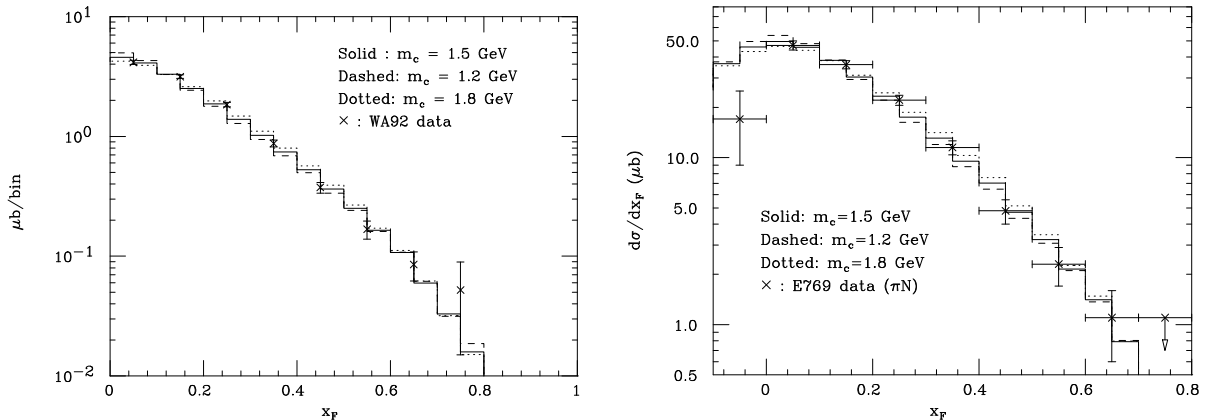


Figure 5: *Experimental  $x_F$  distributions for  $D$  mesons, compared to the NLO QCD prediction for charm quarks.*

result in a hardening of the  $x_F$  distribution for bare quarks. There it was also argued that the usual approach of complementing the perturbative calculation with a fragmentation function in order to describe the  $x_F$  distribution is completely unjustified, since the factorization theorem only holds in the large- $p_T$  region.

The most recent experimental results of WA92 [Adamovich96] and E769 [Alves96a] for the  $D$ -meson  $x_F$  distribution in  $\pi N$  collisions are, instead, in agreement with the perturbative QCD distributions for bare quarks, as can be seen from fig. 5<sup>6</sup>. This is also consistent with previous findings of E769 [Alves92]. The agreement is quite satisfactory in almost the whole range considered for both experiments (which are performed at different beam energies). The shape of the theoretical curve shows a mild sensitivity with respect to the value of the charm mass (all curves have been normalized to the data). Recent results for a proton beam are also available [Alves96a], and an agreement with theoretical predictions similar to the one displayed in fig. 5 is found.

Almost all of the experimental collaborations have observed, in pion–nucleon collisions, the so-called leading-particle effect, that is, an enhanced production at large  $x_F$  of those  $D$  mesons whose light valence quark is of the same flavour as one of the valence quarks of the incoming pion. In ref. [Frixione94] it was shown that the QCD predictions are in better agreement with the data for non-leading particles than with the data for the full  $D$ -meson sample which, as mentioned before, displays on average a harder behaviour than the theory. The difference between the leading and the non-leading sample may be an indication that non-perturbative phenomena (such as

<sup>6</sup>The pion beam used by the E769 collaboration [Alves96, Alves96a] is a mixture of  $\pi^-$  (70%) and  $\pi^+$  (30%). To produce the data appearing in fig. 5, which contain the contributions of both  $D^+$  and  $D^-$ , the distributions obtained with the different beams have been combined together, since no statistically significant discrepancy has been found between them [Alves96a].

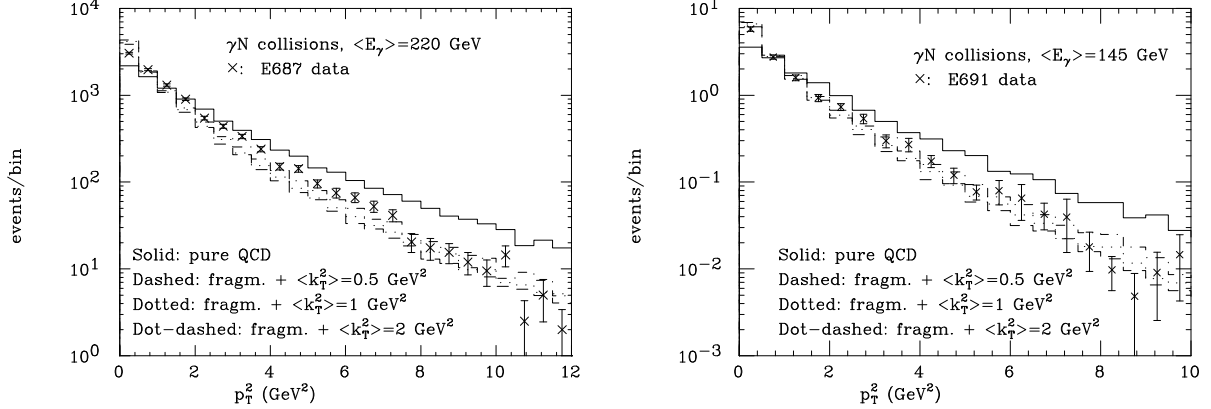


Figure 6: *Experimental  $p_T^2$  distribution compared to the NLO QCD predictions ( $m_c = 1.5$  GeV), with and without the inclusion of non-perturbative effects, in  $\gamma N$  collisions.*

colour-drag effects) are present in the production of leading particles. Recent experimental results on the asymmetry between  $D^-$  and  $D^+$  production were presented in ref. [Aitala96], for  $\pi^- N$  collisions with  $E_b = 500$  GeV. It was found that perturbative QCD, the intrinsic charm hypothesis [Combridge79, Brodsky80], and the standard Monte Carlo simulations cannot describe the measured quantities. The data can only be acceptably reproduced with a special tuning of Monte Carlo models implementing beam-dragging effects. Further studies of colour dragging and hadronization phenomena have been presented in refs. [Aitala96a, Carter96].

In the past, the  $x_F$  and  $p_T^2$  distributions have been fitted with the functions

$$\frac{d\sigma}{dx_F} = A (1 - x_F)^n; \quad \frac{d\sigma}{dp_T^2} = C e^{-bp_T^2}, \quad (2.10)$$

and the data have been presented in the form of measured values for the parameters  $n$  and  $b$ . A possible way of comparing the data with theoretical predictions would be to fit theoretical distributions in the same way, and then compare the values of the parameters  $n$  and  $b$ . This was done in ref. [Frixione94]. However, as pointed out there, this procedure is not satisfactory. In the case of the  $p_T^2$  distribution, for example, it was found that the function

$$\frac{d\sigma}{dp_T^2} = \left( \frac{C}{bm_c^2 + p_T^2} \right)^\beta \quad (2.11)$$

provides an excellent fit to the theoretical curve. Since, as discussed before, the data show the same qualitative behaviour as the theoretical predictions over the whole  $p_T^2$  range explored, the form of eq. (2.11) is clearly preferable, as was explicitly shown more recently in ref. [Alves96a].

Single-inclusive distributions for charm production have also been measured in photon–nucleon collision experiments. In the case of photoproduction, we expect QCD predictions to be more reliable than in the hadroproduction case, since only one hadron is present in the initial state (see refs. [Ellis89, Smith92, Frixione94a] for a detailed discussion). In fig. 6 we show the  $p_T^2$  distributions measured by the E687 [Bellini94] and by the E691 [Anjos89, Anjos90] collaborations. We also show the NLO QCD prediction for bare quarks, and the QCD prediction supplemented with Peterson fragmentation and an intrinsic transverse momentum for the incoming partons with different values of  $\langle k_T^2 \rangle$ . It is interesting to notice that, in this case, the fragmentation effect, combined with a moderate intrinsic transverse momentum of the initial-state partons, is sufficient to reproduce the experimental distributions. Contrary to what happens in the hadroproduction case, the  $p_T^2$  distribution is now less sensitive to the choice of the  $\langle k_T^2 \rangle$ . To show this fact clearly, we have also presented the prediction for  $\langle k_T^2 \rangle = 2 \text{ GeV}^2$ .

The E687 collaboration recently performed a measurement [Frabetti96] of the asymmetries between charm and anticharm states in photon–nucleon collisions, finding no compelling evidence for  $D_s^+$  and  $\Lambda_c^+$  asymmetries, and sizeable asymmetries for  $D^+$ ,  $D^0$  and  $D^{*+}$  states. The very tiny asymmetries predicted by NLO QCD cannot account for these results, which are most likely to originated from some non-perturbative effects, as discussed in the case of hadroproduction. It was found that, by properly tuning Monte Carlo programs based on the Lund string fragmentation model, the data could be reproduced.

In summary, a remarkable amount of experimental information on the single-inclusive distributions for charm quarks is currently available, both in hadroproduction and in photoproduction. Further data with increased statistics are expected in the near future [Kaplan94]. Some modelling of non-perturbative effects is needed in order to describe the transverse-momentum spectrum of charmed hadrons. The inclusion of a fragmentation function tends to give too soft a  $p_T$  spectrum. Assuming the presence of a primordial transverse momentum of the colliding partons, the  $p_T$  spectrum becomes harder, and a better (albeit not fully satisfactory) agreement with the data is found. Longitudinal ( $x_F$ ) distributions are measured to be harder than the theoretical predictions. Similarly, asymmetries in the longitudinal distributions between charm and anticharm states are too large to be explained by perturbative QCD alone. Simple models of hadronization, including colour-dragging effects, can give a satisfactory description of the data.

We remind the reader that the E653 collaboration presented in ref. [Kodama93] the first measurement of single-inclusive distributions for bottom production at fixed target (the azimuthal correlation of the  $b\bar{b}$  pair was also studied). The data appear to be in qualitative agreement with QCD predictions. More investigations with improved statistics will be welcome in this area.

### 2.3 Double-differential distributions

Many experimental results on correlations between charmed particles in hadro- and photoproduction have been obtained by different experiments (see for example refs. [Aguilar85b, Adamovich87, Aguilar88, Barlag91a, Kodama91a, Aoki92a, Alvarez92, Frabetti93]); these reported distributions of the azimuthal distance between the charmed hadrons, the rapidity difference, the invariant mass and the transverse momentum of the pair. A detailed comparison of these results with QCD predictions is performed in ref. [Frixione94]. More recently, new measurements of the azimuthal distance and pair transverse momentum for charmed mesons have been presented by the WA92 collaboration [Adamovich96a]. In what follows we will focus on the distribution of  $\Delta\phi$ , defined as the angle between the projections of the momenta of the pair onto the transverse plane, and of the transverse momentum of the pair  $p_T(Q\bar{Q})$ . We will discuss whether NLO QCD predictions can describe the available experimental data.

In leading-order QCD the heavy-quark pair is produced in the back-to-back configuration, corresponding to  $\Delta\phi = \pi$  and  $p_T(Q\bar{Q}) = 0$ . NLO corrections, as well as non-perturbative effects, can cause a broadening of these distributions, as illustrated in refs. [Mangano93] and [Frixione94a].

We have chosen, as an illustration for hadroproduction, the cases of the WA75 and the WA92 results, which have both been obtained in  $\pi^- N$  collisions at the same energy,  $E_b = 350$  GeV. Let us first consider the  $\Delta\phi$  distribution. In fig. 7 we show (solid curves) the NLO result superimposed on the data of two experiments. The charm mass was set to its default value,  $m_c = 1.5$  GeV. In both cases, we see that the experimental data favour a much broader distribution than the pure NLO QCD result for charm quarks.

One should, however, take into account also non-perturbative effects, as in the case of single-inclusive distributions. We have computed the  $\Delta\phi$  distribution in perturbative QCD with an intrinsic transverse momentum of the incoming partons as described in subsection 2.2 (the use of a fragmentation function has no effect on the  $\Delta\phi$  distribution, since it does not affect momentum directions). The dashed and dotted curves in fig. 7 correspond to the NLO prediction, supplemented with the effect of an intrinsic transverse momentum with  $\langle k_T^2 \rangle = 0.5$  GeV $^2$  and  $\langle k_T^2 \rangle = 1$  GeV $^2$ , respectively. We see that with  $\langle k_T^2 \rangle = 0.5$  GeV $^2$  it is impossible to describe the WA75 and WA92 data. This conclusion differs from the one of ref. [Frixione94] for the WA92 result. This is because in ref. [Adamovich96a] the WA92 collaboration has improved the study of correlations with respect to ref. [Adamovich95] by considering a wider set of correlation variables and by improving the statistics by a factor of 5. WA92 and WA75 data now appear to be consistent with each other. As is apparent from fig. 7, the acceptable value of  $\langle k_T^2 \rangle = 1$  GeV $^2$  is required to describe the data.

We point out that this result has to be interpreted in conjunction with the adopted values of the input parameters entering the calculation. We normally choose the following defaults:

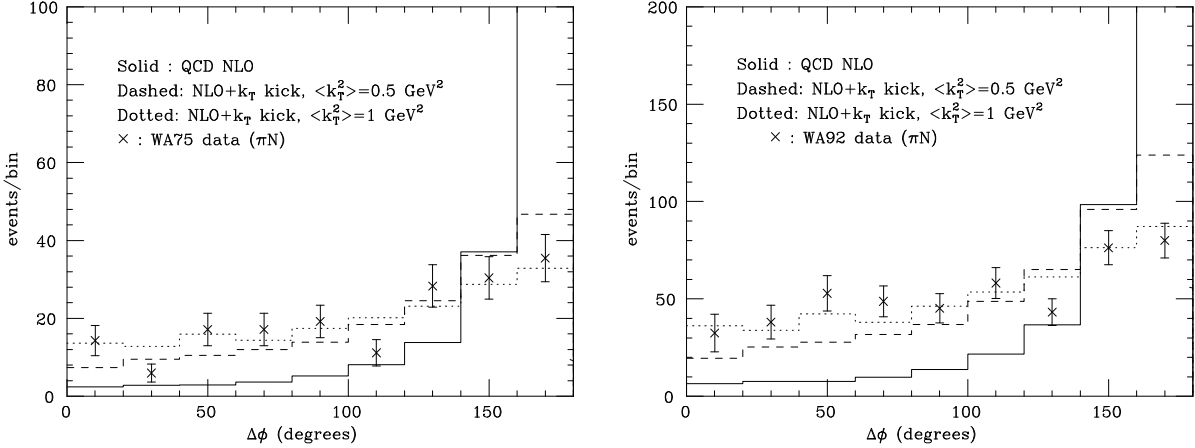


Figure 7: *Azimuthal correlation for charm production in  $\pi N$  collisions: NLO calculation versus the WA75 and WA92 data.*

- $m_c = 1.5 \text{ GeV}$ ,
- $\mu_F = 2\mu_0, \mu_R = \mu_0$ , where

$$\mu_0 = \sqrt{(p_T^2 + \bar{p}_T^2)/2 + m_c^2}, \quad (2.12)$$

- the MRSA' [Martin95] proton parton densities, with the corresponding value of  $\Lambda_5^{\overline{\text{MS}}} = 152 \text{ MeV}$ ,
- the SMRS2 [Sutton92] set for the pion parton densities.

Choosing smaller values for the charm mass, for example, one would get a broader theoretical curve. Alternatively, one could keep the default mass value, but choose  $\mu_R = \mu_0/2$  for the renormalization scale, instead of our default choice  $\mu_R = \mu_0$ . As shown in ref. [Frixione94], this would lead to a broadening of the  $\Delta\phi$  distribution similar to the one caused by an average intrinsic transverse momentum with  $\langle k_T^2 \rangle = 0.5 \text{ GeV}^2$ .

The WA75 collaboration, and recently the WA92 collaboration, published in refs. [Aoki92a, Adamovich96a] the distribution of the transverse momentum of the heavy-quark pair. The theoretical prediction supplemented with a  $k_T$ -kick with  $\langle k_T^2 \rangle = 1 \text{ GeV}^2$  cannot reproduce the WA75 data, while it is in rough agreement with the WA92 measurement, as displayed in fig. 8. Unlike the azimuthal correlation, the  $p_T^2(Q\bar{Q})$  distribution is affected by fragmentation effects, since these can degrade the momenta of the quark and antiquark by different amounts. Fragmentation effects also moderate the pair transverse momentum arising from gluon radiation or from an intrinsic parton transverse momentum. We have verified that at the end, at  $E_b = 350 \text{ GeV}$ , the fragmentation always tends to soften the  $p_T^2(Q\bar{Q})$  distribution.

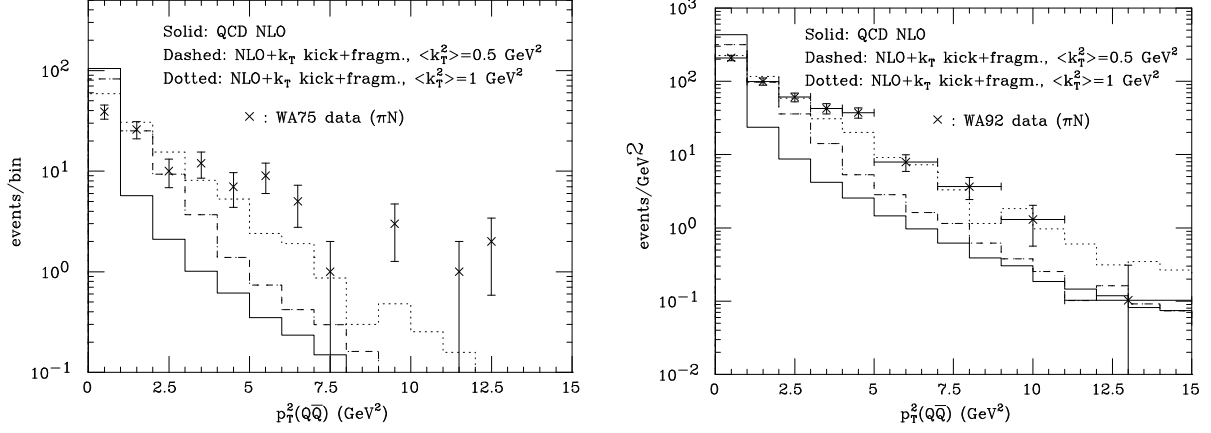


Figure 8: *NLO QCD result for the  $p_T^2(Q\bar{Q})$  supplemented with an intrinsic transverse momentum for the incoming partons, compared with the WA75 (left) and WA92 (right) data.*

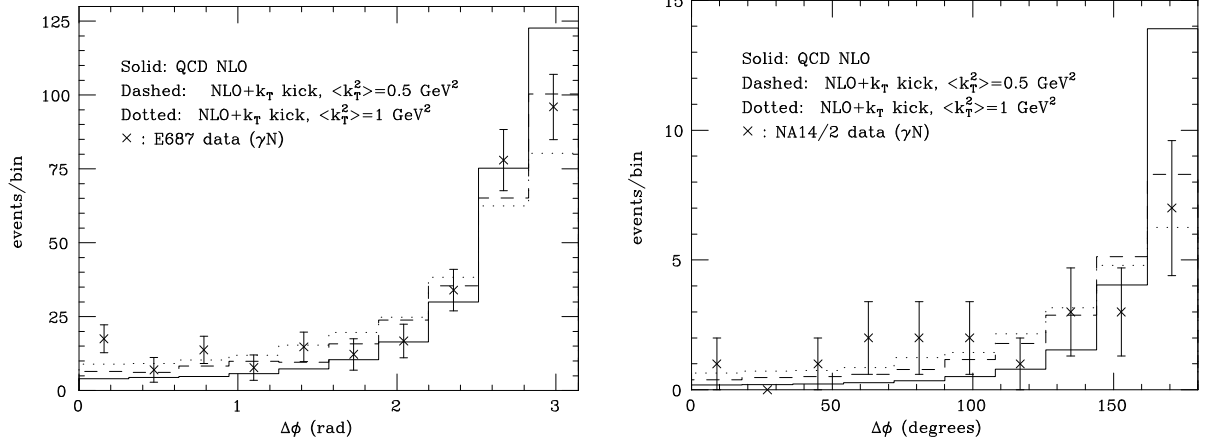


Figure 9: *Azimuthal correlation of  $D\bar{D}$  pair versus the perturbative result in photoproduction for the E687 (left) and NA14/2 (right) experiments.*

Summarizing, the available experimental results for azimuthal  $c\bar{c}$  correlation in hadron–hadron collisions show a tendency to peak in the back-to-back region  $\Delta\phi = \pi$ , but the peak is less pronounced than the one predicted by perturbative QCD. The addition of a  $k_T$  kick of 1  $\text{GeV}^2$  on average gives a satisfactory description of the data, if our default input parameters are chosen. The data on the  $p_T^2(Q\bar{Q})$  distribution do not give a unique indication. While the theoretical prediction obtained with  $\langle k_T^2 \rangle = 1 \text{ GeV}^2$  is in rough agreement with the WA92 measurement, it is sizeably softer than the WA75 data.

Photoproduction of heavy quarks [Alvarez92, Frabetti93, Adamovich87] is another example in which a  $k_T$  kick would induce broader  $\Delta\phi$  and  $p_T(Q\bar{Q})$  correlations. On the left-hand side of fig. 9, the azimuthal correlation measured by the E687 collaboration is given, together with the NLO result. The NLO result supplemented by an intrinsic  $k_T$  of the incoming partons is also shown, for  $\langle k_T^2 \rangle = 0.5 \text{ GeV}^2$  and  $\langle k_T^2 \rangle = 1 \text{ GeV}^2$ . As can be seen, the data do not require a large intrinsic transverse momentum. All curves give a reasonable representation of the data, the one with  $\langle k_T^2 \rangle = 0.5 \text{ GeV}^2$  being slightly better. A similar conclusion applies to the NA14/2 data (which are, however, affected by larger uncertainties), as shown on the right-hand side of fig. 9. The distribution in the transverse momentum of the heavy-quark pair is displayed in fig. 10. In this case, we see that the E687 data favour  $\langle k_T^2 \rangle = 1 \text{ GeV}^2$ .

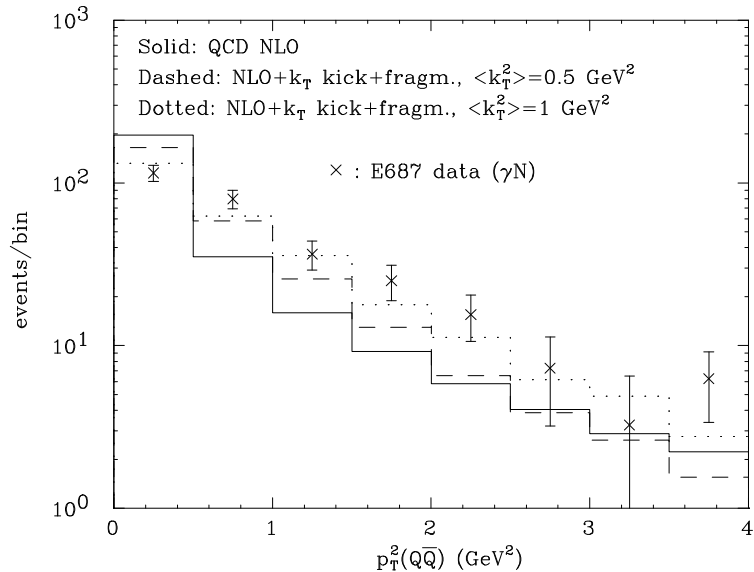


Figure 10: *Transverse momentum distribution of the  $D\bar{D}$  pair versus the perturbative result for the E687 experiment.*

In conclusion, we have seen that the  $\Delta\phi$  and  $p_T(Q\bar{Q})$  distributions are very sensitive to non-perturbative effects, especially in the hadroproduction case. We computed these distributions by assuming that the non-perturbative effects are parametrized by a fragmentation function and an intrinsic transverse momentum of the incoming partons. In general, the azimuthal correlation of the pair is well described by perturbative QCD supplemented by an acceptable  $k_T$  kick. The recent result of ref. [Adamovich96a] on the  $p_T(Q\bar{Q})$  distribution can also be described by the same choice of parameters. This is consistent with what was found in the study of the single-inclusive  $p_T$  distribution. However, the  $p_T(Q\bar{Q})$  distribution reported by WA75 [Aoki92a] is much harder, and would require an unphysically large  $k_T$  kick.

### 3 HEAVY-FLAVOUR PRODUCTION AT HERA

The  $ep$  collider HERA offers new opportunities to study the production mechanism of heavy quarks and to test the predictions of perturbative QCD. The dominant contribution to the cross section is due to those events in which the virtuality of the photon exchanged between the electron and the proton is very small. In this case, the electron can be considered to be equivalent to a beam of on-shell photons, whose distribution in energy (Weizsäcker-Williams function [Weizsaecker34, Williams34]) can be calculated in QED. The underlying production mechanism is therefore a photoproduction one, which has been studied extensively in fixed-target experiments. At HERA, the available centre-of-mass energy is about one order of magnitude larger than at fixed-target facilities (200 GeV versus 20 GeV). This energy regime is totally unexplored in photoproduction, and several new features have to be taken into proper account. In particular, the large contribution of the hadronic photon component introduces in the theoretical predictions a source of uncertainty that is normally negligible at fixed-target energies.

A complementary way of studying heavy-flavour production at HERA is to retain only those events characterized by a large photon virtuality (DIS). Although the total rates are much smaller than the photoproduction ones, the hadronic component is completely eliminated, and more reliable theoretical and experimental results can be obtained. Also, the dependence of the data upon the photon virtuality can be used as a further test of QCD predictions. A significant improvement is expected with the planned luminosity upgrade of the HERA collider [Ingelman96], when the number of charm (bottom) quarks produced will be of the order of  $10^9$  ( $10^6$ ).

In this section, we discuss some aspects of the perturbative QCD calculations of the heavy-flavour photoproduction cross sections of relevance for HERA. We review the phenomenology of charm and bottom production, comparing the available data with the theoretical predictions. We then discuss future perspectives.

#### 3.1 Photoproduction cross sections

It is well known that an on-shell photon has a finite probability to fluctuate into a hadronic state before undergoing a hard collision. In this case, the photon is referred to as “hadronic” (or “resolved”), to contrast with those events in which it directly interacts with the hadron (“point-like” or “direct”). Therefore, a differential photon–hadron cross section can be written as the sum of a point-like and a hadronic photon contribution:

$$d\sigma^{(\gamma H)}(P_\gamma, P_H) = d\sigma_{\text{point}}^{(\gamma H)}(P_\gamma, P_H) + d\sigma_{\text{hadr}}^{(\gamma H)}(P_\gamma, P_H). \quad (3.1)$$

Thanks to the factorization theorems in QCD [Ellis79, Collins89], we have

$$d\sigma_{\text{point}}^{(\gamma^H)}(P_\gamma, P_H) = \sum_j \int dx f_j^{(H)}(x, \mu_F) d\hat{\sigma}_{\gamma j}(P_\gamma, xP_H, \alpha_s(\mu_R), \mu_R, \mu_F, \mu_\gamma), \quad (3.2)$$

$$\begin{aligned} d\sigma_{\text{hadr}}^{(\gamma^H)}(P_\gamma, P_H) &= \sum_{ij} \int dx dy f_i^{(\gamma)}(x, \mu_\gamma) f_j^{(H)}(y, \mu'_F) \\ &\quad \times d\hat{\sigma}_{ij}(xP_\gamma, yP_H, \alpha_s(\mu'_R), \mu'_R, \mu'_F, \mu_\gamma). \end{aligned} \quad (3.3)$$

In eq. (3.3), the  $f_i^{(\gamma)}$  are the partonic densities in the photon. Their physical meaning is analogous to the one of the more familiar partonic densities in the hadron,  $f_j^{(H)}$ . They are universal, but not calculable in perturbation theory. They satisfy a renormalization group equation [Witten77, Llewellyn78, Bardeen79, DeWitt79] that can be obtained by slightly modifying the usual Altarelli–Parisi [Altarelli77] equation

$$\frac{\partial f_i^{(\gamma)}}{\partial \log \mu^2} = \frac{\alpha_{\text{em}}}{2\pi} P_{i\gamma} + \frac{\alpha_s}{2\pi} \sum_j P_{ij} \otimes f_j^{(\gamma)}, \quad (3.4)$$

where, at the lowest order,

$$P_{i\gamma} = e_i^2 \left( x^2 + (1-x)^2 \right) \quad (3.5)$$

and  $e_i$  is the electric charge of the parton  $i$  in units of the charge of the electron (for gluons,  $e_i = 0$ ). The first term on the RHS of eq. (3.4), which is not present in the evolution equation of the hadron densities, is due to the direct coupling of the photon to the quarks.

To understand the strict interplay between the point-like and the hadronic component in eq. (3.1), it is worth while to sketch the derivation of the subtracted partonic cross sections appearing in eqs. (3.2) and (3.3). As a first step, one performs a direct calculation of the partonic cross sections for the processes  $\gamma + j \rightarrow Q + \bar{Q} + X$  and  $i + j \rightarrow Q + \bar{Q} + X$  (here  $i$  and  $j$  represent a generic parton). After the ultraviolet renormalization, one is left with the quantities  $d\sigma_{\gamma j}$  and  $d\sigma_{ij}$ , which still display divergences due to the collinear emission of a massless final-state parton from one of the incoming partons. These divergences are subtracted by applying the prescription of the factorization theorem. Writing the expansion of the partonic cross sections at the next-to-leading order in QCD as

$$d\sigma_{\gamma j} = \alpha_{\text{em}} \alpha_s d\sigma_{\gamma j}^{(0)} + \alpha_{\text{em}} \alpha_s^2 d\sigma_{\gamma j}^{(1)}, \quad (3.6)$$

$$d\sigma_{ij} = \alpha_s^2 d\sigma_{ij}^{(0)} + \alpha_s^3 d\sigma_{ij}^{(1)}, \quad (3.7)$$

and an analogous expansion for the subtracted cross sections  $d\hat{\sigma}_{\gamma j}$  and  $d\hat{\sigma}_{ij}$ , we get, using dimensional regularization ( $d = 4 - 2\epsilon$ ) and order by order in perturbation theory,

$$d\hat{\sigma}_{\gamma j}^{(0)}(p_1, p_2) = d\sigma_{\gamma j}^{(0)}(p_1, p_2), \quad d\hat{\sigma}_{ij}^{(0)}(p_1, p_2) = d\sigma_{ij}^{(0)}(p_1, p_2), \quad (3.8)$$

$$\begin{aligned} d\hat{\sigma}_{\gamma j}^{(1)}(p_1, p_2) &= d\sigma_{\gamma j}^{(1)}(p_1, p_2, \frac{1}{\epsilon}) + \frac{1}{2\pi} \sum_k \int dx \left( \frac{1}{\epsilon} P_{k\gamma}(x) - H_{k\gamma}(x) \right) d\sigma_{kj}^{(0)}(xp_1, p_2) \\ &\quad + \frac{1}{2\pi} \sum_k \int dx \left( \frac{1}{\epsilon} P_{kj}(x) - K_{kj}^{(H)}(x) \right) d\sigma_{\gamma k}^{(0)}(p_1, xp_2), \end{aligned} \quad (3.9)$$

$$\begin{aligned} d\hat{\sigma}_{ij}^{(1)}(p_1, p_2) &= d\sigma_{ij}^{(1)}(p_1, p_2, \frac{1}{\epsilon}) + \frac{1}{2\pi} \sum_k \int dx \left( \frac{1}{\epsilon} P_{ki}(x) - K_{ki}^{(\gamma)}(x) \right) d\sigma_{kj}^{(0)}(xp_1, p_2) \\ &\quad + \frac{1}{2\pi} \sum_k \int dx \left( \frac{1}{\epsilon} P_{kj}(x) - K_{kj}^{(H)}(x) \right) d\sigma_{ik}^{(0)}(p_1, xp_2). \end{aligned} \quad (3.10)$$

On the RHS of eqs. (3.9) and (3.10) we explicitly indicated the dependence of the partonic cross sections upon  $1/\epsilon$  to recall that these quantities are still infrared-divergent. The divergences are nevertheless properly cancelled by the terms proportional to the Altarelli–Parisi kernels appearing in these equations. The functions  $K_{ij}^{(H)}$ ,  $K_{ij}^{(\gamma)}$  and  $H_{k\gamma}$  are completely arbitrary, in that they define an extra finite part of the subtraction; different choices correspond to different subtraction schemes. In eqs. (3.9) and (3.10) the  $\overline{\text{MS}}$  scheme is equivalent to  $H = K \equiv 0$ . For greater generality, we have allowed the possibility to have different subtraction schemes on the photon and hadron legs.

The key feature of eqs. (3.9) and (3.10) is the term proportional to  $P_{k\gamma}(x)$  in eq. (3.9). The physical origin of this contribution is the direct coupling of the photon with the quarks, which in turn implies the presence of the inhomogeneous term in eq. (3.4). In the language of the Altarelli–Parisi equations, this means that the infrared divergences due to the collinear emission of quarks from the incoming photon in the point-like component, eq. (3.2), are re-absorbed into the partonic densities in the photon, which appear in the hadronic component, eq. (3.3). The same argument can be formulated in terms of renormalization group (RG) equations. Equation (3.2) is RG-invariant with respect to the variation of the scales  $\mu_R$  and  $\mu_F$ ; eq. (3.3) is RG-invariant with respect to the variation of the scales  $\mu'_R$  and  $\mu'_F$ . But neither eq. (3.2) nor eq. (3.3) are *separately* RG-invariant with respect to the variation of the scale  $\mu_\gamma$ ; when varying  $\mu_\gamma$  in eq. (3.3), a residual dependence is left, due to the inhomogeneous term in eq. (3.4), which is cancelled only by the explicit dependence of eq. (3.2) upon  $\mu_\gamma$ . A third way of understanding this issue is to consider a change of the subtraction scheme. The partonic densities are modified as follows:

$$f_i^{(H)'} = f_i^{(H)} + \frac{\alpha_s}{2\pi} \sum_j K_{ij}^{(H)} \otimes f_j^{(H)}, \quad (3.11)$$

$$f_i^{(\gamma)'} = f_i^{(\gamma)} + \frac{\alpha_{\text{em}}}{2\pi} H_{i\gamma} + \frac{\alpha_s}{2\pi} \sum_j K_{ij}^{(\gamma)} \otimes f_j^{(\gamma)}. \quad (3.12)$$

The term  $H_{i\gamma}$ , which is due to the change of scheme of the photon densities entering eq. (3.3), affects eq. (3.2), since it defines the finite part of the infrared subtraction in the photon leg via eq. (3.9).

It should now be clear that the point-like and the hadronic components of the photoproduction cross sections are very closely related, and that only their sum is physically meaningful. The separation of a cross section into a point-like and a hadronic component is ambiguous beyond leading order (for a detailed discussion, see refs. [Schuler93, Schuler93a]), as is shown by the discussion on the change of subtraction scheme: finite terms can be subtracted to one piece and added to the other, without affecting physical predictions. One explicit example is presented in ref. [Gluck92], where a factorization scheme ( $\text{DIS}_\gamma$ ) for the photon densities is introduced, which uses  $K^{(\gamma)} = 0$  and  $H \neq 0$ . That notwithstanding, we will keep on talking about the point-like and the hadronic component. The reason for this is twofold: we can use a leading-order approximation to get a physical picture of the separation between the two components; and the term ( $H$ ) that can be exchanged between the two components is numerically small.

The photon parton-densities are quite soft. Therefore, the hadronic component is only important for large CM energies and small masses for the produced system. We will see in the following that it potentially affects charm production at HERA. This process can therefore be used to constrain the densities in the photon, which are experimentally very poorly known at present.

As a final step, in order to obtain the  $Q\bar{Q}$  cross sections in electron–proton collisions, the photoproduction cross sections must be convoluted with the Weizsäcker–Williams distribution:

$$f_\gamma^{(e)}(y) = \frac{\alpha_{\text{em}}}{2\pi} \frac{1 + (1 - y)^2}{y} \log \frac{\mu_{WW}^2(1 - y)}{m_e^2 y^2}. \quad (3.13)$$

The scale  $\mu_{WW}$  is, in general, a function of  $y$  determined by the kinematics of the process considered. It has been pointed out in refs. [Budnev74, Olsen79, Bawa89, Catani91, Frixione93] that the choice of  $\mu_{WW}$  should also take into account the dynamics of the production mechanism. In the case of the production of heavy quarks it is reasonable to set  $\mu_{WW} = \xi m_Q$ , where  $\xi$  is of order 1. It was shown in ref. [Frixione93] that for the point-like component an appropriate choice for the parameter  $\xi$  is  $\xi \equiv 1$ . The hadronic component case is more involved, since the partonic densities in the *virtual* photon introduce in the problem an additional mass scale. The presence of this scale is due to the fact that the densities rapidly fall to zero when the virtuality of the photon approaches the hard scale of the process [Uematsu82, Borzumati93, Drees94], which is of the order of the heavy-quark mass. It follows that the scale  $\mu_{WW}$  must be chosen smaller than  $m_Q$ . In ref. [Frixione95a] it has been argued that  $\xi = 0.6\text{--}0.7$  gives sensible results. Although this is only a rough estimate, the uncertainty due to the choice of the parameter  $\xi$  is much smaller than the uncertainties coming from the phenomenological parameters entering the calculations.

It is interesting to notice that a photoproduction event can be experimentally defined by means of an anti-tag condition: all those events in which the electron is scattered at an angle larger than a given value  $\theta_c$  are rejected. The form of the Weizsäcker–Williams function in the presence of an anti-tag condition can be explicitly worked out [Frixione93]. Indicating with  $E$  the energy of the incoming electron in the laboratory frame, we get

$$f_\gamma^{(e)}(y) = \frac{\alpha_{\text{em}}}{2\pi} \left\{ 2(1-y) \left[ \frac{m_e^2 y}{E^2(1-y)^2 \theta_c^2 + m_e^2 y^2} - \frac{1}{y} \right] + \frac{1+(1-y)^2}{y} \log \frac{E^2(1-y)^2 \theta_c^2 + m_e^2 y^2}{m_e^2 y^2} \right\}. \quad (3.14)$$

The error due to the approximation can be estimated to be  $\mathcal{O}(\theta_c^2, m_e^2/E^2)$  in this case, and it is therefore quite small for applications to HERA physics, where  $\theta_c \approx 5 \times 10^{-3}$ . Also notice that the non-logarithmic term is singular in  $y$  and therefore represents a non-negligible correction.

### 3.2 Charm photoproduction

Taking into account all the relevant sources of uncertainty, which have already been discussed in section 2, we get a theoretical prediction for the total rates with a large error. At the NLO, the point-like cross section changes by a factor of about 4 when varying the mass in the range  $1.2 \text{ GeV} < m_c < 1.8 \text{ GeV}$ , and by a factor of 2 when varying the renormalization scale. The choice of the proton partonic densities induces a 50% uncertainty at  $\sqrt{S_{\gamma p}} = 30 \text{ GeV}$ , and a factor of about 5 [Frixione95b] at  $\sqrt{S_{\gamma p}} = 300 \text{ GeV}$ . These effects are even more dramatic in the case of the hadronic component, where the dominant source of uncertainty is the choice of the partonic densities in the photon. Results from dijet photoproduction at HERA give some indication on the gluon density in the photon [Ahmed95], but the very limited statistics does not allow either a distinction between different NLO parametrizations [Gluck92a, Gordon92, Aurenche92, Aurenche94, Gordon96], or a discrimination between the LAC1 [Abramowicz91] gluon and the flatter ones of the NLO sets. Other LO sets [Hagiwara95] are also consistent with the data. A reasonable way to estimate the effect due to the uncertainty in the gluon density of the photon is to take the sets GRV-HO [Gluck92a] and LAC1 as the two extremes. At the highest photon–proton centre-of-mass energies available at HERA, the prediction for the hadronic component with LAC1 is one order of magnitude larger than the prediction with GRV-HO, and much larger than the point-like component as well.

The comparison between the theoretical predictions and the experimental results [Derrick95, Aid96] is presented in fig. 11, where only the uncertainty on the QCD result due to the choice of the renormalization scale is displayed. Despite the fact that, as discussed before, this only partially accounts for the overall uncertainty on

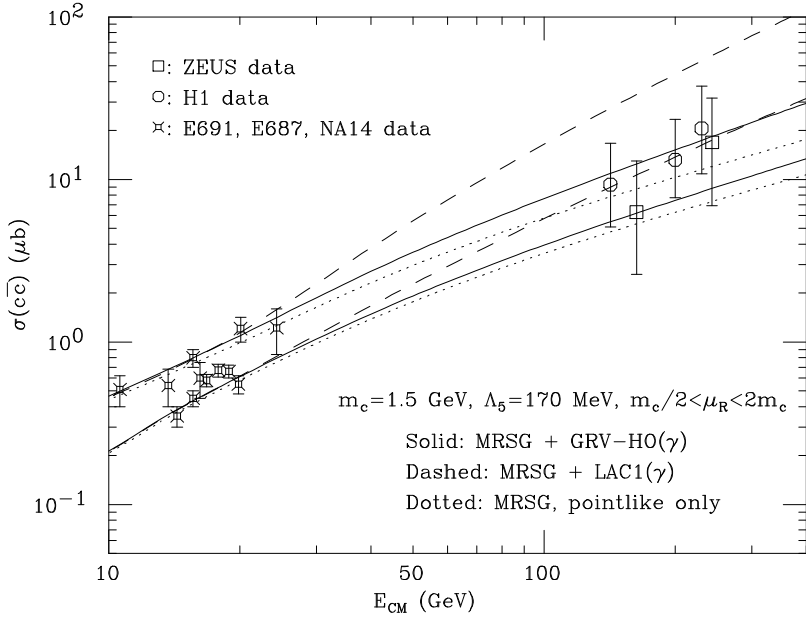


Figure 11: *Total cross section for the photoproduction of  $c\bar{c}$  pairs, as a function of the  $\gamma p$  centre-of-mass energy: next-to-leading order QCD predictions versus experimental results.*

the theoretical predictions, the data show a satisfactory agreement with the curves obtained by choosing  $m_c = 1.5$  GeV and MRSG and GRV-HO for the partonic densities in the proton and the photon respectively. It is important to notice that a single choice of the input parameters allows us to describe the data in the whole energy range considered; this is a non-trivial result, the energies available at HERA being one order of magnitude larger than those available at fixed-target experiments. The importance of the hadronic component of the photon at fixed target and at HERA is also clear from fig. 11.

The experimental determination of the total charm cross section at HERA deserves some further comment. The experiments are sensitive to production in the central rapidity region, typically  $|y| < 1.5$ , where the cross section is far from its maximum (see fig. 13). Furthermore, a small- $p_T$  cut is applied to the data, in order to clearly separate the signal from the background. In order to get the total cross section, one has therefore to extrapolate to the full rapidity and transverse momentum range. Large rapidities and small transverse momenta typically involve small- $x$  values, and the extrapolation is therefore subject to uncertainties due to our ignorance of the small- $x$  behaviour of the parton densities. Since these uncertainties are very large, we believe that it would be useful to present also the measurement of the cross section limited to the directly accessible rapidity region. The lack of sensitivity to large negative rapidities is one of the reasons why it is at present impossible to use the photoproduction of charm quarks at HERA to distinguish among different

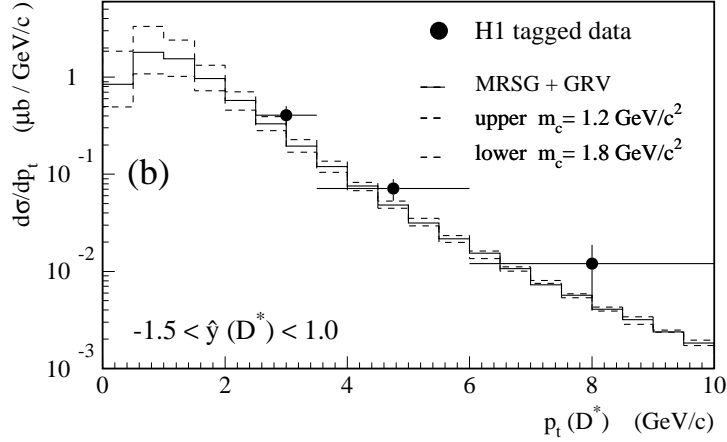


Figure 12: *Transverse-momentum distribution of  $D^*$  mesons in  $ep$  collisions at HERA, for  $Q^2 < 0.01$   $GeV^2$ . Experimental results [Aid96] are compared with next-to-leading order theoretical predictions.*

parametrizations of the gluon density in the proton. An equally important reason (as pointed out in section 2) lies in the presence of inconsistencies in the low-energy data. From fig. 11 no definite conclusion can be drawn on the photon densities either.

The first measurement of single-inclusive distributions for charm photoproduction at HERA has been presented by the H1 Collaboration [Aid96]. The data are integrated over a large range of photon–proton energies, and the results should therefore be compared with the theoretical predictions for electroproduction in the Weizsäcker–Williams approximation.

Since the Weizsäcker–Williams function grows in the small- $x$  region, the bulk of the contribution to the cross section is due to photons of relatively low energy. Therefore, the rôle of the hadronic component of the photon and of the small- $x$  region in the proton densities is marginal. It turns out that, when cuts similar to the experimental ones are applied and electroproduction in the Weizsäcker–Williams approximation is considered, the shape of the theoretically predicted distributions is very stable [Frixione95a]. It follows that single-inclusive charm electroproduction is of little help in constraining the partonic densities of both the proton and the photon, but can be used as a valuable test of the production mechanism.

Figure 12 presents the comparison between theory and H1 data [Aid96] for the  $p_T$  spectrum of the  $D^*$  mesons. The data are relative to the so-called “tagged” sample, defined by the condition  $Q^2 < 10^{-2}$   $GeV^2$ . The QCD predictions for charm quarks have been convoluted with the Peterson fragmentation function [Peterson83]. Given the limited statistics of the measurement, the comparison of the data with the theory appears to be satisfactory, and qualitatively analogous to similar results at fixed-target experiments [Frixione94]. A comparison has also been carried out by the H1

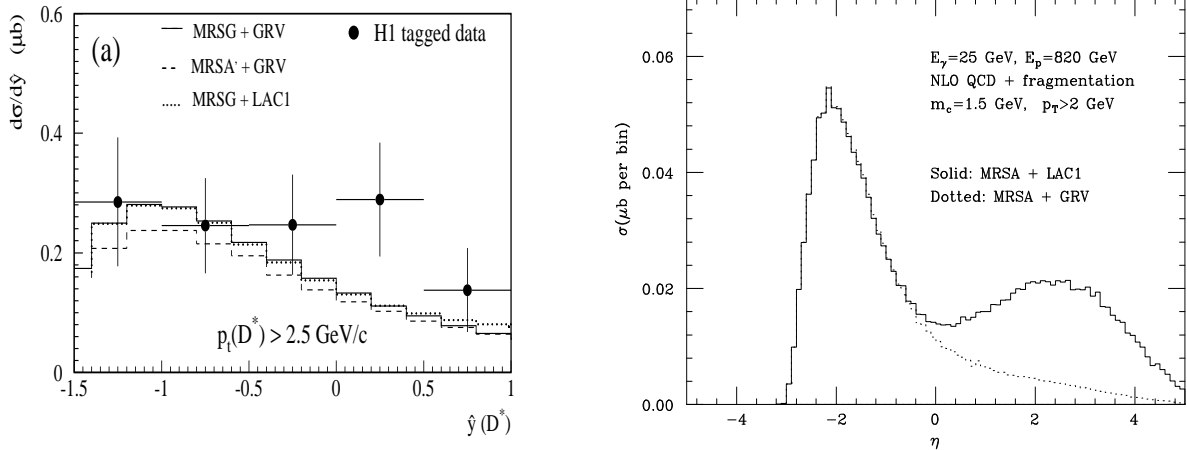


Figure 13: *Left:* rapidity distribution of  $D^*$  mesons in  $ep$  collisions at HERA, for  $Q^2 < 0.01$   $GeV^2$ . Experimental results [Aid96] are compared with next-to-leading order QCD predictions. *Right:* pseudorapidity distribution of fragmented charm quarks in monochromatic photon–proton collisions.

Collaboration [Aid96] for the untagged sample ( $\langle Q^2 \rangle \simeq 0.2$   $GeV^2$ ); the agreement is slightly worse, but still satisfactory. As shown in fig. 12, the uncertainty on the theoretical prediction due to the value of the charm mass is completely negligible when compared to the uncertainties in the experimental data.

The comparison between theory and H1 data for the rapidity distribution is presented on the left-hand side of fig. 13. Although the agreement is acceptable, only one point being more than one standard deviation away from the theoretical predictions, higher statistics are required in order to perform a more significant comparison. Indeed, preliminary H1 results<sup>7</sup> show that, when improving the statistics, the data point at  $\hat{y}(D^*) = 0.25$  is also close to the theoretical curve. We point out, however, that recent preliminary data from ZEUS [Zeus96a] are not in satisfactory agreement with QCD expectations.

If data with larger statistics were available, it would be possible to consider the production processes initiated by very energetic photons only. The right-hand side of fig. 13 shows the theoretical prediction for the pseudorapidity distribution of fragmented charm quarks in monochromatic photon–proton collisions, at a centre-of-mass energy of  $\sqrt{S_{\gamma p}} = 286$   $GeV$ , and for different choices of the partonic densities in the photon. As is apparent from the figure, the results obtained with the LAC1 and GRV-HO sets are completely different in the forward region. Even at the moderate pseudorapidity values covered by the present configuration of the detectors, the large difference induced by the two photon sets should have measurable effects.

<sup>7</sup>C. Grab, private communication.

Because of the large photon–proton centre-of-mass energy available at HERA, the  $\log(S/m_c^2)$  terms appearing in the charm cross section may get large and spoil the convergence of the perturbative series. The problem of resumming these terms (*small- $x$  effects*) has been tackled by several authors [Ellis90, Catani89, Catani90, Collins91], mainly in the context of  $b$  production in hadronic collisions. In ref. [Frixione95b] an estimate has been given of the importance of the small- $x$  effect for charm physics in the HERA energy range. It has been found that, resumming the  $\log(S/m_c^2)$  terms, the total rate can be increased by by 20% to 40% with respect to the next-to-leading order prediction for the point-like contribution, and by 20% to 45% for the hadronic contribution, depending on the partonic densities used in the calculation (as a rule of thumb, the flatter is the gluon density at small  $x$ , the larger is the contribution expected from the resummation of the small- $x$  effects). These effects are therefore negligible with respect to the other sources of uncertainty on the theoretical predictions.

We finally observe that the transverse-momentum distribution is in principle affected by the presence of  $\log(p_T/m_c)$  terms. These logarithms can be resummed by observing that, at high  $p_T$ , the heavy-quark mass is negligible, and by using perturbative fragmentation functions [Cacciari96, Kniehl95]. Remarkably enough, the fixed-order and the resummed results of [Cacciari96] agree in a very wide range in  $p_T$ . Recently, the massless approach has been used in ref. [Kniehl96] to predict the  $D^*$  spectrum at HERA.

### 3.3 Bottom photoproduction

Thanks to the higher value of the quark mass, perturbative QCD predictions for bottom production are more reliable than those for charm. In fact, all the uncertainties we have discussed for charm are in this case strongly reduced. The resummation of the small- $x$  effects has been estimated in ref. [Frixione95b] to increase the next-to-leading order result by  $\approx 5\%$ . In monochromatic photon–proton collisions, the point-like component has an uncertainty of a factor of 2 if all the parameters are varied *together* in the direction that makes the cross section larger or smaller. At  $\sqrt{S_{\gamma p}} = 100$  GeV, the lower and upper limits of the point-like component are 16 nb and 35 nb respectively, while at  $\sqrt{S_{\gamma p}} = 280$  GeV we get 41 nb and 101 nb [Frixione95b]. The hadronic component has larger uncertainties, but much smaller than in charm production. As discussed above, the main source of uncertainty is the parton density set for the photon. Nevertheless, in bottom production the small- $x$  region is probed to a lesser extent than in charm production, and the sensitivity of the result to the photon densities is therefore milder; we get an uncertainty of a factor of 3 (to be compared with a factor of 10 in the case of charm). The hadronic component can still be the dominant contribution to the photoproduction cross section, if the gluon in the photon is as soft as the LAC1 parametrization suggests.

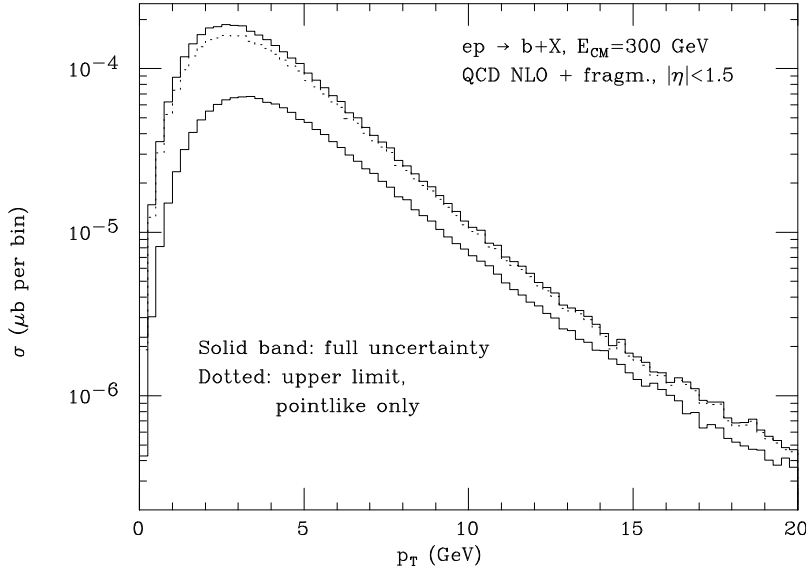


Figure 14: *Full uncertainty on the transverse-momentum distribution for bottom electroproduction (Weizsäcker-Williams approximation) with Peterson fragmentation and a pseudorapidity cut.*

The bottom rates are about a factor of 200 smaller than the charm ones. To perform a statistically significant study of bottom production, the luminosity upgrade at HERA is necessary. In any case, it is very likely that a comparison with the theory could only be done by considering electroproduction in the Weizsäcker-Williams limit. In this case, consistently with what was discussed for charm, the sensitivity of the theoretical predictions to the input parameters is sizeably reduced, and a reliable comparison between theory and data can be performed. For example, in electroproduction the hadronic component contribution to the total cross section is at most 75% of the point-like contribution, even if the LAC1 set is used. The most interesting results are, however, obtained when considering more exclusive quantities, such as single-inclusive distributions. In particular, as shown in fig. 14, the transverse momentum of the bottom quark at HERA can be predicted by perturbative QCD quite accurately. It is clear that even with the LAC1 set the hadronic component affects the prediction only marginally; this fact is basically a consequence of the applied pseudorapidity cut. We can therefore regard fig. 14 as a reliable prediction of QCD for the  $p_T$  spectrum of  $b$  hadrons at HERA. The comparison of this prediction with the data would be extremely useful in the light of the status of the comparison between theory and data for  $b$  production at the Tevatron (see section 4).

### 3.4 Deep-inelastic production

The first data on charm production in the deep-inelastic regime at HERA have recently become available [Zeus96, Adloff96]. On the theoretical side, NLO QCD calculations for total and single-inclusive deep-inelastic production have been performed

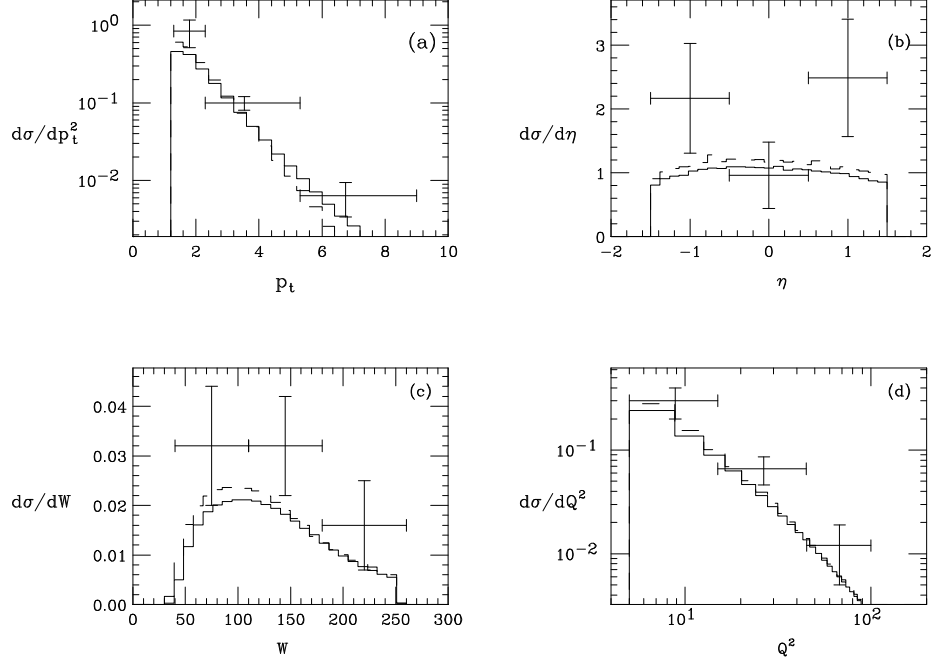


Figure 15: *Comparison between theoretical predictions and experimental data for single-inclusive distributions in DIS charm production.*

in refs. [Laenen92a, Laenen93, Laenen93a]. Recently, fully exclusive cross sections have been computed [Harris95, Harris95a]. In this context, it is possible to perform comparisons between theory and experiment in different aspects.

To start with, one can consider the contribution of charm quarks to the proton structure functions  $F_2$  and  $F_L$ . It turns out that NLO corrections to these quantities are non-negligible. The full NLO results display a mild dependence upon the renormalization and factorization scales (well below 10% for  $Q^2$  larger than  $10 \text{ GeV}^2$ , when varying scales between half and twice the default value  $\sqrt{Q^2 + m_c^2}$ ). The dominant uncertainty in the calculation is the small- $x$  behaviour of the gluon density in the proton. For this reason, it is possible to conclude that structure-function measurements may provide useful information about the gluon distribution in the proton (see ref. [Laenen96a] for a discussion of this issue). For  $Q^2 \gg 4m_c^2$  the calculation of  $F_2$  and  $F_L$  requires the inclusion of large logarithmic effects arising from evolution. Approaches to this problem can be found in refs. [Aivazis94, Aivazis94a, Lai97] and [Martin96].

In fig. 15, taken from ref. [Laenen96a], we show experimental data for some single-inclusive distributions, superimposed on QCD theoretical predictions at NLO. The following distributions are shown: a) the  $D^*$  transverse momentum  $p_T^{D^*}$ , b) its pseudorapidity  $\eta^{D^*}$ , c) the hadronic final state invariant mass and d) the  $Q^2$  one, for the kinematic range  $5 \text{ GeV}^2 < Q^2 < 100 \text{ GeV}^2$ ,  $1.3 \text{ GeV} < p_T^{D^*} < 9 \text{ GeV}$  and  $|\eta^{D^*}| < 1.5$ .

A cut on the DIS  $y$  variable  $0 < y < 0.7$  is also applied. The  $D^*$  momenta are obtained by applying a Peterson fragmentation function to the produced charm quark. Also shown are experimental data of the ZEUS collaboration [Zeus96].

The shape of the distributions considered is significantly modified by the introduction of radiative corrections. As we can see, the data are in reasonable agreement with theoretical predictions. More statistics is needed for a meaningful comparison with the theory.

### 3.5 Future physics

In this subsection we will discuss a few topics on future physics possibilities in heavy-flavour production at HERA. With the planned upgrades of the HERA collider, an integrated luminosity of  $100 \text{ pb}^{-1}$  or larger will be achieved. This will probably allow the production of a sizeable sample of double-tagged charm events [Eichler96], and therefore to study double-differential cross sections. The possibility of having polarized beams has also been considered [Ingelman96]. Furthermore, the HERA-B fixed-target program will become operational.

#### 3.5.1 Determination of $f_g^{(p)}$

An interesting application of double-differential measurements is the determination of the proton gluon density  $f_g^{(p)}$  [Buchmueller91, Riemersma92, Frixione93a]. At present, this quantity is not directly measured: DIS data allow its indirect extraction from the  $Q^2$  evolution of the structure functions, and direct photon and inclusive jet measurements constrain it in complementary regions of  $x$  and  $Q^2$ .

In photon or electron–hadron collisions, the advantage is that the gluon density enters the cross section in a simpler way than in the case of hadronic collisions. It is easy to show that this in turn implies that, if one could determine the invariant mass and rapidity of the produced system, the cross section would be directly proportional to  $f_g^{(p)}$  and to other calculable factors. For example, the LO heavy-flavour electroproduction cross section can be written, in the Weizsäcker–Williams approximation, and neglecting the hadronic component, in the following way:

$$\frac{d\sigma^{(0)}}{dy_{Q\bar{Q}} dM_{Q\bar{Q}}^2} = x_g \frac{d\sigma^{(0)}}{dx_g dM_{Q\bar{Q}}^2} = \frac{1}{E^2} f_\gamma^{(e)}(x_\gamma, \mu_0^2) f_g^{(p)}(x_g, \mu_F^2) \hat{\sigma}_{\gamma g}^{(0)}(M_{Q\bar{Q}}^2), \quad (3.15)$$

where  $M_{Q\bar{Q}}$  is the invariant mass of the heavy-quark pair, and  $y_{Q\bar{Q}}$  is the rapidity of the pair in the electron–proton centre-of-mass frame (we choose positive rapidities in the direction of the incoming proton);  $E = \sqrt{S}$  is the electron–proton centre-of-mass energy, and

$$x_\gamma = \frac{M_{Q\bar{Q}}}{E} \exp(-y_{Q\bar{Q}}), \quad (3.16)$$

$$x_g = \frac{M_{Q\bar{Q}}}{E} \exp(y_{Q\bar{Q}}). \quad (3.17)$$

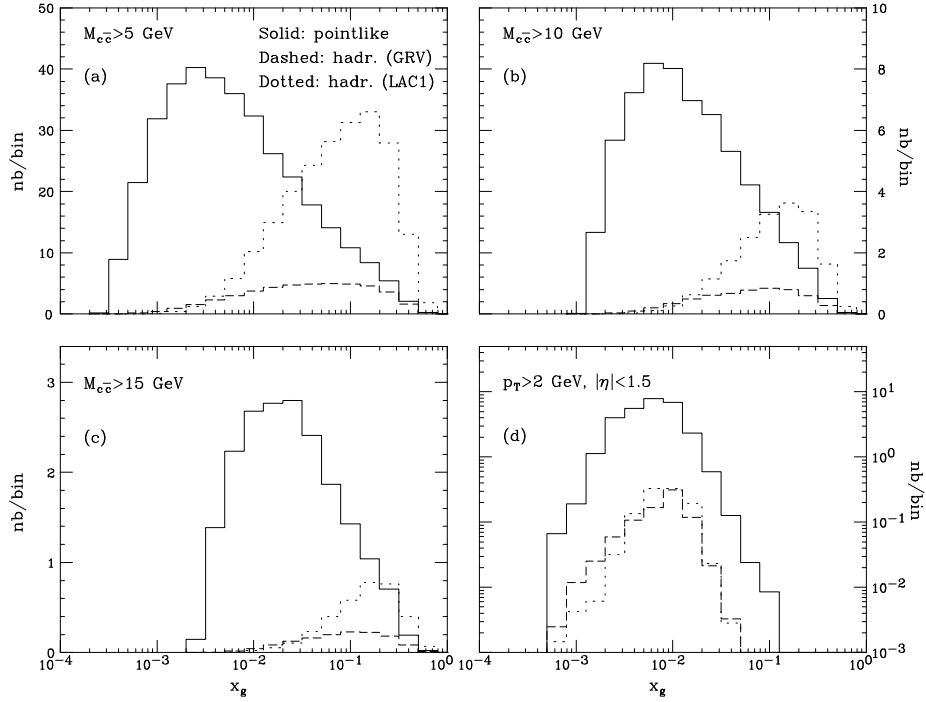


Figure 16:  $x_g$  distribution in  $ep$  collisions (Weizsäcker-Williams approximation) at HERA, for  $m_c = 1.5$  GeV and the MRSG proton parton-densities.

The function  $f_\gamma^{(e)}$  is the Weizsäcker-Williams function we already discussed in subsection 3.1. We observe that all quantities on the right-hand side of eq. (3.15) are calculable, except for  $f_g^{(p)}$ , which can therefore be measured. The inclusion of radiative corrections does not pose any problem. This issue is discussed in detail in ref. [Frixione93a], where it is shown that  $f_g^{(p)}$  can be measured up to NLO accuracy by using double-differential charm data.

As discussed previously, the heavy-flavour cross section receives a large contribution from the hadronic component. In order to extract the gluon density of the proton with the method outlined above, we have to consider only those kinematical regions where the hadronic component is suppressed. We study this possibility in fig. 16, where we present the NLO QCD distribution in the variable  $x_g$ , in electron-proton collisions at  $\sqrt{S} = 314$  GeV. The partonic densities in the proton are given by the MRSG set, while we considered both the LAC1 and GRV-HO sets for the photon. Figures 16a)–16c) show the effect of applying a cut on the invariant mass of the pair. Even in the case of the smallest invariant-mass cut, there is a region of small  $x_g$  where the hadronic component is negligible with respect to the point-like one. When we increase the invariant-mass cut, we notice that the hadronic component decreases faster than the point-like one. This is due to the fact that, for large invariant masses, the production process of the hadronic component is suppressed by the small value of the

gluon density of the photon at large  $x$ . By pushing the invariant-mass cut to 20 GeV, it turns out that the point-like component is dominant over the hadronic one for  $x_g$  values as large as  $10^{-1}$ . We then conclude that the theoretical uncertainties affecting the charm cross section, in the range of  $10^{-3} < x_g < 10^{-1}$ , are small enough to allow for a determination of the gluon density in the proton by using invariant-mass cuts to suppress the hadronic component. In a more realistic configuration, as the present one of the detectors at HERA, additional cuts are applied to the data. Figure 16d) shows the effect, on the  $x_g$  distribution, of a small- $p_T$  and a pseudorapidity cut applied to both the charm and the anticharm. In this case, even without applying an invariant-mass cut, the point-like component is dominant in the whole kinematically accessible range.

### 3.5.2 Polarization asymmetries

It is conceivable that, in the future, the HERA collider will be operated in a polarized mode. At present, a good result for the polarization of the positron beam has been obtained, and feasibility studies for the polarization of the proton beam are under way [Ingelman96]. At leading order in QCD, the heavy-flavour production cross section in polarized  $ep$  collisions is proportional to the polarized gluon density in the proton,  $\Delta g$ . Therefore, data on charm production could be used to measure  $\Delta g$  directly, as previously shown for the unpolarized case. In practice, the situation for the polarized scattering is much more complicated. First of all, it is not possible to perform a complete NLO analysis, because NLO cross sections for polarized charm photoproduction have never been computed. Furthermore, there is no experimental information on parton densities in the polarized *photon*. It is reasonable, however, that charm production at the HERA collider in the polarized mode can help in constraining the polarized gluon density in the proton. This possibility was first suggested in refs. [Gluck88, Gluck91, Vogelsang91], and recently reconsidered in refs. [Frixione96b, Stratmann96].

In order to reduce the impact of the uncertainties induced by radiative corrections, it is useful to present predictions [Frixione96b] for the ratio  $\Delta\sigma/\sigma$  (asymmetry), where  $\sigma$  is the unpolarized cross section and

$$\Delta\sigma = \frac{1}{2} (\sigma^{\uparrow\uparrow} - \sigma^{\uparrow\downarrow}). \quad (3.18)$$

Here  $\sigma^{\uparrow\uparrow}$  and  $\sigma^{\uparrow\downarrow}$  are the cross sections for  $c\bar{c}$  production with parallel and antiparallel polarizations of the incoming particles respectively. One might expect that the effect of the radiative corrections approximately cancels in the ratio. It must be stressed that, for consistency, the unpolarized cross section  $\sigma$  appearing in the asymmetry must be calculated at the leading order, as the polarized one. The NLO value of  $\sigma$  can then be used to estimate the sensitivity of the experiment.

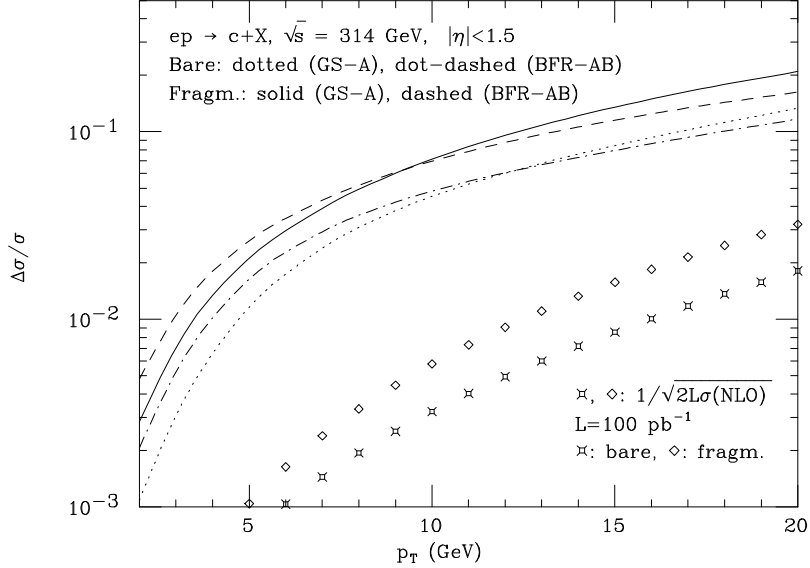


Figure 17: *Asymmetry cross section versus transverse momentum in polarized ep collisions (Weizsäcker-Williams approximation) at  $\sqrt{s} = 314$  GeV. The minimum observable asymmetry, computed at next-to-leading order, is also displayed.*

A rough estimate of the minimum value of the asymmetry observable at HERA can be obtained by requiring the difference between the numbers of events with parallel and antiparallel polarizations of the initial-state particles to be larger than the statistical error on the total number of observed events. This gives

$$\left[ \frac{\Delta\sigma}{\sigma} \right]_{min} \simeq \frac{1}{\sqrt{2\sigma\mathcal{L}\epsilon}}, \quad (3.19)$$

where  $\mathcal{L}$  is the integrated luminosity and the factor  $\epsilon$  accounts for the experimental efficiency for charm identification and for the fact that the colliding beams are not completely polarized. This procedure can be applied to total cross sections, as well as to differential distributions; in this case, the values of  $\sigma$  and  $\Delta\sigma$  have to be interpreted as *cross sections per bin* in the relevant kinematical variable.

In ref. [Frixione96b] it was shown that total cross section asymmetries for the point-like component are quite small in absolute value, and can be measured only if  $\epsilon$  is equal to or larger than 1% (0.1%), assuming  $\mathcal{L} = 100 \text{ pb}^{-1}$  ( $1000 \text{ pb}^{-1}$ ). Therefore, even with a vertex detector (see ref. [Eichler96]), it appears unlikely that this kind of measurements will be performed at HERA. Furthermore, in ref. [Stratmann96] a rough estimate of the hadronic contribution to the polarized cross section has been given, assuming polarized parton densities in the photon to vary between zero and the corresponding unpolarized densities in order to get a lower and an upper bound on

the cross section. It was found that a non-negligible contamination of the point-like result might indeed come from the hadronic process. The situation clearly improves when considering more exclusive quantities; in ref. [Frixione96b] it was found that at moderate  $p_T$  values the asymmetry for the point-like component can be rather large, well above the minimum observable value (in this region, the experimental efficiency is sizeable [Eichler96]); this is shown in fig. 17. In ref. [Stratmann96] it was argued that the hadronic component should have a negligible impact in this case.

We conclude that charm data in high-energy polarized  $ep$  collisions will help in the determination of the polarized gluon density of the proton, provided that the integrated luminosity and the experimental efficiencies will allow a study of at least single-inclusive distributions.

### 3.5.3 HERA-*B*

The HERA-*B* program will allow a detailed study of  $b$  production in proton–copper collisions, at  $\sqrt{S} = 39.2$  GeV. Since this energy is relatively close to threshold, one may worry about the presence of large soft gluon resummation effects. Large resummation effects were found in ref. [Kidonakis95]. In ref. [Catani96a] it was instead argued that these large effects have a spurious origin, and a properly performed resummation gives corrections of the order of 10%. This issue will be discussed in more detail in section 5. For example, from the NLO calculation with the MRSA' [Martin95] parton densities and  $m_b = 4.75$  GeV, we get  $\sigma_{b\bar{b}} = 10.5^{+8.2}_{-4.7}$  nb, a range obtained by varying the renormalization and factorization scales from  $m_b/2$  to  $2m_b$ . Thus the upper band is 80% higher than the central value, to be compared with a 10% increase from the resummation effects of ref. [Catani96a]. This result is much less dramatic than the results of ref. [Kidonakis95]. For completeness we report in table 2 cross section values obtained using different sets of structure functions, corresponding to different values of  $\Lambda_5^{\overline{\text{MS}}}$ , and to different values of the bottom quark mass. Observe that measurements of  $b$  cross sections in  $pN$  collisions at a beam energy of 800 GeV, close to the HERA-*B* regime, have been presented in refs. [Jansen95, Spiegel96]. These measurements (see fig. 2 in section 2) are consistent with the range reported in table 2.

## 4 HEAVY-QUARK PRODUCTION AT HADRON COLLIDERS

Hadron collisions are by far the largest source of heavy quarks available today. While the environment of high-energy hadronic interactions does not allow to trigger on the largest fraction of charm and bottom produced, the production rates are so large that the number of recorded events allows today  $b$ -physics studies that are competitive with those of  $e^+e^-$  experiments. The introduction of new experimental techniques, such as the use of silicon vertex detectors, which enable the tagging of events containing bottom quarks, led in the recent years to high-statistics and low-background measurements of the  $b$ -production properties over a large range of

$m_b$ (GeV)	MRS, $\alpha_s(M_Z) = 0.105$	MRSA'	MRS, $\alpha_s(M_Z) = 0.125$
4.5	$12.9^{+7.7}_{-5.1}$	$16.5^{+12.8}_{-7.3}$	$30.2^{+43.3}_{-16.6}$
4.75	$8.2^{+5.0}_{-3.3}$	$10.5^{+8.2}_{-4.7}$	$18.6^{+27.0}_{-10.2}$
5.0	$5.2^{+3.2}_{-2.1}$	$6.6^{+5.4}_{-3.0}$	$11.5^{+16.9}_{-6.3}$

Table 2: *Total cross sections in nb for bottom production at HERA-B. The central values correspond to  $\mu = m_b$ , upper and lower values to  $\mu = m_b/2$  and  $\mu = 2m_b$  respectively. The structure functions are those of refs. [Martin95, Martin95a].*

transverse momenta. The high energies and luminosities available at the Tevatron  $p\bar{p}$  collider, in addition to the enhanced  $b$ -tagging capability, have furthermore led to the discovery of the top quark [Abe94, Abe95, Abachi95], opening the way to a new set of tests of the heavy-quark production dynamics.

From the point of view of QCD studies, heavy-flavour production in high-energy hadronic collisions has better potentials than in fixed-target experiments. The  $b$  quarks produced at large  $p_T$  can be studied in perturbative QCD with smaller contamination from non-perturbative effects. For example, the impact of the initial-parton transverse momentum is largely reduced with respect to fixed-target charm production. Furthermore, the fragmentation properties of heavy flavours in high transverse momentum jets can be directly studied, since the transverse momenta involved are typically perturbative. Finally, top production should be fully perturbative, and therefore the ultimate testing ground for the theory of heavy-flavour hadroproduction.

In this section we review the current status of these measurements and their implications for the study of QCD. We discuss here first the phenomenology of charm and bottom production. We cover the inclusive production of  $b$  quarks,  $b$  hadrons, jets containing  $b$  and  $c$  quarks,  $b\bar{b}$  correlations, and we finally discuss the associate production of heavy flavours and electroweak gauge bosons. We then discuss the phenomenology of top-quark production. The large mass of the top quark implies that theoretical predictions based on NLO calculations should provide a rather accurate description of its inclusive production properties, with uncertainties in the range of 10%. The experimental statistics currently available cannot probe the theory at this level of accuracy, and significant improvements will only occur with the next round of data taking at the Tevatron and with the LHC. Nevertheless, the current data are an important step forward, and it is encouraging that they basically confirm the theoretical expectations.

## 4.1 Inclusive bottom production

### 4.1.1 Preliminaries

The distribution most commonly studied by the hadron-collider experiments is the  $b$ -quark differential  $p_T$  spectrum, integrated within a fixed rapidity range and above a given  $p_T$  threshold ( $p_T^{min}$ ):

$$\sigma(p_T^{min}) = \int_{|y| < y_{max}} dy \int_{p_T > p_T^{min}} dp_T \frac{d^2\sigma}{dy dp_T}. \quad (4.1)$$

The UA1 experiment at the CERN  $p\bar{p}$  collider used  $y_{max} = 1.5$ , while the CDF and D0 experiments at the Tevatron use  $y_{max} = 1$ . QCD calculations for this distribution are available at NLO [Nason89, Beenakker91].

In analogy to the case of fixed-target charm production, the study of NLO  $b$  cross sections indicates a strong dependence on the choice of factorization and renormalization scales. We show in fig. 18 this dependence at various values of  $p_T$  for the two energies  $\sqrt{S} = 630$  and  $1800$  GeV. Notice the growth of the cross sections at small scale values. Notice furthermore that for values of  $p_T^{min} < 40$  GeV the scale dependence at  $630$  GeV and  $1800$  GeV are approximately the same. The large scale dependence indicates that corrections of higher orders are significant both at  $630$  and at  $1800$  GeV. Above  $p_T^{min} = 40$  GeV, on the other hand, the scale dependence at  $630$  GeV is significantly reduced, suggesting a more reliable perturbative expansion.

In the following we will present results obtained by varying simultaneously  $\mu_R$  and  $\mu_F$  within the range<sup>8</sup>  $\mu_0/2 < \mu < 2\mu_0$  ( $\mu_0^2 = p_T^2 + m_b^2$ ), which represents an acceptable window within which to explore the scale dependence.

The uncertainty induced by the choice of different sets of parton density functions (PDF) is rather marginal, given the tight constraints set by the DIS and HERA data. One should, however, remember that the gluon density, which is the most important ingredient in  $b$  and  $c$  production at colliders, has not yet been measured directly for the values of  $x$  probed by the  $b$  measurements at CERN and at the Tevatron, approximately limited to the range  $0.01 < x < 0.1$ . As a standard set of parton densities we will choose here the MRSA' set [Martin95], for which  $\Lambda_5^{\overline{\text{MS}}\gamma} = 152$  MeV. It should be pointed out, however, that this value of  $\Lambda_5^{\overline{\text{MS}}\gamma}$  yields a value of  $\alpha_s$  significantly lower than that extracted from different observables [Barnett96]. Parton distribution fits have therefore also been performed with fixed values of  $\Lambda_5^{\overline{\text{MS}}\gamma}$  [Martin95a, Lai96]. To explore the dependence of our results on the choice of  $\alpha_s$ , we will also present results obtained using the PDF set MRS125 [Martin95a], which was extracted by forcing  $\alpha_s(M_Z) = 0.125$ . Notice that this procedure is not necessarily consistent, since the inconsistency in the extraction of  $\alpha_s$  is present in the data themselves. Should the future DIS measurements of  $\alpha_s$  become closer to the LEP value, as suggested by recent results [Harris96, Seligman97, Schmelling96], it is very likely that also the PDF fits, and with them our results, will change.

Given the large values of  $p_T$  probed by the collider experiments, the  $b$ -mass dependence of the theoretical result is small. We will choose as a default the value  $m_b = 4.75$  GeV, and allow for variations in the range  $4.5$  GeV  $< m_b < 5$  GeV.

---

<sup>8</sup>Unless otherwise specified we will always assume the renormalization and factorization scales to be equal, and will simply denote them by  $\mu$ .

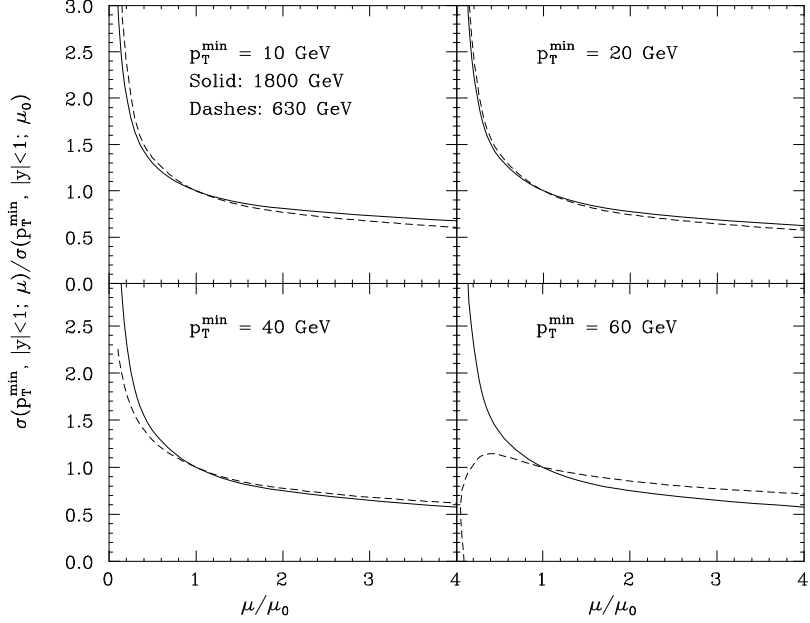


Figure 18: *Scale dependence of the integrated b-quark  $p_T$  distribution at 630 GeV (dashed lines) and at 1800 GeV (solid lines), for different values of  $p_T^{\min}$ .*

#### 4.1.2 The effect of higher-order corrections

The significant scale dependence of the NLO results for bottom production is a symptom of large contributions from higher orders. We briefly discuss here two possible sources of higher-order corrections: small- $x$  effects, possibly relevant in the low- $p_T$  domain, and large logarithms, which appear at high  $p_T$ .

The possibility that higher-order corrections at the Tevatron may be very large had been pointed out early on in ref. [Nason88]. One can show that, in the high-energy limit ( $\rho = 4m_Q^2/S \rightarrow 0$ ), large corrections arise to all orders in perturbation theory. The source of these large corrections is the presence, starting from  $\mathcal{O}(\alpha_s^3)$ , of diagrams where a gluon exchanged in the  $t$  channel becomes soft. In this limit, it is easy to show that the dominant behaviour of the Born and of the  $\mathcal{O}(\alpha_s^3)$  term are

$$\hat{\sigma}_{\text{Born}}(gg \rightarrow Q\bar{Q}) \stackrel{\hat{\rho} \rightarrow 0}{\propto} \frac{\alpha_s^2}{m_Q^2} \hat{\rho}, \quad (4.2)$$

$$\hat{\sigma}_{(3)}(gg \rightarrow Q\bar{Q}) \stackrel{\hat{\rho} \rightarrow 0}{\propto} \frac{\alpha_s^3}{m_Q^2}, \quad (4.3)$$

where  $\hat{\rho} = 4m_Q^2/\hat{s}$ . A crude but revealing estimate of the relative size of leading-order and higher-order terms can be obtained by assuming a simple form of the gluon

densities at small  $x$ , e.g.  $f(x) = A/x^{1+\delta}$ , with  $\delta < 1$ . It is easy to show that the total cross sections scale as follows:

$$\frac{\sigma_{(3)}(gg \rightarrow Q\bar{Q})}{\sigma_{Born}(gg \rightarrow Q\bar{Q})} \sim \begin{cases} \alpha_s \log \frac{1}{\rho} & (\text{if } \delta \log 1/\rho < 1) \\ \alpha_s \frac{1+\delta}{\delta} & (\text{if } \delta \log 1/\rho > 1) \end{cases} \quad (4.4)$$

Notice that in the Feynman scaling approximation (e.g.  $x g(x)$  constant at small  $x$ ), the  $\mathcal{O}(\alpha_s^3)$  correction is enhanced by a large logarithm of the ratio between the total hadronic CM energy and the heavy-quark mass. Logarithms of this type, also known as *small- $x$*  logarithms, arise at all orders of perturbation theory, and need to be resummed. The resummation theory for this class of corrections has been applied to the problem of heavy-flavour production in refs. [Ellis90, Collins91, Catani90, Catani91, Levin91]. The results contained in ref. [Collins91] indicate an enhancement of the NLO total bottom cross section at the Tevatron by no more than 30% due to the resummation of small- $x$  effects, the highest values being obtained with small- $\delta$  gluon densities. Naive reasoning based upon eq. (4.4) would lead to a similar pattern.

These results suggest that small- $x$  effects at the current collider energies are not large enough to justify discrepancies as large as those initially found at the Tevatron. Use of a gluon density more singular than  $1/x$ , such as for example recent parametrizations obtained from the HERA data, should reduce these effects even more.

Another class of potentially large higher-order corrections appears when  $b$  quarks are produced at high transverse momentum. At large momentum, in fact, the  $b$  quark behaves more and more like a massless particle, radiating an increasingly large amount of its energy in the form of hard, collinear gluons. This physical phenomenon is associated with the presence of logarithms of the form  $\log(p_T/m)$ , which appear at all orders in perturbation theory. This problem was already examined in ref. [Nason89]. Some logarithmically enhanced higher-order terms were estimated, and found to be negative and small up to transverse momenta of the order of 20 GeV.

Techniques are available to resum this class of logarithms. Two different groups have approached this problem in the recent past. Cacciari and Greco [Cacciari94] have folded the NLO cross section for production of a massless parton  $i$  ( $i = g, q$ ) [Aversa89] with the NLO fragmentation function for the transition  $i \rightarrow b$  [Mele90, Mele91]. The evolution of the fragmentation functions resums all terms of order  $\alpha_s^n \log^n(p_T/m)$  and  $\alpha_s^{n+1} \log^n(p_T/m)$ . All the dependence on the  $b$ -quark mass lies in the boundary conditions for the fragmentation functions. This approach ensures a full NLO accuracy, up to corrections of order  $m^2/(m^2 + p_T^2)$ . In particular, this formalism describes NLO corrections to the gluon splitting process, which in the  $\mathcal{O}(\alpha_s^3)$  calculation is only included at the leading order. One can verify, by looking at the Born-level production process as a function of the quark mass, that, in order for the mass corrections not to exceed the 10% level, it is necessary to limit the applications of this formalism to the region of  $p_T \gtrsim 20$  GeV.

Figure 19 shows the differential  $b$ -quark  $p_T$  distribution obtained in the fragmentation-function approach, compared to the standard fixed-order NLO result. Several features of this figure should be noticed. To start with, the scale dependence is significantly reduced with respect to the fixed-order calculation. Furthermore, in the range of applicability of this calculation (i.e.  $p_T \gtrsim 20$  GeV) the result of the fragmentation-function approach lies on the upper side of the fixed-order NLO calculation. The resummed calculation is, however, always within the uncertainty band of the fixed-order one. Finally, notice that the overall effect of the inclusion of higher-order logarithms is a steepening of the  $p_T$  spectrum, as is natural to expect.

Another calculation has recently appeared, by Scalise, Olness and Tung [Scalise96]. In this approach the authors employ a strategy developed in the case of DIS in refs. [Aivazis94, Aivazis94a]. Here initial- and final-state mass singularities are resummed as in the fragmentation-function approach, and the result is then matched in the low- $p_T$  region to the fixed-order NLO massive calculation. At large  $p_T$  this calculation does not include as yet, however, the full set of NLO corrections to the hard-process matrix elements.

The preliminary numerical results of this study [Scalise96] are consistent with those of the approach by Cacciari and Greco; in particular, they support the conclusion that in the  $p_T$  range explored by the Tevatron experiments the resummed results are consistent with the fixed-order ones, provided a scale  $\mu$  of the order of  $\mu_0/2$  or smaller is selected.

The fragmentation function formalism discussed so far can also be applied to high transverse momentum charm-meson production [Cacciari96b].

#### 4.1.3 Comparison with experimental results

The comparison of the final experimental data from UA1 [Albajar91] with theory is shown in fig. 20. The data are (approximately) a factor of 2 higher than the central prediction. Good agreement can be obtained by selecting the largest theoretical prediction.

Initially, the comparison with the Tevatron data led to pessimistic conclusions on the capability of NLO QCD to describe the data. Limited statistics in the channels with fully reconstructed  $b$ -meson decays [Abe92a], and the insufficient theoretical understanding of the  $J/\psi$  production mechanisms, which was required at that time for the extraction of the  $b$  cross section from the measurement of inclusive  $J/\psi$ 's [Abe92b, Abe93b], led to evidence that the production rate of  $b$  quarks exceeded by several times the one predicted by NLO QCD. The disagreement with theory was less pronounced in the case of higher-statistics measurements using semileptonic  $b$  decays [Abe93, Abe93a], which however probe production at  $p_T$  values higher than those based on exclusive and  $J/\psi$  decays.

The analysis of the large data samples accumulated during the Tevatron data taking of 1992–93 has recently been completed, and the first results from the data

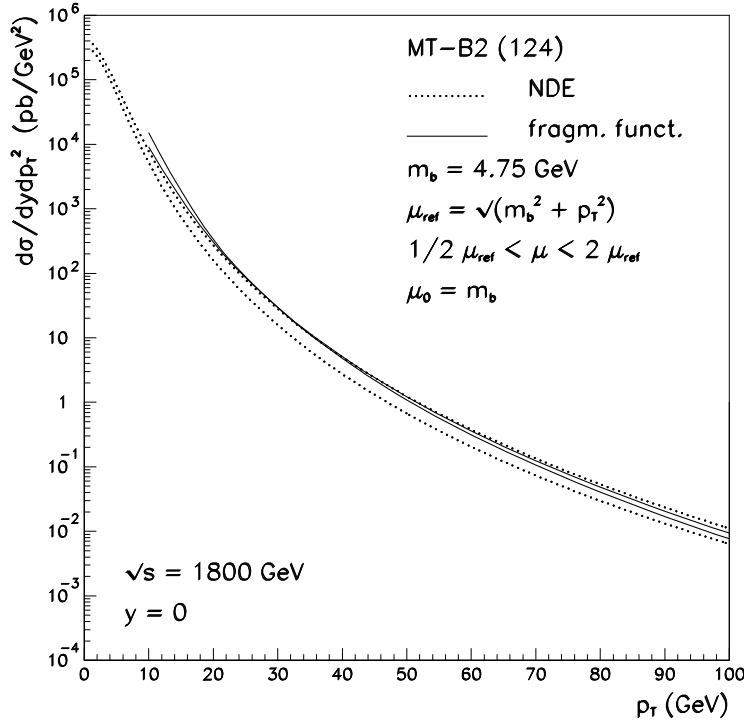


Figure 19: *Differential  $b$ -quark  $p_T$  distribution: comparison of the fixed-order NLO calculation (NDE stands for [Nason88]) with the fragmentation-function approach [Cacciari94];  $\mu_0$  is the scale at which the boundary conditions for the fragmentation functions are set.*

of the 1994–96 run are being released. This wealth of data and the improved detection capabilities offer today a rather precise picture of inclusive  $b$  production at 1800 GeV. The CDF experiment primarily used its silicon vertex detector to improve the background rejection in the reconstruction of fully exclusive  $b$ -hadron decays and to separate the  $J/\psi$ 's coming from  $b$  decays from those promptly produced, thus eliminating an important source of systematic error. The measurement of fully reconstructed  $b$ -hadron decays also allows a precise determination of the differential  $p_T$  spectrum of  $b$  hadrons, free of the uncertainties related to the modelling of fragmentation and decay. The experiment D0 exploited its low muon backgrounds to extend the measurement of the  $b$  spectrum to high values of  $p_T$  [Abachi95a], as well as using dimuon pairs [Abachi96, Abachi96a] and forward muons for a measurement of small-angle  $b$  production [Abachi96b].

The results obtained by the two collaborations are shown in figs. 21 and 22, compared with the theoretical predictions.

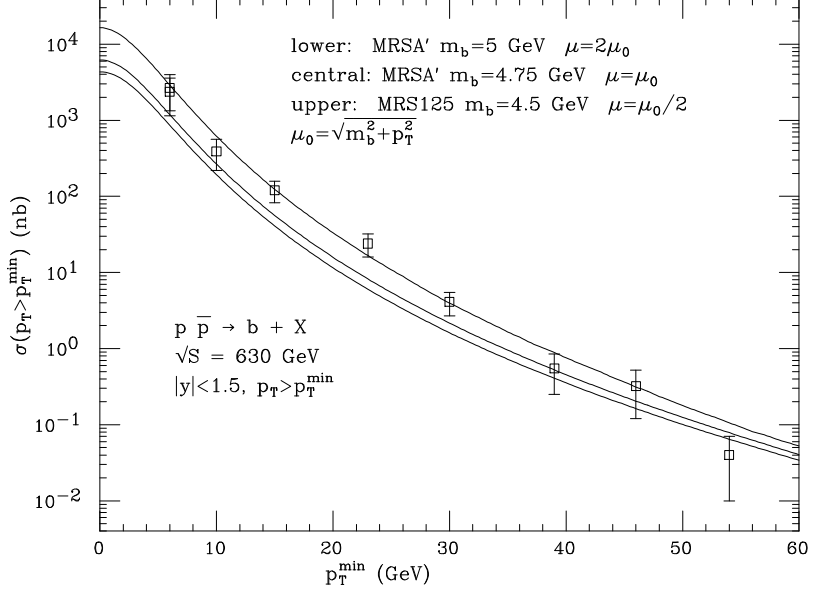


Figure 20: *UA1 data on the integrated b-quark  $p_T$  distribution, compared to the results of NLO QCD.*

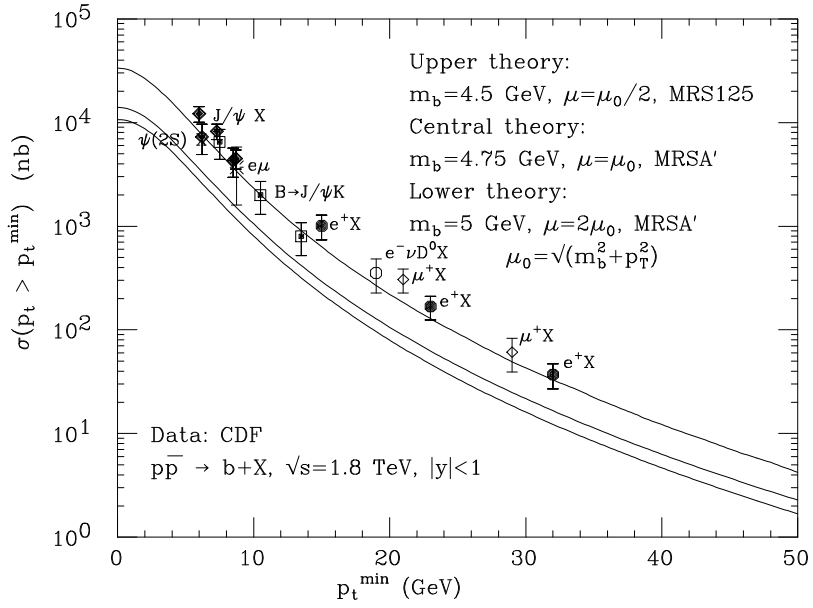


Figure 21: *CDF data on the integrated b-quark  $p_T$  distribution, compared to the results of NLO QCD.*

For an easier evaluation of the results, we present them on a linear scale in the form Data/Theory in fig. 23, where we include the UA1 data as well. We divided

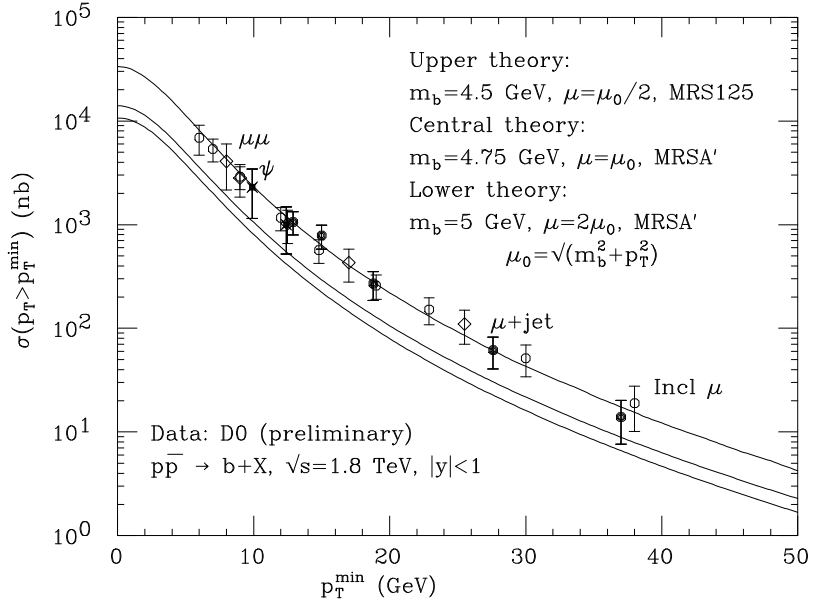


Figure 22: *D0 data on the integrated  $b$ -quark  $p_T$  distribution, compared to the results of NLO QCD.*

the data by our central theoretical prediction. The dot-dashed straight lines are constant fits to the ratios, weighed by the inverse of the experimental uncertainties. For comparison, we also include the upper and lower theoretical curves divided by the central one (solid lines).

The first important thing to notice is that, independently of the chosen input parameters, the shape of the theoretical curves agrees very well with the data. Secondly, it must be pointed out that the results at  $\sqrt{S} = 630$  GeV are consistent with those at  $\sqrt{S} = 1800$  GeV. The average ratio Data/Theory measured by UA1 differs by less than 10% from the ratio measured by D0, independently of the input parameters chosen. The difference is between 40 and 50% if one uses the CDF data. If we naively average the Tevatron data, we conclude that the relative discrepancy between theory and data when changing the value of  $\sqrt{S}$  from 630 to 1800 GeV is about 30%, a number of the same order as the estimate of small- $x$  effects.

Independently of the beam energy, the data are higher by a factor of about 2 than the default prediction based on  $\mu = \mu_0$ . They are, however, well reproduced by the upper theoretical curve. Therefore, while the overall uncertainty of the theoretical prediction due to the scale choice is large, there is currently no inconsistency between theory and data for the inclusive  $p_T$  distribution of  $b$  quarks at the Tevatron. The 30% discrepancy between the results of CDF and D0 is comparable to the discrepancy between the extrapolation of the UA1 data to CDF, while UA1 and D0 data agree at the level of 10%.

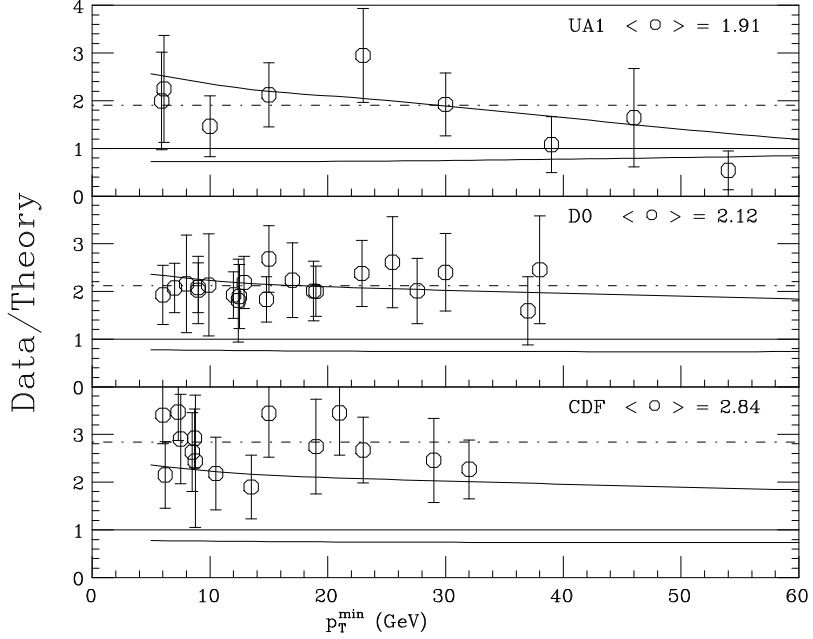


Figure 23: *Linear comparison between experimental data and theory for the integrated  $b$ -quark  $p_T$  distribution. See the text for details.*

Recently, new data on  $b$  production at 630 GeV have been presented by CDF [Abe96a]. The measurement was performed during a special Tevatron run at  $\sqrt{S} = 630$  GeV, using large-impact-parameter muons from  $b$ -meson decays. The measurement was compared with a similar one carried out at  $\sqrt{S} = 1800$  GeV, to reduce common systematic errors. The preliminary result of this study is:

$$\frac{\sigma_b(p_T > 9.5 \text{ GeV}, |y| < 1, \sqrt{S} = 630 \text{ GeV})}{\sigma_b(p_T > 9.5 \text{ GeV}, |y| < 1, \sqrt{S} = 1800 \text{ GeV})} = 0.193 \pm 0.025 \text{ stat} \pm 0.023 \text{ syst} . \quad (4.5)$$

To compare this result with a theoretical expectation, we have to choose the scales to be used at the two different energies. While there is no theorem on how to do this, it is however reasonable to choose the scales to be the same. This can be partly justified by the similarity of the scale dependence at the two energies, shown in fig. 18. Assuming  $\mu(630) = \mu(1800) = \mu_0$  and using MRSA' parton densities, we find a theoretical ratio of  $0.189 \pm 0.012$ . The theoretical error is obtained by varying  $\mu$  in the range  $\mu_0/2 < \mu < 2\mu_0$  and  $m_b$  in the range  $4.5 \text{ GeV} < m_b < 5 \text{ GeV}$ . The ratio  $(\text{Data/Theory})(630)/(\text{Data/Theory})(1800)$  measured by CDF is therefore equal to  $1.0 \pm 0.2$ . This is a very important measurement, because a large fraction of the systematic uncertainties present in the individual measurements cancel out in the ratio. This result indicates that possible sources of corrections to the theoretical calculations (e.g. higher-order corrections, small- $x$  effects) should have the same impact at 630 and at 1800 GeV. One would reach the same conclusion by comparing

the results of UA1 and D0, although the comparison of the systematic errors is in this case more complex.

A recent measurement by D0 [Abachi96b], using muonic semileptonic decays of  $b$  quarks, explored the production of  $b$  quarks in the forward region ( $2.4 < |y^\mu| < 3.2$ ). The results, shown in fig. 24, indicate a rate in excess by a factor of approximately 4 over the central theoretical prediction. The large samples collected at 1800 GeV have

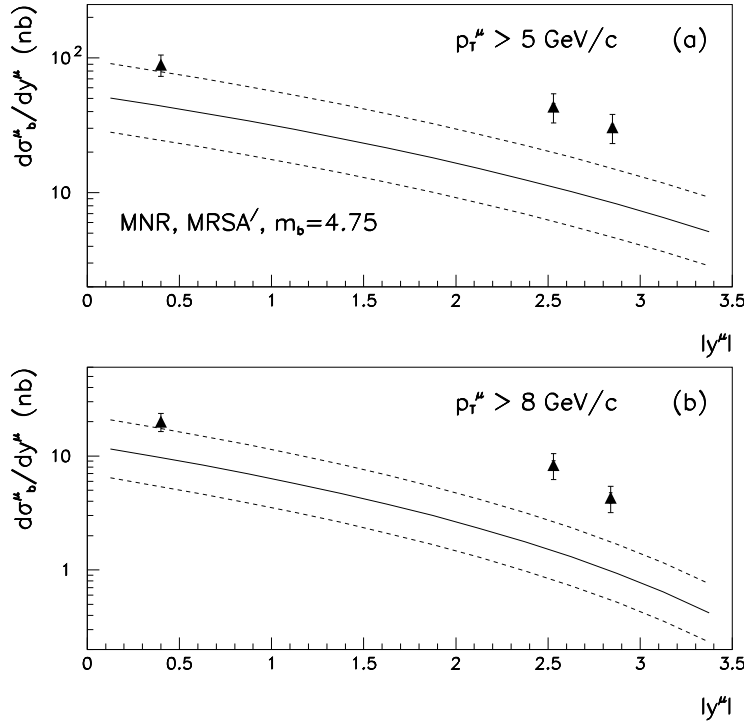


Figure 24: Comparison between D0 data and theory for the  $p\bar{p} \rightarrow (b \rightarrow \mu) + X$  cross section at large rapidity.

also allowed a measurement of the differential  $p_T$  spectrum of fully reconstructed  $B$  mesons. CDF performed this measurement by detecting several hundreds of events in the final states  $B \rightarrow J/\psi K^{(*)}$  [Abe92a, Abe95a, Abe96f]. The full reconstruction of the final state allows a precise measurement of the hadron momentum, therefore providing a direct measurement of the differential  $p_T$  spectrum. The systematic errors due to the modelling of the  $b$ -hadron decays are significantly reduced relative to the measurements in the inclusive channels. The comparison with the NLO QCD calculations, however, still requires a description of the  $b$ -quark to  $b$ -hadron fragmentation function. The NLO calculation of the  $b$ -quark  $p_T$  distribution contains the effects of final-state gluon radiation, although limited to the emission of one gluon. As was

done in the fixed-target section, we then fold the NLO quark  $p_T$  spectrum with a phenomenological parametrization of the non-perturbative quark-to-hadron transition. We use the so-called Peterson fragmentation function [Peterson83], already described in section 2. For the parameter  $\epsilon$  that defines the shape of the distribution we choose the value  $\epsilon_b = 0.006 \pm 0.002$  [Chrin87]. We furthermore assume that the fraction of  $b$  quarks that fragments into the hadron species identified in the experimental analyses ( $B_{u,d}$ ) is 75%, a number supported by recent direct measurements [Abe96c].

Figure 25 shows the latest CDF data [Abe96f], compared to the NLO QCD predictions. The ratio Data/Theory is consistent with that found in the inclusive measurements, with the possible exception of the point at the lowest  $p_T$ , which is higher than expected. It is premature to conclude whether this is just a statistical fluctuation, or whether this is a sign of small- $x$  effects.

As in the case of charm production at fixed target, we should comment here that the use of the Peterson fragmentation function might not be justified in the context of hadroproduction of heavy quarks. As a simple observation, we point out here that while the measurement of heavy-quark spectra in  $e^+e^-$  data is mostly sensitive to the first moment of the fragmentation function, corresponding to the average jet energy carried by the heavy hadron, the  $p_T$  distributions in hadronic collisions are sensitive to higher moments of the non-perturbative fragmentation function. In fact, assuming for simplicity a perturbative  $p_T$  spectrum of the form:

$$\frac{d\sigma}{dp_T} = \frac{A}{p_T^n} , \quad (4.6)$$

it is easy to prove that the resulting hadron spectrum, after convolution with a given fragmentation function  $f(z)$ , will be given by:

$$\frac{d\sigma}{dp_T} = \frac{A}{p_T^n} \times \int dz z^{n-1} f(z) . \quad (4.7)$$

In the case of the Tevatron,  $n$  turns out to be approximately 5. It is not unlikely, therefore, that alternative models for the non-perturbative fragmentation of heavy quarks, which could equally well fit the  $e^+e^-$  data, could give rise to significant differences when applied to production in hadronic collisions. We also remark that the gluon component of the fragmentation function is not important in  $e^+e^-$  physics, while it may be crucial in hadroproduction.

To display the size of the hadronization corrections induced by the Peterson fragmentation, we also include in fig. 25 the  $b$ -quark  $p_T$  distribution. Notice that, neglecting the lowest- $p_T$  point, both shape and normalization of the data are well described by the central theoretical prediction without fragmentation.

We summarize the main conclusions of the studies presented in this section:

1. There is good agreement between the shape of the  $b$ -quark  $p_T$  distribution predicted by NLO QCD and that observed in the data for central rapidities.

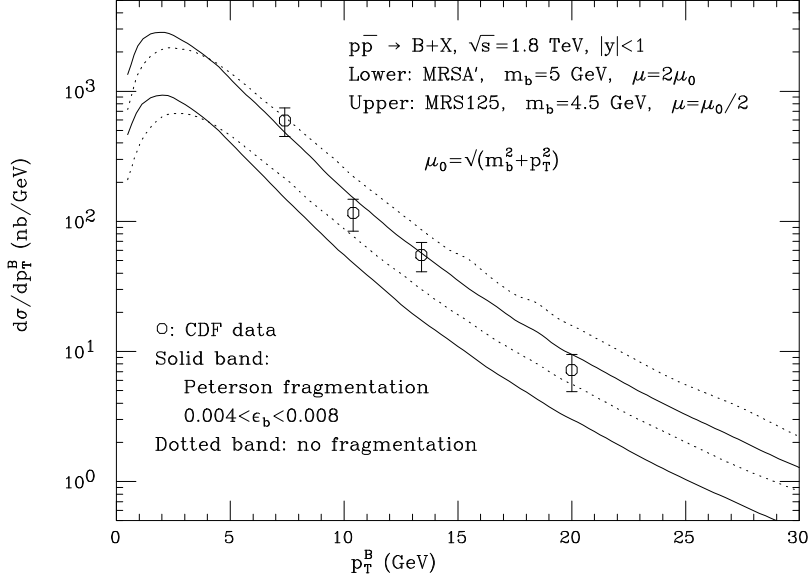


Figure 25: Comparison between CDF data and theory for the differential  $B$ -meson  $p_T$  distribution.

2. Although the data are higher by a factor of approximately 2 with respect to the theoretical prediction with the default choice of parameters, extreme (although acceptable) choices of  $\Lambda_5^{\overline{\text{MS}}}$  and of renormalization and factorization scales bring the theory in perfect agreement with the data of UA1 and D0, and within 30% of the CDF measurements.
3. The choice of low values of  $\mu_R$  and  $\mu_F$  is favoured by studies of higher-order logarithmic corrections.
4. There is a difference at the level of 30% between the measurements of CDF and D0 at 1800 GeV, and between CDF and UA1 at 630 GeV.
5. The CDF measurements at 630 and 1800 GeV indicate that theory correctly predicts the scaling of the differential  $p_T$  distribution between 630 and 1800 GeV, a fact that had often been questioned in the past and now finds strong support.
6. Forward production of  $b$  quarks indicates a larger discrepancy between theory and data.
7. More theoretical studies should be devoted to the understanding of the non-perturbative fragmentation function for heavy quarks. As already stressed in the section on fixed target, there is no firm evidence, either theoretically or experimentally, that the standard Peterson parametrization is well suited for the description of the hadroproduction data.

## 4.2 $b\bar{b}$ correlations

Studies of the one-particle inclusive distributions are a benchmark test of QCD. However, these tests do not probe all of the important features of the production mechanism. In several cases the correlations between the quark and the antiquark can provide additional important information. We already discussed how, in the case of fixed-target charm production, the shape of the azimuthal correlations between the  $c$  and  $\bar{c}$  quarks is sensitive to the amount of intrinsic transverse momentum carried by the partons in the hadron. Given the large mass of the  $b$  quark and the large  $p_T$  values at which  $b$ 's are probed in hadronic collisions, these effects should be negligible. However, one could observe similar behaviours induced by the build-up of large transverse momentum due to the perturbative evolution of the initial state (i.e. multi-gluon emission). This phenomenon would be even more pronounced at small  $p_T$  and in the presence of important small- $x$  effects.

The knowledge of heavy-quark correlations is also an important element in the study of detector acceptances and detection systematics. For example, in studies of  $b$  tagging in samples where both  $b$ 's have been tagged, it is important to know what the correlations between the  $b$  and  $\bar{b}$  momenta are, since the tagging efficiency depends on the  $b$  momentum. These studies have implications on the determination of tagging efficiencies for a multitude of important measurements, from the study of top production [Abe94] to the study of  $R_b$  [Nason96].

The study of  $b\bar{b}$  correlations in hadronic collisions was pioneered by UA1 [Geiser92, Albajar94, Albajar96]. For these measurements they used their sample of high-mass and non-isolated dimuon events. The shapes of the  $\Delta\phi$  and  $\Delta R$  distribution for the data are both in good agreement with the theoretical expectations [Albajar94]. The rate is approximately 30% higher than the central value of the theoretical predictions, a result consistent with the UA1 determination of the inclusive cross section. They also separated the sample of dimuon events into two classes, defined by two-body and three-body topologies. Contributions to the three-body topology come from events with hard-gluon bremsstrahlung, and are therefore proportional to  $\alpha_s^3$ . Two-body final states, with the  $b$  and the  $\bar{b}$  almost back-to-back, are dominated by Born-like processes, and their rate is of  $\mathcal{O}(\alpha_s^2)$ . A comparison between the two samples, carried out as a function of the  $p_T$  of the  $b$  quark, allowed UA1 to study the dynamical evolution of  $b\bar{b}$  correlations and to extract the value of  $\alpha_s(M_Z) = 0.113^{+0.007}_{-0.006}{}^{\text{exp}}{}^{\text{+0.008}_{-0.009}{}^{\text{th}}}$  [Albajar96]. The same study led to a  $3\sigma$  evidence for the running of  $\alpha_s$ .

CDF presented their first study of  $b\bar{b}$  correlations using a sample of  $e\mu$  pairs [Abe94a]. Once again, good agreement was found between the shape of the data and the QCD expectations. A second measurement has been recently reported by CDF, using muons plus tagged  $b$  jets [Abe96b]. The shape of the  $\Delta\phi$  distribution is in reasonable agreement with QCD, while the distributions of the jet  $E_T$  and of the muon  $p_T$  are not (see fig. 26).

Contrary to the case of  $c\bar{c}$  correlations measured in fixed-target experiments, the measurement at hadron colliders is sensitive to the modelling of the heavy-quark

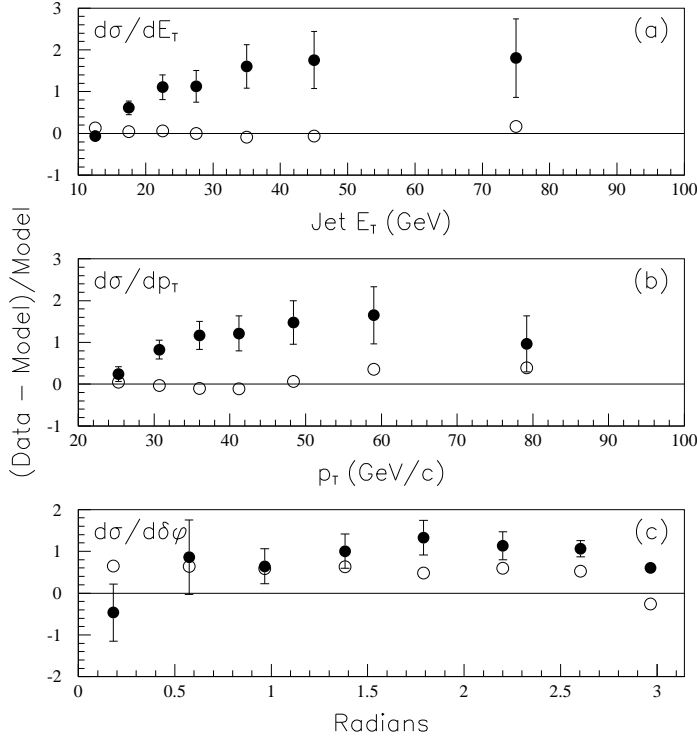


Figure 26: *CDF results on the  $b\bar{b}$  correlations using  $\mu+b$ -tagged jet final states [Abe96b], compared to NLO QCD. Solid points correspond to the default theoretical prediction, with scales  $\mu = \mu_0$ , empty circles correspond to the difference between the choice  $\mu = \mu_0/2$  and  $\mu = \mu_0$ .*  
*Top figure: tagged-jet  $E_T$  distribution. Central: muon  $p_T$  spectrum. Bottom: azimuthal correlations.*

fragmentation, because of possible trigger biases. A harder (softer) fragmentation function would enhance (decrease) the efficiency for the detection of the softest of the two  $b$  quarks. These effects could have an impact on the distributions reported in this study by CDF. This collaboration explored the effects of changes in the  $\epsilon_b$  parameter within the Peterson fragmentation model, finding them negligible. As we argued earlier, it cannot be excluded that a systematic study of other possible parametrizations for the fragmentation modelling could lead to significant effects. Also the possible effects of the  $k_T$  kick have been studied by CDF [Abe96b], with the conclusion that not even an average  $k_T$  as large as 4 GeV could improve the agreement between theory and data for the measurements considered.

Both CDF and D0 recently presented studies based on samples of high-mass dimuons [Abe96d, Abachi96a]. The shapes for both  $\Delta\phi$  and  $p_T^b$  for a given  $p_T^b$  are well reproduced by theory, within the large uncertainties, while there is a normalization discrepancy relative to the central predictions (fig. 27).

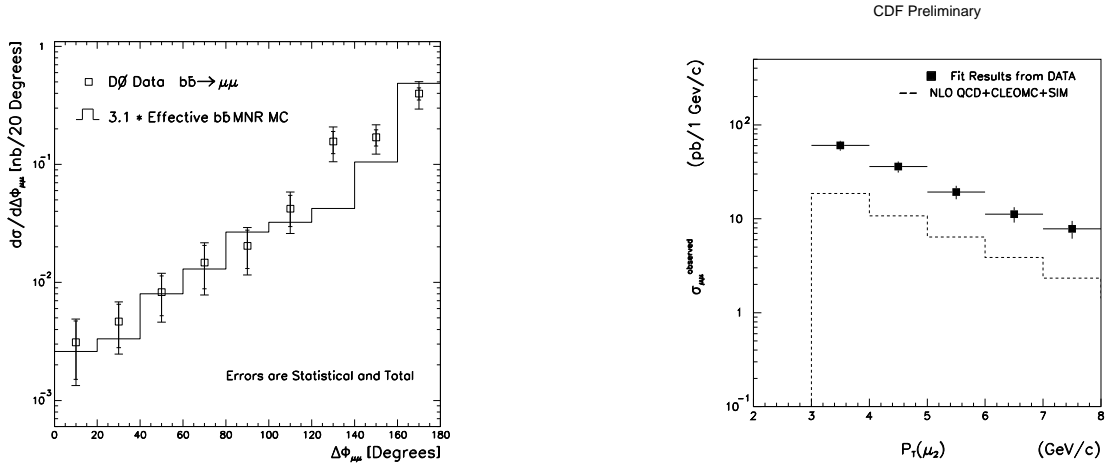


Figure 27: *Results on  $b\bar{b}$  correlations using dimuon final states, compared to NLO QCD. Left: azimuthal-correlation results from D0. Right:  $p_T$  distribution of the slowest muon from CDF.*

In conclusion we can say that, overall, there are good indications that NLO QCD correctly describes the correlations between  $b$  pairs produced in hadronic collisions. Most of the large theoretical systematics present in the case of fixed-target charm production are not relevant here. The discrepancies observed in the CDF measurement using the muon+tagged-jet final states, however, indicate that there still is a possible interplay between the theoretical and experimental systematics, which is not entirely understood as yet.

### 4.3 Heavy-quark jets in perturbative QCD

#### 4.3.1 Preliminaries

An interesting way of understanding the production mechanism of heavy flavours is to consider the cross section of jets that contain a heavy quark (in short: heavy-quark jets) [Frixione96]. The main difference between the study of a heavy quark and of a heavy-quark jet is that in the former we are interested in the momentum of the quark itself, regardless of the properties of the event in which the quark is embedded, while in the latter we are interested in the properties of a jet containing one or more heavy quarks, regardless of the momentum fraction of the jet carried by the quark. A priori it is expected that variables such as the  $E_T$  distribution of a heavy-quark jet should be described by a finite-order QCD calculation more precisely than the  $p_T$  distribution of open quarks. This is because the large logarithms  $\log(p_T/m_b)$  arising from the emission of collinear gluons from the heavy quark cancel in this case. Furthermore, the experimental measurement of the  $E_T$  distribution of heavy-quark jets does not depend on the knowledge of the heavy-quark fragmentation functions, contrary to the

case of the  $p_T$  distribution of open heavy quarks. Experimental systematics, such as the knowledge of decay branching ratios for heavy hadrons or of their decay spectra, are also largely reduced.

The calculation of the heavy-quark jet rate is very similar to the one of the generic jet cross section. Two important differences have nevertheless to be stressed: by its very definition, a heavy-quark jet is not flavour-blind; one has to look for those jets containing a heavy flavour. Furthermore, the mass of the heavy flavour is acting as a cutoff against final-state collinear divergences. This in turn implies that the structure of the singularities of the heavy-quark jet cross section is identical to that of the open-heavy-quark cross section. The heavy-quark jet cross section at NLO can therefore be written in the following way, which implicitly defines  $d\Delta/dE_T$  (this term will be denoted in the following as the “jet-like” component of the cross section)

$$\frac{d\sigma}{dE_T} = \frac{d\sigma^{(open)}}{dE_T} + \frac{d\Delta}{dE_T}, \quad (4.8)$$

where  $d\sigma^{(open)}/dE_T$  is the open-heavy-quark cross section. Observe that  $d\Delta/dE_T$  has no contributions at the Born level. Gluon-radiation effects start contributing to it at order  $\alpha_s^3$ . Normally the heavy-quark jet is defined by a cone algorithm. In our phenomenological applications, we will use the Snowmass convention [Huth91], whereby particles are clustered in cones of radius  $R$  in the pseudorapidity–azimuthal angle plane. One then requires that the  $b$  quark be inside the jet. At the NLO, the heavy-quark jet can be the heavy quark, or it can contain the heavy quark and the light parton, or the heavy quark and the heavy antiquark. In other words, there is the possibility to cluster more than one parton to get the heavy-quark jet, which will be eventually observed. It turns out that, if the jet definition is appropriately infrared-safe, all the subtractions needed to get an infrared-safe result are contained in the term  $d\sigma^{(open)}/dE_T$ . This is shown in details in ref. [Frixione96]. This result is however quite intuitive. In fact, singularities arise because of radiation collinear to the incoming partons, which cannot enter the jet cone, or to soft radiation, which does not sensibly alter the jet  $E_T$ .

#### 4.3.2 The structure of heavy-quark jets at the Tevatron

We present in this section some results of interest for the Tevatron collider [Koehn95]. We consider jets produced within  $|\eta| < 1$ , in order to simulate a realistic geometrical acceptance of the Tevatron detectors. We will use the parton distribution set MRSA' [Martin95a]. Our default values of the parameters entering the calculations are  $m_c = 1.5$  GeV,  $m_b = 4.75$  GeV and  $\mu_R = \mu_F = \mu_0 \equiv \sqrt{E_T^2 + m_Q^2}$ . In practice, since we will consider jets of energy much larger than the heavy-quark mass, the dependence of our results upon the mass value is almost negligible. We will therefore study only the uncertainties associated with the choice of renormalization and factorization scales.

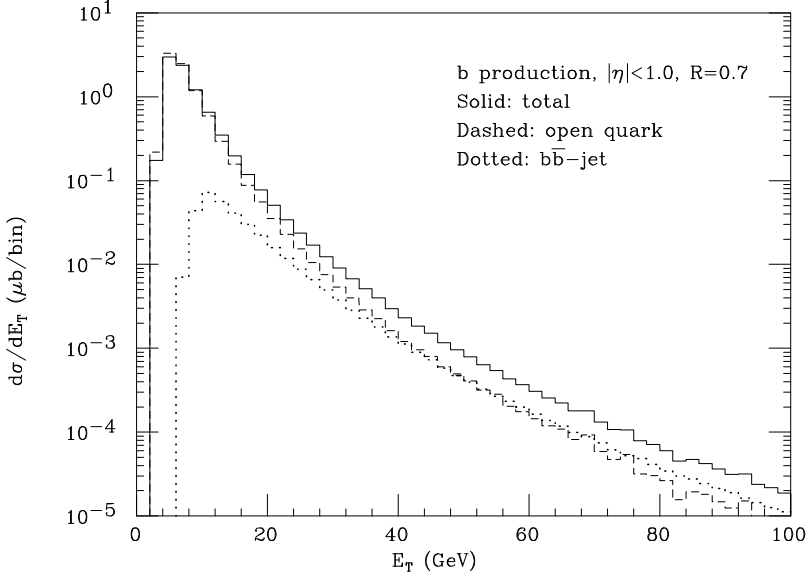


Figure 28:  $b$  jet inclusive  $E_T$  distribution in  $p\bar{p}$  collisions at 1.8 TeV, for  $|\eta| < 1$ ,  $R = 0.7$  and  $\mu_F = \mu_R = \mu_0$  (solid line). For comparison, we also show the open-quark inclusive  $E_T$  distribution (dashed line). The component of the jet-like contribution due to jets containing both  $b$  and  $\bar{b}$  is represented by the dotted line.

Figure 28 shows the prediction for the  $E_T$  distribution of  $b$  jets at the Tevatron for  $R = 0.7$ . For the purpose of illustration, the open-quark component is presented separately. It is apparent that the jet-like component becomes dominant as soon as  $E_T$  becomes larger than 50 GeV. It can be shown [Frixione96] that this value depends significantly on the cone size, being equal to 25 and 100 GeV for  $R = 1$  and 0.4 respectively. Also, for a fixed  $R$ , the value of  $E_T$  at which the jet-like component becomes dominant is smaller for  $c$  jets than for  $b$  jets. This is in agreement with naive expectations. The relative probability of finding a heavy-quark pair inside a high- $E_T$  gluon scales in fact like  $\log(E_T/m_Q)$  [Mueller85, Mueller86, Mangano92, Seymour95].

We also show the part of the jet-like component due to jets including the  $b\bar{b}$  pair (we will call these  $b\bar{b}$  jets). The figure suggests that for this  $E_T$  range and with  $R = 0.7$  this is the dominant part of the jet-like component. This is consistent with the expectation that, for large enough  $E_T$ , and provided that the majority of the final-state generic jets are composed of primary gluons, heavy-quark jets are dominated by the process of gluon splitting, with the jet formed by the heavy-quark pair. As we will show later, the situation changes at higher values of  $E_T$  where heavy quarks are mostly produced via the  $s$ -channel annihilation of light quarks.

The left-hand side of fig. 29 presents the theoretical prediction for the absolute  $b$ -jet rate at  $E_T = 50$  GeV versus the cone size, for different choices of the factorization

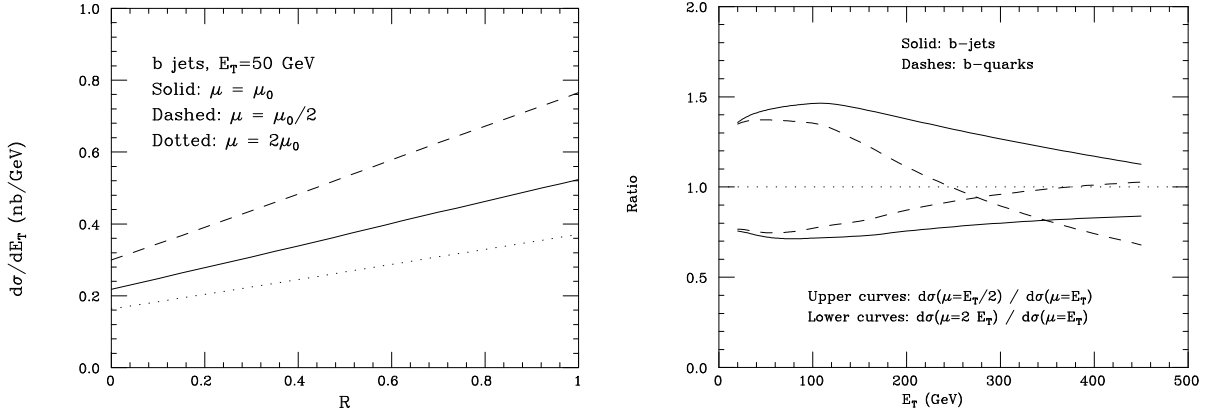


Figure 29: *Left:*  $b$  jet inclusive  $E_T$  rate, as a function of the cone size  $R$ , at  $E_T = 50$  GeV and for various scale choices ( $\mu_R = \mu_F \equiv \mu$ ). *Right:* Scale dependence of the  $b$ -jet  $E_T$  distribution ( $R = 0.4$ , solid lines) and of the open-quark inclusive  $E_T$  distribution (dashed lines).

and renormalization scales. The cross section at  $R = 0$  is well defined, and it is equal to the open-bottom cross section. This should be contrasted with the case of generic jets, in which the cross section at  $R = 0$  is not well defined, being negative at any fixed order in perturbation theory [Aversa89, Aversa90a, Ellis89S, Ellis90S]. Completely analogous results hold in the case of  $c$ -jet production. The right-hand side of fig. 29 shows the scale dependence of the  $b$ -jet cross section ( $R = 0.4$ ) as a function of  $E_T$ , for values up to 450 GeV.

The strong scale dependence exhibited by the absolute rate at low and moderate  $E_T$  values is of the same size as the one present in the inclusive  $p_T$  distribution of open bottom quarks. This scale dependence is usually attributed to the importance of the gluon splitting contribution. One therefore expects that, in a regime where the gluon-splitting contribution is suppressed by the dynamics, the scale dependence should be milder. We will show later that this suppression does indeed take place for high transverse energies. This explains why, in the high- $E_T$  region, the scale dependence is indeed reduced to the value of 20% when the scale is varied in the range  $\mu_0/2 < \mu < 2\mu_0$ , a result consistent with the limited scale dependence of the NLO inclusive-jet cross sections [Aversa89, Aversa90a, Ellis89S, Ellis90S]. In spite of the strong scale sensitivity at the smaller values of  $E_T$ , it is reasonable to expect that the ratio of the  $b$ - and  $c$ -jet rates be a stable quantity under scale variations. It can be shown [Frixione96] that this is indeed the case: by taking  $\mu_0/2 < \mu < 2\mu_0$  the ratio changes at most by 10% with respect to the default prediction; furthermore, the ratio of  $b$  to  $c$  jets is more stable than the one of  $b$  to  $c$  quarks.

Of direct interest for studies of heavy-flavour tagging and for searches of possible new physics is the fraction of heavy-quark jets relative to generic jets. This is also in principle the most straightforward measurement from the experimental point of

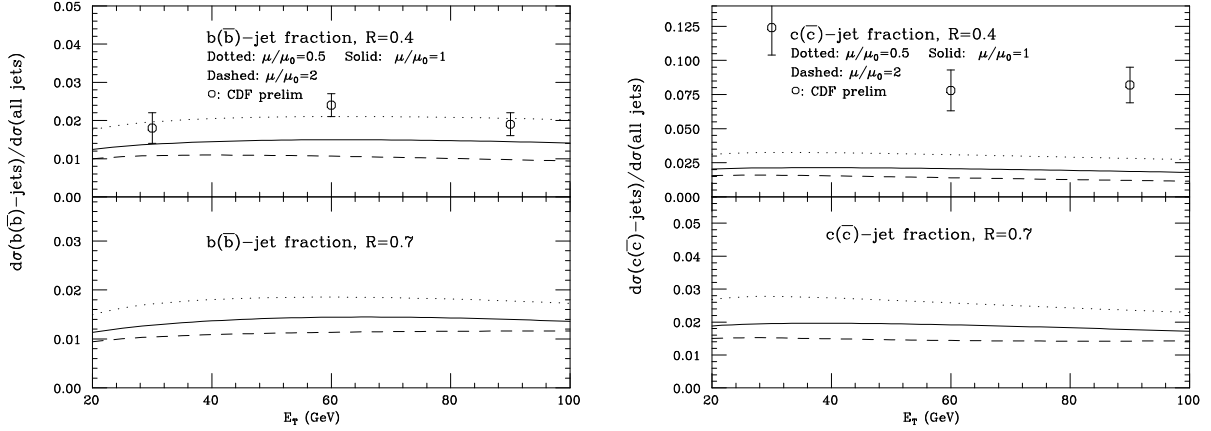


Figure 30: *Ratio of the heavy-quark jet (for bottom, left, and charm, right) to inclusive-jet  $E_T$  distributions, for different choices of renormalization and factorization scales ( $\mu_R = \mu_F \equiv \mu$ ), for  $R = 0.4$  (top) and  $R = 0.7$  (bottom). The data points for  $R = 0.4$  represent preliminary results from the CDF experiment, for which only the statistical uncertainty is shown.*

view. We present in fig. 30 the ratio of the heavy-quark jet to the inclusive-jet  $E_T$  distributions [Aversa89, Aversa90a, Ellis89S, Ellis90S] for bottom (left) and charm (right). The inclusive-jet  $E_T$  cross section used here was calculated with the JETRAD program [Giele94], using the same choices of parton densities and  $(\mu_R, \mu_F)$  that were adopted for the  $b$ -jet and  $c$ -jet calculations. Contrary to the figures presented so far, which showed results for the heavy quark only (i.e. no antiquark contribution), we adopt for this figure the prescription used in the definition of the data presented by CDF [Koehn95]. The  $Q$ -jets are defined there as jets containing either a  $Q$  or a  $\bar{Q}$  quark, jets containing both being counted only once. We will call these  $Q(\bar{Q})$  jets. This distribution can be obtained by subtracting the contribution of  $Q\bar{Q}$  jets from twice the total  $Q$ -jet rate.

It is interesting to notice that, as far as  $b$  production is concerned, there is a good agreement between the CDF data and the theoretical prediction obtained with  $\mu_R = \mu_F = \mu_0/2$ ; this choice of scale is also supported by the inclusive-jet  $E_T$ -spectrum data [Abe92, Abe96, Blazey96]. This is particularly significant since the choice of scale for the heavy-quark jet cross section is not independent from the scale chosen to predict the open-heavy-quark one (see eq. (4.8)). On the other hand, to get a satisfactory description of the data for the open-bottom  $p_T$  spectrum, smaller scale values (of the order of  $\mu_0/4$ ) or larger  $\Lambda_{QCD}$  values (compatible with LEP measurements) have to be chosen [Frixione94, Frixione96a]. Should this situation persist when additional data on  $b$  jets will become available, it would indicate an inconsistency in describing two phenomena due to the same underlying physics. The poor understanding of the

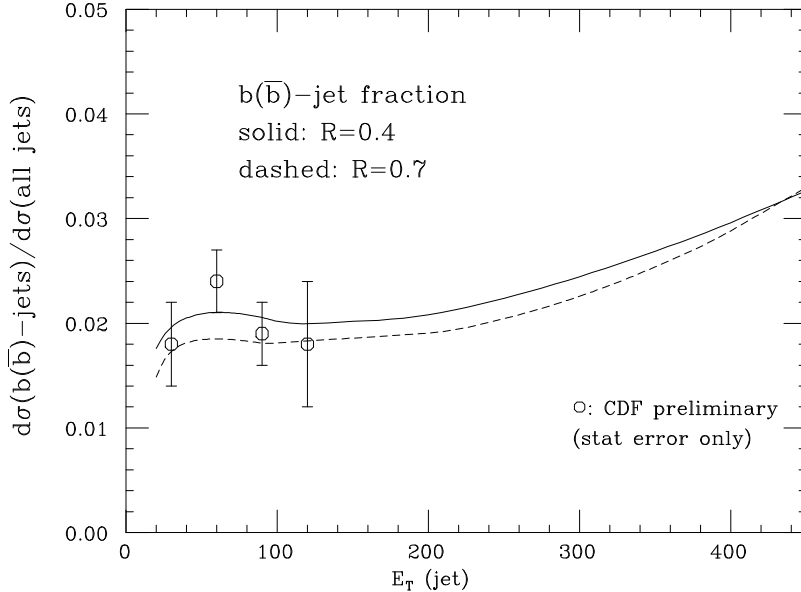


Figure 31: *Ratio of the  $b(\bar{b})$  jet to inclusive-jet  $E_T$  distributions for  $\mu_R = \mu_F = \mu/2$  and with  $R = 0.4$  (solid) or  $R = 0.7$  (dashes). The data points are preliminary CDF data [Koehn95], obtained with  $R = 0.4$ .*

fragmentation mechanism is very likely a source of this inconsistency. As for the large disagreement with the charm data, we have no significant comment to make. Hopefully, additional data will soon be available, as well as estimates of the experimental systematics. Notice that the largest contribution expected from higher-order perturbative corrections is given by the production of  $c\bar{c}$  pairs from soft gluons emitted during the gluon-shower evolution. However, these effects have been estimated in refs. [Mueller85, Mueller86, Mangano92, Seymour95], and have been shown to be negligible at the energies of interest for the current measurements.

To conclude this section, we discuss the behaviour of the  $b$ -jet production cross section at high  $E_T$ . The interest of this item stems from the discrepancy reported by CDF [Abe92, Abe96] in the tail of the jet distribution. If this discrepancy could not be accommodated by new theoretical developments in QCD [Catani96a] or in the fitting of parton densities [Huston95, Glover96], a study of the flavour composition of these high-energy jets could help in understanding the nature of the phenomenon.

Figure 31 shows the  $b(\bar{b})$ -jet fraction for  $E_T$  values up to 450 GeV, for two different values of the cone size ( $R = 0.4$  and  $R = 0.7$ ) and at  $\mu_R = \mu_F = \mu_0/2$ . Notice that while the fraction remains constant through most of the  $E_T$  range, a rise is observed above 300 GeV. To better understand the origin of this rise, we present in fig. 32a the separate contribution to the  $b$ -jet cross section of the three possible initial states,  $gg$ ,  $q\bar{q}$  and  $qg$ . Notice that the  $q\bar{q}$  contribution becomes dominant for  $E_T > 250$  GeV. Figures 32b-d show, for each individual channel, the separate

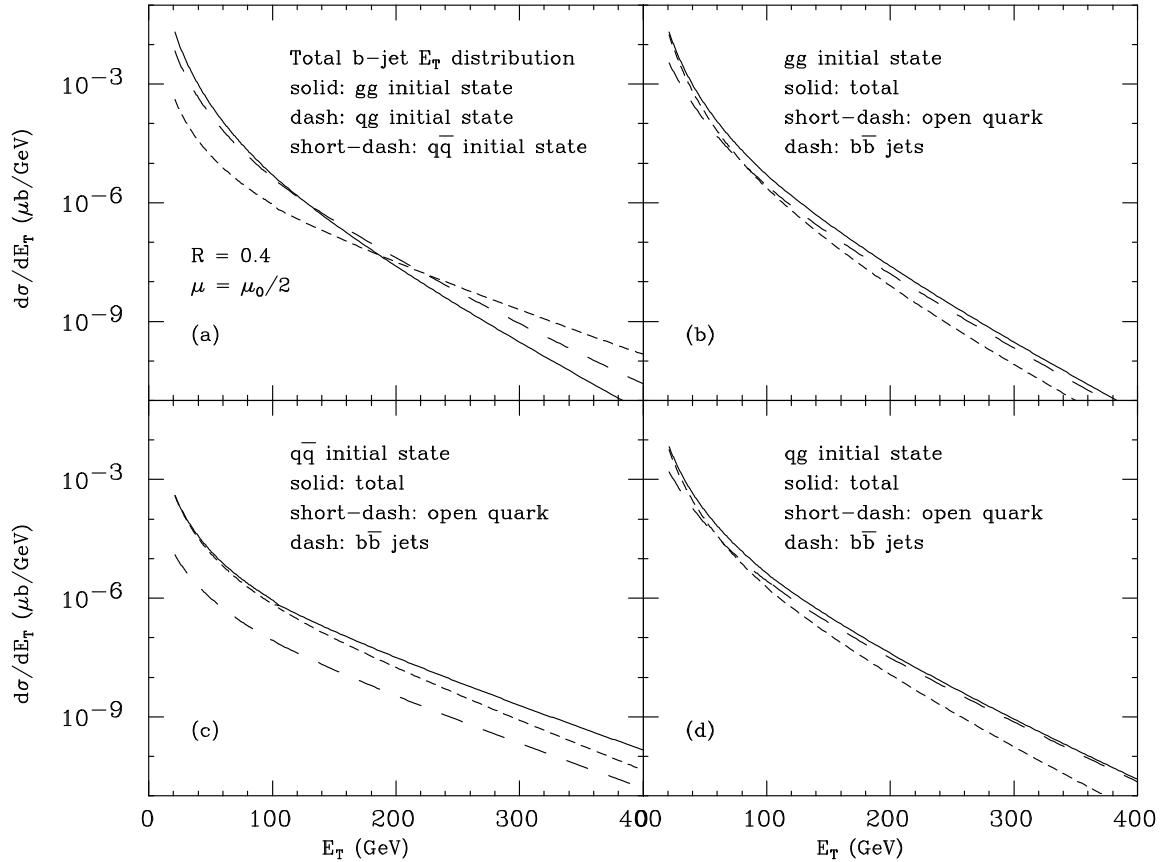


Figure 32: *Initial-state composition of the  $b$ -jet production processes, calculated for  $\mu_R = \mu_F = \mu_0/2$  and  $R = 0.4$  (upper left). Different components of the production processes:  $gg \rightarrow b$ -jet (upper right),  $q\bar{q} \rightarrow b$ -jet (lower left) and  $qg \rightarrow b$  jet (lower right).*

contribution of the open-quark and  $b\bar{b}$ -jet components. For  $E_T$  large enough, the dominant component of the  $gg$  and  $qg$  channels is given by the  $b\bar{b}$ -jet contribution, because of the gluon-splitting dominance. In the case of the  $q\bar{q}$  channel, on the contrary, the  $b\bar{b}$ -jet term is always suppressed, and most of the  $b$  jets are composed of a single  $b$  quark, often accompanied by a nearby gluon. We conclude that at high  $E_T$  the dominant mechanism for the production of a  $b$  jet is the  $s$ -channel annihilation of light quarks. Since mass effects are negligible at high  $E_T$ ,  $1/5$  of the jets produced in  $s$ -channel annihilation are  $b$  jets. A simple LO calculation shows that the fraction of the two-jet rate due to  $s$ -channel light-quark annihilation is about  $20\%$  at  $E_T = 450$  GeV, giving an overall  $b$ -jet over inclusive-jet fraction of approximately  $4\%$ . This explains the rise of the  $b$  fraction at high  $E_T$ , and provides a nice consistency check of our results. Notice also that while the probability that a gluon jet will split into a  $b\bar{b}$  pair grows at large  $E_T$  faster than the  $\mathcal{O}(\alpha_s^3)$  result [Mueller85, Mueller86, Mangano92,

Seymour95]<sup>9</sup>, the fraction of primary gluons in the final state is so small that the overall effect on our predictions is negligible.

#### 4.4 Associated production of heavy quarks with $W$ or $\gamma$ .

In addition to the standard measurements of inclusive heavy-quark production, the high energies and luminosities available at the Tevatron collider allow the detection of the associated production of heavy quarks and electroweak vector bosons ( $\gamma$ ,  $W$  and  $Z$ ). The study of these processes goes beyond the goal of testing perturbative QCD, and has a wide range of applications, which will be briefly described in this section.

##### 4.4.1 Photon plus heavy quarks

The associate production of a photon recoiling against a jet is dominated by the Compton scattering of a gluon and a quark in the proton sea. This process, in the most common experimental configurations, dominates over the quark–antiquark annihilation channel. In the case of a heavy-flavoured jet we would then be sensitive to the heavy-flavour component of the proton sea. The measurement of the  $p_T$  spectrum of photons produced in association with charm jets, and the knowledge of the gluon parton density, could therefore provide in principle a direct measurement of the charm density inside the proton [Fletcher89]. The similar process  $gb \rightarrow \gamma b$  would allow the study of the  $b$  density. In addition, these processes provide a useful control sample for the study of heavy-quark tagging.

Figure 33 contains the distributions of jets of various flavours produced with photons, as estimated with a LO QCD calculation and CTEQ1M parton densities [Botts93]. Because of the difference in charge and partonic density, associate production with a bottom quark is suppressed by a factor of 8–10 relative to charm. Notice also the curious fact that, because of the suppression of the light-quark annihilation channel, it is more likely for a jet produced in association with a photon to be a charm jet rather than a gluon jet, at least for transverse momenta up to 30 GeV.

There is a theoretical interest in these processes because the density of a heavy quark inside the proton is in principle calculable perturbatively. Neglecting higher-order logarithmic corrections, which can be resummed using the Altarelli–Parisi evolution, the inclusive process  $p\bar{p} \rightarrow \gamma Q + X$  can be calculated by evaluating the partonic process  $gg \rightarrow Q\bar{Q}\gamma$  and integrating over the phase space of the  $\bar{Q}$  [Mangano94, Stratmann95]. This process is dominated by configurations where the quark being integrated over is produced at large rapidity and small  $p_T$ . No divergence will appear, because of the heavy-quark mass. A consistent definition of the heavy-quark density, including threshold effects [Collins86], should then reproduce the result of this calculation, at least at moderate  $p_T$ . Comparison against the experimental data is however important, to verify that no additional non-perturbative effect is at work.

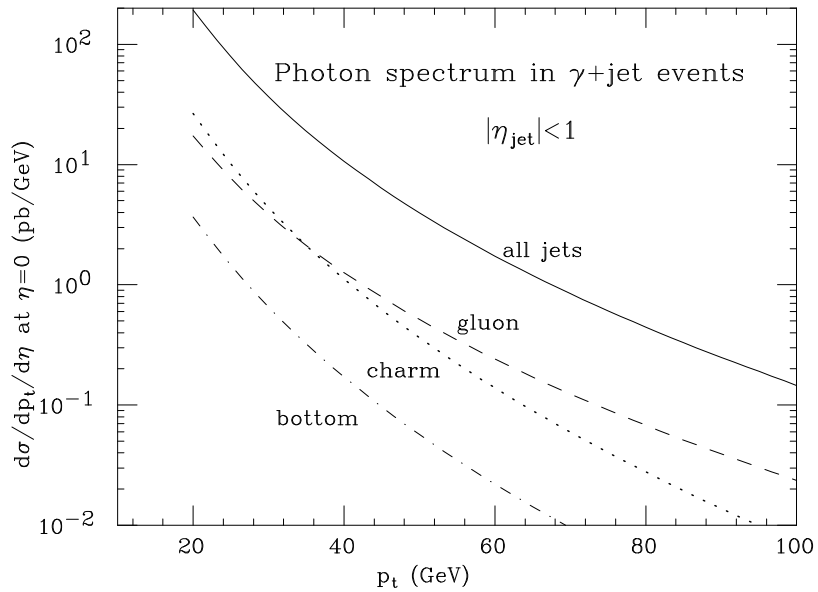


Figure 33: *Jet-type composition in  $\gamma$ +jet events.*

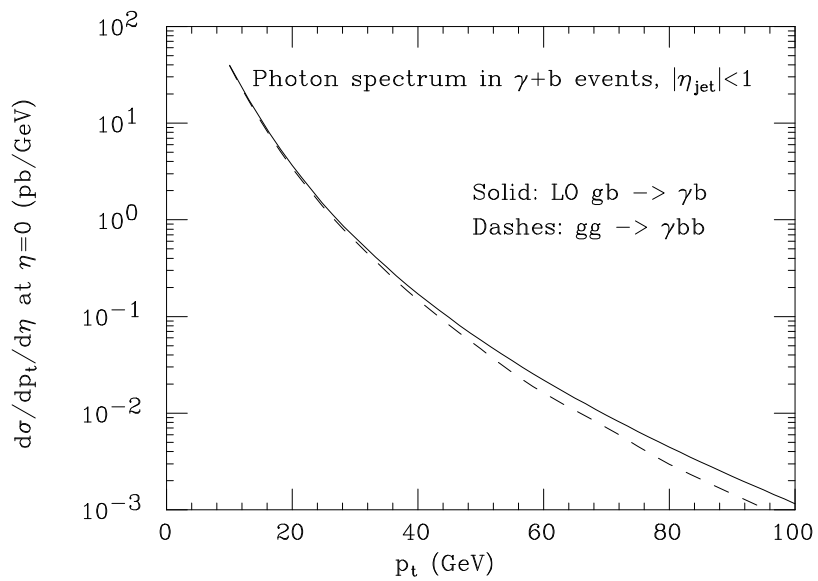


Figure 34: *Photon  $p_t$  distribution in events with a central  $b$  jet in direct photon events, showing the results of the LO structure-function approach and of the  $\mathcal{O}(\alpha_s^2)$  calculation.*

We show in fig. 34 the photon  $p_T$  distribution in events with a central  $b$ , calculated [Mangano94] using the structure function approach ( $bg \rightarrow b\gamma$ , solid line, CTEQ1M PDF's [Botts93]) and using the exact matrix elements for the  $gg + q\bar{q} \rightarrow \gamma Q\bar{Q}$  processes [Ellis88] (dashed line). The  $q\bar{q}$  channel produces a heavy-quark pair via gluon splitting, and cannot be accounted for by the structure-function calculation. As the plot shows, there is perfect agreement between the two approaches, at least in the region where gluon splitting is small. This indicates that the effects of initial-state evolution for the  $b$  quark at these values of  $x$  and  $Q^2$  are not important. Notice that this conclusion is important for the consistency of the NLO evaluation of the inclusive  $b$  cross sections, which contains only the flavour excitation diagrams present in the  $\mathcal{O}(\alpha_s^3)$  matrix elements.

Similar results are obtained in the case of charm production, where there is, however, some larger sensitivity to the choice of the charm mass. A more comprehensive study of the charm case can be found in ref. [Stratmann95].

A NLO QCD calculation of this process has also been recently performed [Bailey96]. This calculation uses massless charm quarks; it is therefore valid in the limit of large transverse momentum. The inclusion of photon isolation and of a  $c \rightarrow \gamma$  fragmentation function is then necessary to remove the divergences due to the collinear emission of a photon from the final-state charm quark. The first experimental results on the associated production of photons and charm have recently appeared from CDF [Abe96e]. The quoted result is the cross section for the process  $p\bar{p} \rightarrow \gamma D^{*+} + X$ , for  $p_T(\gamma) > 16$  GeV,  $p_T(D^{*+}) > 6$  GeV,  $|\eta(\gamma)| < 0.9$  and  $|\eta(D^{*+})| < 1.2$ . The reported measurement is  $\sigma = 0.38 \pm 0.15 \pm 0.11$  nb. While the statistics of this study (based on approximately  $19 \text{ pb}^{-1}$ , i.e. a 20% fraction of the full data set currently available) are not sufficient to produce a distribution in  $p_T$ , the agreement of theory and data is satisfactory. Estimates performed using the LO PYTHIA Monte Carlo program [Sjostrand87], using as renormalization scale  $\mu = p_T(\gamma)$ , give rates in the range 0.18–0.22 nb, depending on the set of parton densities used. Given the large K-factor values found in ref. [Bailey96] between the LO and NLO predictions, the CDF results disfavour a significant presence of a non-perturbative component of charm quarks inside the proton in the regions of  $x$  explored by this measurement.

#### 4.4.2 $W$ bosons plus heavy quarks

The associated production of  $W^\pm$  bosons and heavy quarks is interesting for several reasons. Production of  $W$  plus charm is, in analogy to the  $\gamma$  plus charm case, a potential probe of the partonic densities of the proton. In this case, the Cabibbo-allowed channel  $gs \rightarrow Wc$  is the leading production mechanism, and provides a direct probe of the strange content of the proton at large  $Q^2$  [Baur93].

The  $Wc$  final state is also one of the dominant sources of events with a  $W$  plus one jet with a reconstructed secondary vertex. As such, these events enter in the

---

<sup>9</sup>This happens because of pairs emitted at higher orders from the gluons of the shower.

analysis of the low jet multiplicity  $W +$ jet events, which is performed as ancillary work to the isolation of the  $t\bar{t}$  signal (see the extensive discussion in ref. [Abe94]). Although no cross sections for the  $W + c$  process have been explicitly quoted by the experiments, the agreement of the data with the LO theoretical predictions, modelled for the presence of several analysis cuts, is good [Abe94, Abe95, Abachi95]. The full set of NLO ( $\mathcal{O}(\alpha_s^2)$ ) corrections to this process has recently been evaluated [Giele96], resulting in an improved stability with respect to renormalization and factorization scale variations.

Because of the small value of  $V_{cb}$  and of the charm density in the proton, which suppress the LO process  $gc \rightarrow Wb$ , associate production of  $W$  and bottom quarks has its dominant contribution from the higher-order process  $q\bar{q} \rightarrow Wb\bar{b}$  [Kunszt84, Mangano93a]. Interest in this process is once again related to its relevance for the isolation of the  $t\bar{t}$  final state, which has always among its decay products a  $W$  boson and a  $b\bar{b}$  pair. Direct evidence for the prompt production of  $Wb\bar{b}$  events comes from the study of tagged jets in the  $W + 2J$  sample, performed by the CDF and D0 collaborations in the top analyses (for a detailed discussion, see ref. [Abe94]). Because of the small tagging efficiencies for charm quarks, and because of the limited statistics, there is currently no experimental result on the production of  $Wc\bar{c}$  events.

Additional interest in the  $Wb\bar{b}$  process comes from the studies of direct backgrounds to the detection of an intermediate-mass Higgs. This could be observed with possible future luminosity upgrades of the Tevatron collider in the mass range  $65 < M_H < 110$  GeV using the  $p\bar{p} \rightarrow WH \rightarrow Wb\bar{b}$  channel [Stange94, Stange94a, Amidei96]. The D0 collaboration has recently presented the first study of a direct search for Higgs bosons in the  $Wb\bar{b}$  channel [Abachi96d]. The findings are consistent with the QCD background estimates, providing preliminary evidence for the correctness of the QCD calculations of the  $Wb\bar{b}$  rate, although no explicit cross section has as yet been quoted for this process.

## 4.5 Production of top quarks

### 4.5.1 Total $t\bar{t}$ production cross sections

The top quark having been found [Abe94, Abe95, Abachi95], the comparison between its observed production properties and those expected from the Standard Model will be an important probe of the possible existence of new phenomena. One of the most important tests to be performed concerns the total production cross section. This is the most inclusive quantity available, and is *a priori* the least sensitive to a detailed understanding of the higher-order corrections that influence the evolution of the initial and final states. Within QCD, one expects the perturbative expansion in powers of  $\alpha_s(m_t)$  to be well behaved and to provide an accurate estimate of the total cross section already at low orders. In particular, the first estimates of the total production cross section using the full NLO matrix elements [Nason88, Beenakker89, Ellis91] gave an increase (relative to the Born result) of the order of 30% for masses above 100 GeV.

The residual perturbative QCD uncertainty, evaluated by varying the renormalization and factorization scales, was estimated to be no larger than 10%. The choice of parametrization for the input parton densities was also shown to give effects of this order of magnitude, by using the available sets.

It was later pointed out in refs. [Laenen92, Laenen94] that logarithmic contributions associated with the emission of soft gluons from the initial state could significantly enhance the NLO result. Similar conclusions were reached in refs. [Berger95, Berger96]. More recent studies [Catani96, Catani96a], which will be described in more detail in Section 5, have proved that the effect of soft-gluon resummation is actually very small, of the order of a 1% correction to the total cross section.

Beside the soft-gluon emission effects, also Coulomb effects [Sommerfeld39] may enhance or deplete the cross section near threshold, as originally discussed in ref. [Fadin90]. These effects can be evaluated in the following way. We separate the partonic Born cross-section formulae into their colour singlet and octet components

$$\hat{\sigma}^{(gg)} = \hat{\sigma}_{(8)}^{(gg)} + \hat{\sigma}_{(1)}^{(gg)} \quad (4.9)$$

$$\hat{\sigma}^{(q\bar{q})} = \hat{\sigma}_{(8)}^{(q\bar{q})} \quad (4.10)$$

where  $\hat{\sigma}^{(q\bar{q}, gg)}$  can be found in ref. [Nason88], and

$$\hat{\sigma}_{(1)}^{(gg)}(\rho) = \frac{\alpha_s^2}{m^2} \frac{\beta\rho\pi}{384} \left[ \frac{1}{\beta} \log \frac{1+\beta}{1-\beta} (4 + 4\rho - 2\rho^2) - 4 - 4\rho \right]. \quad (4.11)$$

Here  $\beta = \sqrt{1-\rho}$  and  $\rho = 4m^2/\hat{s}$ . The Coulomb-resummed cross section is given as

$$\hat{\sigma}^{\text{Coul}}(\rho) = \hat{\sigma}_{(8)}(\rho) \frac{\pi\alpha_s/(6\beta)}{\exp(\pi\alpha_s/(6\beta)) - 1} + \hat{\sigma}_{(1)}(\rho) \frac{4\pi\alpha_s/(3\beta)}{1 - \exp(-4\pi\alpha_s/(3\beta))}. \quad (4.12)$$

We do not include bound-state effects, which, as shown in ref. [Fadin90], are much smaller. As shown in ref. [Catani96], the relative correction due to the resummation of Coulomb effects not already included into the NLO results is an effect smaller than 1% of the NLO cross section. Together with soft-gluon resummation effects, higher-order Coulomb corrections can therefore be entirely neglected, given the theoretical NLO uncertainties and the current experimental accuracy.

Electroweak processes can give rise to single top production. This happens through the so-called  $Wg$  fusion process [Dawson85, Willenbrock86, Yuan90, Ellis92, Bordes95], whereby a virtual  $W$ , emitted from an initial-state light quark, interacts with an initial-state gluon and produces a  $t\bar{b}$  pair, and through the decay of an off-shell  $W$  boson into a  $t\bar{b}$  pair [Cortese91, Stelzer95]. While in principle these processes do not contribute to the observation of  $t\bar{t}$  pairs, and therefore should not interfere with the measurement and study of the QCD production properties of top quarks, in practice they constitute an irreducible background to the detection of  $t\bar{t}$  events. From the

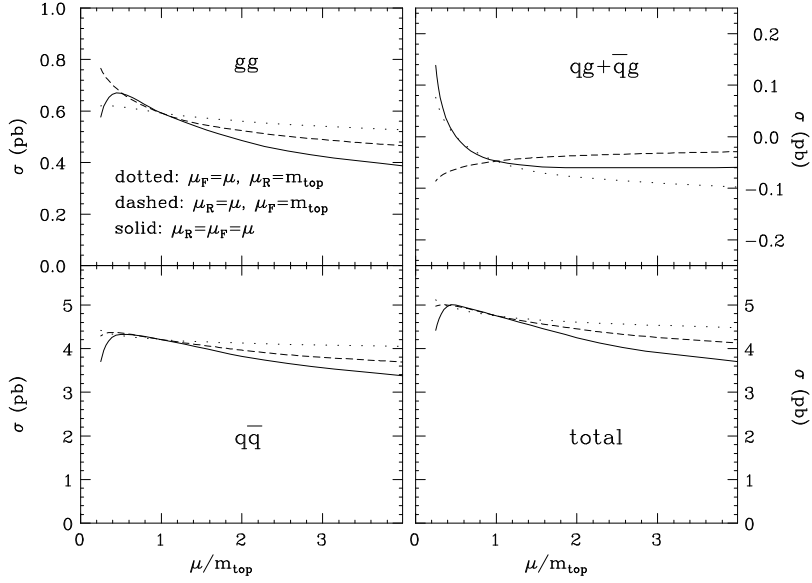


Figure 35: *Scale dependence of the top cross section at the Tevatron, for  $m_t = 175$  GeV. Dotted lines are the  $\mu_F$  dependence at fixed  $\mu_R$ , dashed lines are the  $\mu_R$  dependence at fixed  $\mu_F$ , and solid lines are obtained by the simultaneous variation of  $\mu_R$  and  $\mu_F$ .*

point of view of QCD studies, it is therefore a welcome fact that their total contribution to the inclusive top-production cross section is only a fraction of the order of 25%. Their study is however important for electroweak measurements, as it probes the  $Wtb$  vertex and the value of  $V_{tb}$  directly. A complete review of the phenomenological applications of single top production, in addition to a complete list of the relevant references, can be found in ref. [Amidei96].

Electroweak radiative corrections to top production in hadronic collisions have been considered in refs. [Kao93, Stange93, Beenakker94, Harlander95]. They range from  $-0.97\%$  to  $-1.74\%$  of the Born cross section, for a Higgs mass of 60 and 1000 GeV respectively<sup>10</sup>.

In this section we will confine our theoretical analysis to results obtained within the QCD  $\mathcal{O}(\alpha_s^3)$  approximation. It should be pointed out that this study is performed within the strict domain of the Standard Model. Corrections to the top cross section much larger than the Standard Model QCD uncertainties can be obtained in the presence of new phenomena. Virtual corrections due to loops of supersymmetric particles have been studied, for example, in refs. [Li95, Li96, Alam96, Kim96, Sullivan96]. For a partial list of examples of alternative production mechanisms for top quarks, arising in theories beyond the SM such as Supersymmetry or Technicolor, see for instance refs. [Eichten94, Hill94, Holdom95, Casalbuoni96, Kane96].

<sup>10</sup>W. Hollik and D. Wackerlo, private communication.

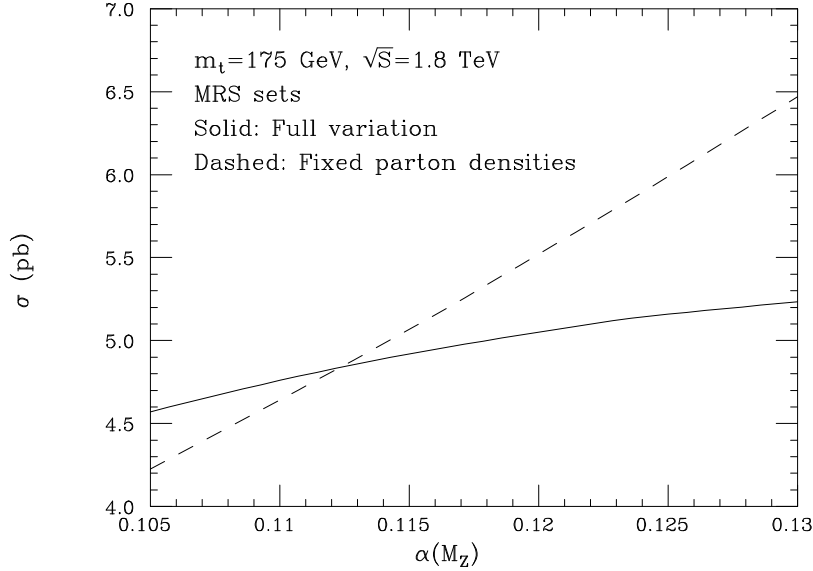


Figure 36: *Top cross section as a function of  $\alpha_s(M_Z)$ . The dashed line (obtained with the MRSA' set) does not include the variation of the parton densities due to the change in  $\alpha_s$ .*

We now proceed to a review of the theoretical uncertainties on the total cross section for  $t\bar{t}$  production, which arise at NLO. Uncertainties due to unknown higher-order effects are usually accounted for by varying the renormalization ( $\mu_R$ ) and factorization ( $\mu_F$ ) scales. In principle, independent variations of the two scales should be considered. In fig. 35 we show the scale dependence of the top cross section. Notice that there is a compensation of the renormalization-scale dependence when the different subprocesses are added up. In fact, the renormalization-scale dependence in the  $gg$  and  $qq$  channels has a behaviour opposite to that in the  $qg$  channel. It is only the combined scale dependence that can be considered an estimate of the neglected sub-leading corrections. As a second point, we observe that the maximum of the cross section is reached around  $m_t/2$ . Thus, the usual choice of the range  $m_t/2 < \mu < 2m_t$  appears to be particularly justified in this case. As a third point, we observe that the scale dependence in the cross section goes in the same direction for the two scales, so that, for the purpose of estimating the associated uncertainty, it is sufficient to consider the simultaneous variation of  $\mu_R$  and  $\mu_F$ .

Aside from the scale uncertainties, which reflect the limitations of the perturbative QCD calculation, there are uncertainties associated with our imprecise knowledge of the physical parameters involved. In particular, the strong coupling constant is determined within a certain accuracy.

In the case of top production at the Tevatron, there is fortunately a compensating mechanism that reduces the dependence of the cross section upon  $\alpha_s$ . In fact, the top cross section is dominated by the  $q\bar{q}$  annihilation process. Quark densities in

$\mu_R = \mu_F$	CTEQ1M	CTEQ'	MRSA'	MRS, variable $\Lambda$ , $\alpha_s(M_Z) =$				
				0.105	0.110	0.115	0.120	0.125
$m_t/2$	5.24	5.07	5.00	4.78	4.99	5.18	5.34	5.48
$m_t$	4.96	4.86	4.75	4.57	4.76	4.92	5.05	5.16
$2m_t$	4.38	4.38	4.25	4.13	4.27	4.38	4.47	4.52

Table 3: *Total cross sections (in pb) for  $m_t = 175$  GeV at NLO. The set CTEQ' is taken from ref. [Huston95].*

the proton are directly measured in DIS at a scale around 10 GeV<sup>2</sup>, and the QCD evolution to scales of the order of the top mass makes them softer. Therefore, for larger coupling, the partonic cross section increases, but the quark luminosity decreases.

In order to perform a fair estimate of the uncertainty due to  $\Lambda_{\text{QCD}}$ , we need sets of parton densities fitted with different values of the strong coupling. The sets of ref. [Martin95a] meet our purpose<sup>11</sup>. In fig. 36 we show the cross section as a function of the strong coupling.

For comparison we also show the  $\alpha_s$  dependence if the parton densities are kept fixed to the MRSA' set. We see the remarkable reduction in the  $\alpha_s$  dependence, due to the compensation of the rise of the partonic cross section and the decrease of the quark parton densities.

Our results for the top cross section for  $m_t = 175$  GeV are collected in table 3. We also show results obtained with the recent parametrization derived in ref. [Huston95] by including the CDF jet data. We stress that the numbers in the table are obtained with a standard one-loop calculation. No resummation effects are included.

Our range for the top cross section at  $m_t = 175$  GeV ( $m_t = 170$  GeV) is given by  $4.75^{+0.73}_{-0.62}$  pb ( $5.57^{+0.86}_{-0.73}$  pb). This should be compared with the current experimental results:

$$\sigma_{\bar{t}t}(m_t = 175 \text{ GeV}) = 7.5 \pm 1.6 \text{ pb} \quad (\text{CDF [Caner96]}) ; \quad (4.13)$$

$$\sigma_{\bar{t}t}(m_t = 170 \text{ GeV}) = 5.2 \pm 1.8 \text{ pb} \quad (\text{D0 [Narain96]}) . \quad (4.14)$$

<sup>11</sup>The values of  $\Lambda_4$  that accompany the FORTRAN program for the structure function sets of ref. [Martin95a] are not consistent with the values of  $\alpha_s$  quoted there, the differences being of the order of 1%. In the present work, we extract the values of  $\Lambda_5$  from their quoted values of  $\alpha_s$  using the standard two-loop formula [Barnett96].

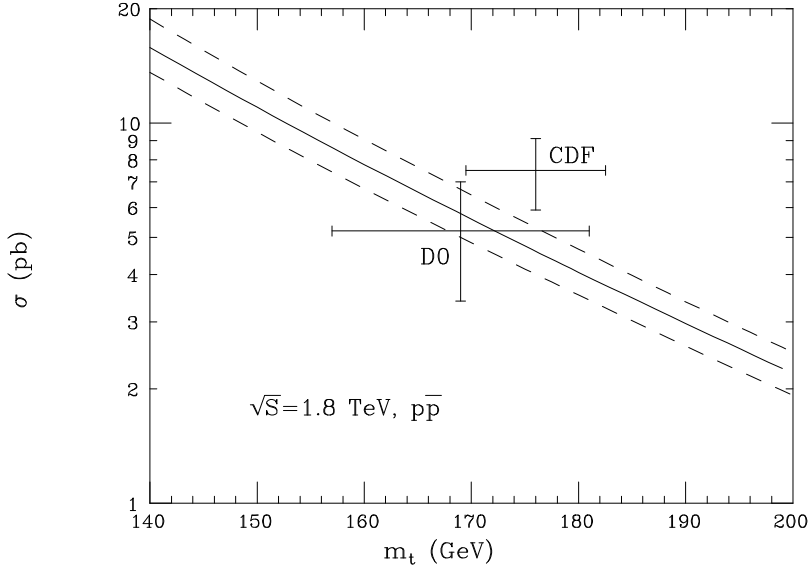


Figure 37: Top cross-section at the Tevatron at  $\sqrt{S} = 1.8$  TeV. The solid line is obtained with MRSA' parton density, and the dashed lines correspond to the upper and lower values obtained in table 3. The experimental data are taken from refs. [Caner96, Narain96].

As a central value for our determination we have chosen the MRSA' [Martin95] result with  $\mu_R = \mu_F = m_t$ , in association with a value of  $\Lambda_5 = 0.152$  GeV (which corresponds to  $\alpha_s(M_Z) = 0.1113$ , according to the standard two-loop formula [Barnett96]). For the MRS sets with variable  $\Lambda$ , we have used  $\Lambda_5 = 0.0994, 0.140, 0.190, 0.253, 0.328$  GeV (which correspond to  $\alpha_s(M_Z) = 0.105, 0.110, 0.115, 0.120, 0.125$ ).

The cross section bands are also shown in fig. 37. The agreement of theory and data is good, but it is clear that higher statistics should be collected before a significant test is achieved.

For reference, we also quote the cross section for top production at the LHC. We get  $\sigma(t\bar{t}) = 0.77^{+0.25}_{-0.12}$  nb, for  $m_t = 175$  GeV and  $\sqrt{S} = 14$  TeV. The error is obtained with the same scale and  $\alpha_s$  variations that we used for the Tevatron cross section. Notice that the relative error is much larger than at the Tevatron, because of the greater importance of the  $gg$  initial-state contribution at the LHC energy.

#### 4.5.2 Top kinematical distributions

Because of the high precision of the theoretical prediction, the measurement of the top cross section could become a sensitive probe of new physics. The only way to unambiguously disentangle the standard sources of top production from possible new physics will nevertheless rest on the detection of significant discrepancies in

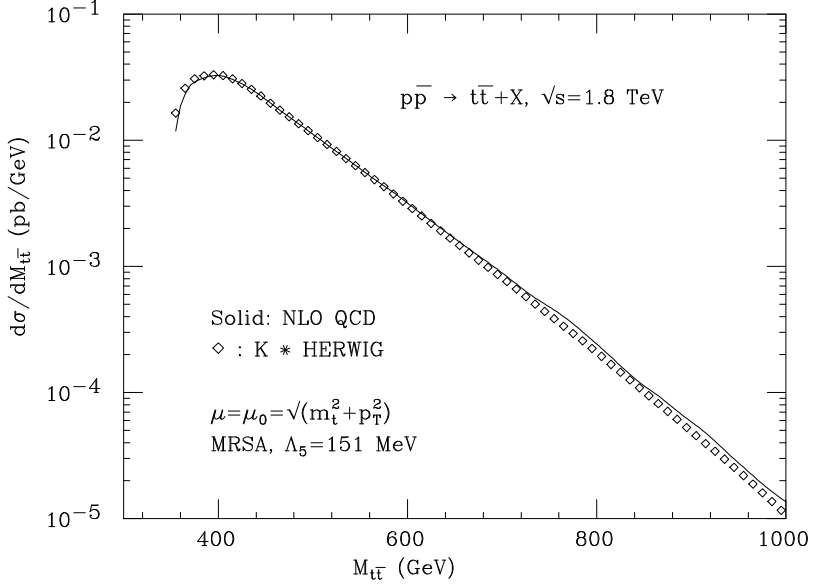


Figure 38: *Invariant-mass distribution of the  $t\bar{t}$  pair. The HERWIG prediction has been rescaled by a constant factor  $K = 1.34$ .*

the kinematical features of top production from what is expected from QCD. For example, the detection of mass peaks in the invariant mass distribution of top pairs would indicate the possible presence of  $s$ -channel resonances strongly coupled to the top [Eichten94, Hill94].

Kinematical distributions for top-quark pairs produced at the Tevatron have been calculated at NLO in ref. [Frixione95]. Since top quarks manifest themselves experimentally in a rather indirect way, their identification relies on complex series of experimental cuts [Abe94, Abe95, Abachi95, Campagnari96, Sinervo96]. The study of their kinematical properties therefore strongly relies on the modelling of the top-quark production mechanism itself. In particular, experimental analyses are performed using parton shower Monte Carlo (MC) programs, such as HERWIG [Marchesini88, Marchesini92], ISAJET [Paige86] or PYTHIA [Sjostrand87]. It is therefore important to compare the distributions predicted by these MC calculations with what is expected from NLO QCD. The study performed in ref. [Frixione95] indicates an excellent agreement between these results, at least for distributions that are non-trivial at LO in perturbation theory, such as the top inclusive  $p_T$  distribution or the invariant-mass distribution of the top-quark pair (fig. 38). The theoretical uncertainty from higher-order corrections and from hadronization effects is very small for these variables, making them a rather solid term of comparison in the search for new physics. Distributions that are non-trivial only at  $\mathcal{O}(\alpha_s^3)$ , such as the  $p_T$  of the top pair, show instead significant higher-order corrections. This is visible, for the example of the top-pair  $p_T$  distribution, in fig. 39, where a comparison is made between the NLO QCD predictions and those of the HERWIG MC. The multiple gluon emission

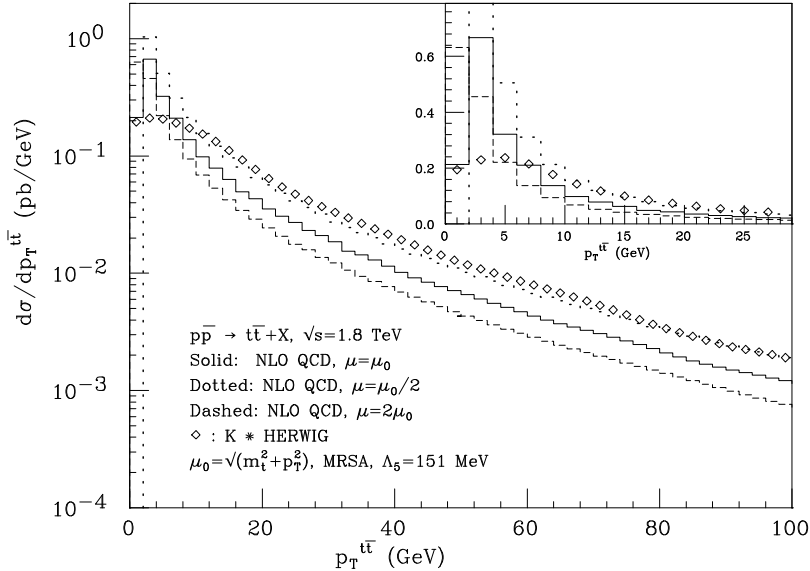


Figure 39: Transverse-momentum distribution of the  $t\bar{t}$  pair. The *HERWIG* prediction has been rescaled by a constant factor  $K = 1.34$ .

from the initial state of the hard process, included in the MC calculation, significantly increases the average transverse momentum of the pair, as can also be seen by the numbers quoted in table 4. Notice the significant scale dependence of the NLO result. Similar discrepancies between the results of higher-order exact matrix element calculations and shower MC predictions have been reported in [Orr95, Orr95a].

It should be pointed out that the transverse momentum of the top pair, directly related to the jet activity that accompanies a top production event, has important consequences on the determination of the experimental top detection efficiency, as well as a large impact on the reliability with which the mass of the top quark can be measured [Abe94, Abe95, Abachi95, Campagnari96]. The uncertainty related to the modelling of the gluon radiation emitted by initial and final state, in  $t\bar{t}$  production and decay, is in fact one of the largest systematics present in the most recent top-mass determinations [Galtieri96, Grannis96].

Although the statistics of the data on top production are still low, the first distributions have been presented by CDF [Caner96]. The top-pair invariant-mass spectrum is in good agreement with the theoretical expectations, and currently shows no evidence of an anomalous production source in the  $s$ -channel (fig. 40). On the contrary, the pair transverse momentum is harder than the *HERWIG* MC predicts (fig. 41). As was pointed out above, this distribution is not, at the moment, predicted very accurately. It is therefore premature to conclude that the present discrepancy is physically significant, especially in view of the limited statistics.

To summarize this section on top production, we conclude that nothing surprising has been discovered so far in the comparison of data with the predictions of NLO

	$\langle p_T^{t\bar{t}} \rangle$ (GeV)	$F(p_T^{t\bar{t}} > 10 \text{ GeV})$ (%)	$F(p_T^{t\bar{t}} > 20 \text{ GeV})$ (%)
NLO QCD, $\mu_R = \mu_F = \mu_0$	11.9	30	15
NLO QCD, $\mu_R = \mu_F = 2\mu_0$	9.1	23	11
NLO QCD, $\mu_R = \mu_F = \mu_0/2$	16.6	44	22
HERWIG, $\mu_R = \mu_F = \mu_0$	17.5	51	28

Table 4: *Average value of  $p_T^{t\bar{t}}$  and fraction of the cross section with  $p_T^{t\bar{t}} > 10$  and 20 GeV for different calculations.*

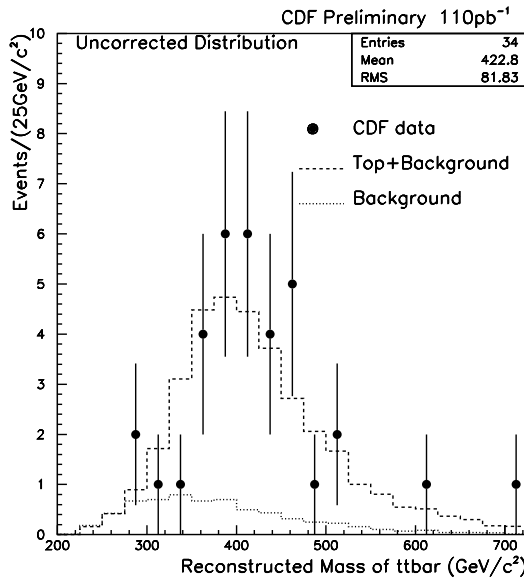


Figure 40: *CDF data on the invariant mass of top pairs, from  $W + 4$  jets (one of which tagged as a  $b$ ), compared with the HERWIG MC expectations.*

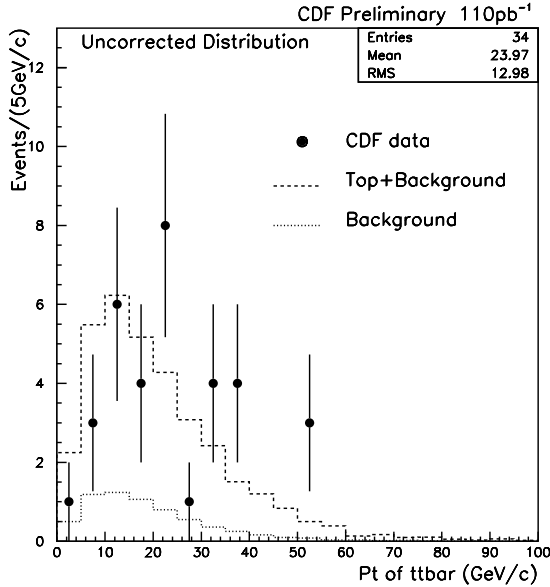


Figure 41: *CDF data on the transverse momentum distribution of top pairs, from  $W + 4$  jets (one of which tagged as a  $b$ ), compared with the HERWIG MC expectations.*

perturbative QCD. As expected, the agreement between data and theory is already more solid than in the case of bottom or charm production. Given the claimed accuracy of the theoretical predictions, at least for the total cross section and for inclusive quantities, only additional statistics will however make these comparisons more compelling. Detailed features of the structure of the final state in top production, such as studies of the jet activity, have so far been probed only indirectly in the context of the mass measurements. It is likely that a lot will be learned in the future from these more detailed analyses, and that significant progress will be made in their MC modelling.

## 5 HIGHER ORDERS AND RESUMMATION

In this section we will deal with the problem of the resummation of logarithmically enhanced effects in the vicinity of the threshold region in hard hadroproduction processes. Drell–Yan lepton-pair production has been in the past the best studied example of this sort. The threshold region is reached when the invariant mass of the lepton pair approaches the total available energy. A large amount of theoretical and phenomenological work has been done on this subject. The articles in refs. [Sterman87, Catani89] summarize the theoretical status of the subject, and also include references to the extensive literature in this field. For the Drell–Yan

process the resummation of soft gluons has been computed to NLO accuracy. Extension of the NLO resummation formalism to heavy-flavour production is under way [Kidonakis96, Contopanagos96].

Resummation formulae have also been used in estimating heavy-flavour production [Laenen92, Laenen94, Berger95, Berger96, Kidonakis95]. These works indicate the presence of very large higher-order corrections to heavy-flavour production at colliders, in particular in the  $gg$  production channel. Since top production at the Tevatron is dominated by the  $q\bar{q}$  channel, the claimed size of the resummation effects is about 15%, below the current experimental uncertainties on the cross section. Nevertheless, it is important to establish whether threshold resummation effects are really so large, a fact that would cast doubts on every QCD calculation of hadronic cross sections. Recently, in ref. [Catani96, Catani96a], it was argued that in fact resummation effects are not as large as found in previous computations. In particular, it was pointed out there that large spurious terms are present in certain formulations of the resummation problem that are not justified by the threshold approximation. Furthermore, it was also shown that resummation may be formulated in such a way that these terms are absent. In the following we will present a brief review of this problem.

### 5.1 What are soft-gluon effects

Coloured particles emit soft gluons with high probability. Normally, the effect of soft-gluon emission is small (at least in inclusive quantities), since they only slightly affect the kinematics of a process. However, in a production process of high-mass objects, when we approach the threshold, soft-gluon emission becomes important. Let us fix our attention on heavy-flavour production in hadronic collisions near threshold. The process is schematically depicted in fig. 42. The incoming protons make a big

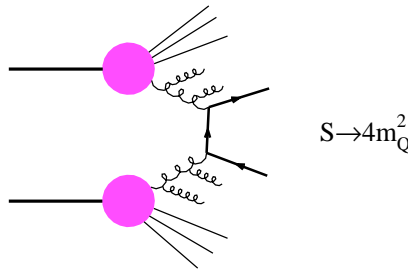


Figure 42: *Heavy-flavour production near threshold.*

effort in providing partons with a large fraction of the longitudinal momentum, thus going towards the very large  $x$  region of the structure functions. Under these circumstances, even the small amount of energy wasted by soft-gluon radiation yields an

important suppression of the cross section. In the usual application of the factorization theorem, part of the radiative corrections due to gluon radiation are included in the structure functions. Thus, depending upon the factorization scheme, the left-over suppression may be positive or negative. In the  $\overline{\text{MS}}$  and DIS scheme the left-over is negative, so that the suppression effect appears instead as an enhancement of the cross section.

In the case of heavy-flavour production, the perturbative expansion for the partonic cross section at  $\mathcal{O}(\alpha_s^3)$  (omitting obvious indices, such as the incoming parton types) has the structure

$$\hat{\sigma}(\hat{s}) = \sigma_0(\hat{s}) \left[ 1 + C\alpha_s \log^2(1 - \hat{\rho}) + \mathcal{O}(\alpha_s \log(1 - \hat{\rho}), \alpha_s^2) \right], \quad (5.1)$$

where  $\hat{s}$  is the square of the partonic centre-of-mass energy,  $\hat{\rho} = 4m^2/\hat{s}$ ,  $\sigma_0(\hat{s})$  is the Born cross section

$$\sigma_0(\hat{s}) = \frac{\alpha_s^2}{m^2} f^{(0)}(\hat{\rho}), \quad (5.2)$$

and  $\alpha_s = \alpha_s(m^2)$ . The reader can find in ref. [Nason88] explicit formulae for the functions  $f^{(0)}(\hat{\rho})$ , as well as for the constant coefficient  $C$ . The precise value of  $C$  depends upon the type of incoming partons (i.e. quarks or gluons) and upon the factorization scheme. In both the  $\overline{\text{MS}}$  and the DIS scheme it is positive, so that in the following we can think of it as being a positive constant. Resummation, according to refs. [Laenen92, Laenen94], gives

$$\hat{\sigma}^{(\text{res})}(\hat{s}) = \frac{\alpha_s^2}{m^2} f^{(0)}(\hat{\rho}) \exp \left[ C\alpha_s(s') \log^2(1 - \hat{\rho}) \right], \quad (5.3)$$

where  $s'$  is a scheme-dependent function of  $\hat{s}$  that goes to zero as  $\hat{s} \rightarrow 4m^2$ . We have  $s' = (1 - \hat{\rho})^\eta m^2$ , where  $\eta = 1$  in the DIS scheme, and  $3/2$  in the  $\overline{\text{MS}}$  scheme. Formula (5.3) is supposed to include all terms of order  $\alpha_s^m \log^n(1 - \hat{\rho})$  with  $n > m$  in the exponent. Remember in fact that

$$\alpha_s(s') = \frac{1}{b_0 \log \frac{s'}{\Lambda^2}} = \frac{1}{b_0 \log \frac{m^2}{\Lambda^2} + b_0 \eta \log(1 - \hat{\rho})} = \alpha_s (1 - \alpha_s b_0 \eta \log(1 - \hat{\rho}) + \dots), \quad (5.4)$$

so that in the exponent there are terms with arbitrary powers of  $\alpha_s$ , and a power of the logarithm that is always larger than the power of  $\alpha_s$ . The first subleading terms have the form  $\alpha_s^k \log^k(1 - \hat{\rho})$ .

In order to get a physical cross section, the partonic cross section given above should be convoluted with parton luminosities:

$$\sigma^{(\text{res})} = \frac{\alpha_s^2}{m^2} \int \mathcal{L}(\tau) f^{(0)}(\hat{\rho}) \exp \left[ C\alpha_s ((1 - \hat{\rho})^\eta m^2) \log^2(1 - \hat{\rho}) \right] d\tau, \quad (5.5)$$

where, omitting obvious parton indices,

$$\mathcal{L}(\tau) = \int F(x_1) F(x_2) \delta(x_1 x_2 - \tau) dx_1 dx_2. \quad (5.6)$$

Here we can spot a problem in the resummation formula. When performing our integral over  $\tau$ , as  $\hat{\rho} \rightarrow 1$  the argument of  $\alpha_s$  in the exponential approaches zero. Before it actually hits the zero, it will hit a singularity in the running coupling  $\alpha_s(s')$ , causing the integral to diverge. In order to avoid this divergence, a cutoff  $\mu_0$  was introduced in the literature [Laenen92, Laenen94, Appel88]. Observe that this cutoff has nothing to do with the standard factorization and renormalization scale  $\mu$ . It is essentially a cutoff on soft-gluon radiation, imposed in order to avoid the blowing up of the running coupling associated with soft-gluon emission.

The use of a cutoff seems an ad hoc procedure in this case. However, it can be justified to some extent. Suppose, for example, that we end up in a QCD calculation with a formula like

$$G = \int_0^Q \alpha_s(k^2) G(k^2) dk , \quad (5.7)$$

where  $G(k^2)$  is a smooth function as  $k^2 \rightarrow 0$ . Integrals of this kind are often found, for example, in the computation of shape variables in jet physics. This expression is divergent as  $k^2 \rightarrow 0$ , since at some point  $\alpha_s$  approaches the Landau pole. The divergence can be handled by a cutoff  $\mu_0$ , which has to be large enough for  $\alpha_s$  to be barely perturbative. For example, we may choose  $\mu_0 = 5\Lambda$ , a value around 2 GeV. We can then argue that

$$G = \int_{\mu_0}^Q \alpha_s(k^2) G(k^2) dk + C \frac{\mu_0}{Q} . \quad (5.8)$$

In fact, the divergence of the 1-loop expression of  $\alpha_s$  does not signal a real physical divergence. More likely, the point at which  $\alpha_s$  becomes of order 1 signals the breakdown of perturbation theory. We therefore exclude this region, estimate its contribution by dimensional analysis, and obtain a power correction. A slightly more formal justification makes use of the concept of IR (infrared) renormalons. We expand eq. (5.7) in powers of  $\alpha_s = \alpha_s(Q^2)$ , using

$$\alpha_s(k^2) = \frac{1}{b_0 \log \frac{k^2}{\Lambda^2}} = \frac{1}{b_0 \log \frac{Q^2}{\Lambda^2} + b_0 \log \frac{k^2}{Q^2}} = \alpha_s \sum_{j=0}^{\infty} \left( -\alpha_s b_0 \log \frac{k^2}{Q^2} \right)^j , \quad (5.9)$$

and we get

$$\begin{aligned} G &\propto \int_0^Q \alpha_s \sum_{j=0}^{\infty} \left( -\alpha_s b_0 \log \frac{k^2}{Q^2} \right)^j dk \\ &= \alpha_s \sum_{j=0}^{\infty} (\alpha_s b_0)^j \int_0^{\infty} t^j e^{-t/2} dt , \end{aligned} \quad (5.10)$$

where  $t = \log Q^2/k^2$ . The integral can be performed, and one gets

$$G \propto 2\alpha_s \sum_{j=0}^{\infty} j! (2\alpha_s b_0)^j , \quad (5.11)$$

which is a divergent series, since a factorial grows faster than any power. This lack of convergence is in fact a general feature of the perturbative expansion in field theory. The perturbative expansion should be interpreted as an asymptotic one. The terms of the expansion (5.11) decrease for moderate values of  $j$ . As  $j$  grows, the factorial takes over, the terms stop decreasing and begin to increase. This happens at the value of  $j$  at which the next term is equal to the current one

$$(j+1)! (2\alpha_s b_0)^{j+1} = j! (2\alpha_s b_0)^j \quad (5.12)$$

or roughly

$$j_{\min} \simeq \frac{1}{2\alpha_s b_0}. \quad (5.13)$$

Asymptotic expansions are usually handled by summing their terms as long as they decrease. Of course, in this resummation prescription there is an ambiguity, which is of the order of the size of the first neglected term. In our case

$$j_{\min}! (2\alpha_s b_0)^{j_{\min}} \approx e^{j \log j - j} \frac{1}{j^j} = e^{-\frac{1}{2\alpha_s b_0}} \approx \frac{\Lambda}{Q}, \quad (5.14)$$

which gives a power-suppressed ambiguity with the same power law that we found using the cutoff procedure.

From the discussion given above, we would expect that the resummation formulae should include a cutoff of the order of a typical hadronic scale; varying the cutoff within a factor of order 1 should affect the cross section by terms of order  $\Lambda/Q$ . In fact, this is not the case. The cutoff has a dramatic effect on the cross section, as can be seen from figs. 2 and 3 of ref. [Laenen92]. For example, the uncertainty band obtained by varying the scale  $\mu_0$  between  $0.2m$  and  $0.3m$ , for top production in the  $gg$  channel, brings about a change in the cross section by a factor of 2, for a top mass between 100 and 200 GeV. These two values of  $\mu_0$  correspond to cutting off the gluon radiation at energies of the order of 20 to 30 GeV, therefore much larger than a typical hadronic scale.

Other proposals for the resummation procedure have appeared in the literature. In refs. [Contopanagos94, Alvero95] a method was developed in the context of Drell–Yan pair production, which was applied to the heavy-flavour case in ref. [Berger95]. There, as can be seen from formula (116) and the subsequent discussion, unphysically large cutoffs are present, much larger than the typical hadronic scale one would expect.

In the following section, we will show that the presence of large cutoffs and of large ambiguities in the resummation formula is not at all related to the blowing up of the coupling constant. In other words, there are other sources of factorial growth of the perturbative expansion for the resummation of soft gluons, and they largely dominate the factorial growth due to the running coupling. We will also show that these terms are spurious, and that soft-gluon resummation can be easily formulated in such a way that these terms are not present.

## 5.2 Problems with the $x$ -space resummation formula

For definiteness, let us focus upon the resummation formula (5.5). We pointed out earlier that this formula is divergent when the argument of  $\alpha_s$  becomes too small and the coupling constant blows up. In fact, formula (5.5) is divergent, even for fixed coupling constant. At fixed coupling it can be written as

$$\begin{aligned}\sigma^{(\text{res})} &= \frac{\alpha_s^2}{m^2} \int d\tau \mathcal{L}(\tau) f^{(0)}(\hat{\rho}) \exp \left[ \alpha_s C \log^2(1 - \hat{\rho}) \right] \\ &= \frac{\alpha_s^2}{m^2} \int_{\rho}^1 d\hat{\rho} \frac{\rho}{\hat{\rho}^2} \mathcal{L}(\rho/\hat{\rho}) f^{(0)}(\hat{\rho}) \exp \left[ \alpha_s C \log^2(1 - \hat{\rho}) \right],\end{aligned}\quad (5.15)$$

where  $\rho = 4m^2/S$ , and the integral diverges as  $\hat{\rho} \rightarrow 1$ , since the exponential

$$\exp(a \log^2(1 - \hat{\rho})) = (1 - \hat{\rho})^{a \log(1 - \hat{\rho})} \quad (5.16)$$

grows faster than any inverse power of  $1 - \hat{\rho}$  as  $\hat{\rho} \rightarrow 1$ . This divergence can again be related to the factorial growth in the perturbative expansion. Expanding formula (5.15) in powers of  $\alpha_s$ , we get

$$\sigma^{(\text{res})} = \frac{\alpha_s^2}{m^2} \sum_{k=0}^{\infty} \frac{1}{k!} (C\alpha_s)^k \int_{\rho}^1 d\hat{\rho} \frac{\rho}{\hat{\rho}^2} \mathcal{L}(\rho/\hat{\rho}) f^{(0)}(\hat{\rho}) \log^{2k}(1 - \hat{\rho}). \quad (5.17)$$

It is now easy to see that, because of its singularity for  $\hat{\rho} \rightarrow 1$ , the integral of  $\log^{2k}(1 - \hat{\rho})$  grows like  $(2k)!$ . Let us make here the simplifying assumption that  $f^{(0)}(\hat{\rho}) \approx \theta(1 - \hat{\rho})$ . In a neighbourhood of the singularity, the integral behaves like

$$\int_{1-\epsilon}^1 d\hat{\rho} \log^{2k}(1 - \hat{\rho}) = \int_{\log 1/\epsilon}^{\infty} dt e^{-t} t^{2k}, \quad (5.18)$$

where we have performed the substitution  $t = |\log(1 - \hat{\rho})|$ . The above integral equals

$$\int_{\log 1/\epsilon}^{\infty} dt e^{-t} t^{2k} = \int_0^{\infty} dt e^{-t} t^{2k} - \int_0^{\log 1/\epsilon} dt e^{-t} t^{2k} = (2k)! - \int_0^{\log 1/\epsilon} dt e^{-t} t^{2k}. \quad (5.19)$$

Since

$$\int_0^{\log 1/\epsilon} dt e^{-t} t^{2k} < (\log 1/\epsilon)^{2k+1} \quad (5.20)$$

we see that the contribution to the integral near the singularity is dominated by the term  $(2k)!$ . The power expansion for the cross section is then

$$\sigma^{(\text{res})} \approx \sum_{k=0}^{\infty} \frac{(2k)!}{k!} (C\alpha_s)^k \approx \sum_{k=0}^{\infty} k! (4C\alpha_s)^k. \quad (5.21)$$

The above formula is in fact appropriate for the case of the heavy-flavour cross section with a lower cut on the invariant mass of the pair<sup>12</sup>. As in the previous example,

<sup>12</sup> In the case of the total cross section, using the known behaviour of  $f^{(0)}$  near threshold, one would get an extra factor of 4/9 in front of  $C$  in eq. (5.21).

the factorial growth of formula (5.21) will give rise to ambiguities in the resummation of the perturbative expansion. These ambiguities are not, however, related to renormalons, since they occur also at fixed coupling constant. In fact, they are in general fractional powers of  $\Lambda/Q$ , where  $Q$  is the scale involved in the problem, and  $\Lambda$  is a typical hadronic scale. For example, as shown in ref. [Catani96a], in the case of heavy-flavour production through the gluon-fusion mechanism, at fixed invariant mass of the heavy-quark pair, the ambiguity would have the form  $(\Lambda/Q)^{0.16}$ , and it would thus be extremely relevant, even for very massive heavy-quark pairs.

These large terms in the perturbative expansion are in fact spurious. They are an artefact of the  $x$ -space resummation procedure. This can be easily understood with the following argument. Exponentiation of the gluon emission is possible because, roughly speaking, each soft gluon is emitted independently. However, this independence is only approximate: the total momentum must be conserved. Momentum conservation, however, is a subleading effect in the soft resummation formula. Yet, its violation leads to factorially growing terms. These terms are subleading from the point of view of the logarithmic behaviour, but very important from the point of view of the factorial growth of the perturbative expansion. The presence of large factorial terms due to momentum non-conservation can be understood also by simple arguments. The emission of  $k$  gluons, where each gluon has a limit on its energy  $E_i < \eta$ , leads to a phase space that is larger by a factor of  $k!$  than the case when the total energy of emission is bounded  $\sum E_i < \eta$ . Thus phase space alone provides a  $k!$  factor. We can see in more detail the origin of the  $(2k)!$  term by considering the formula for the partonic cross section with two emitted soft gluons, implementing momentum conservation. We have

$$\sigma^{(2)}(\hat{\rho}) = \frac{1}{2} (2C\alpha_s)^2 \frac{\alpha_s^2}{m^2} \int \left[ \frac{\log(1-z_1)}{1-z_1} \right]_+ \left[ \frac{\log(1-z_2)}{1-z_2} \right]_+ f^{(0)}(\hat{\rho}') \delta(\hat{\rho} - z_1 z_2 \hat{\rho}') dz_1 dz_2 d\hat{\rho}' . \quad (5.22)$$

The leading-logarithmic term of the above integral is given by

$$\sigma^{(2)}(\hat{\rho}) = \frac{1}{2} (2C\alpha_s)^2 \frac{\alpha_s^2}{m^2} \log^4(1 - \hat{\rho}) f^{(0)}(\hat{\rho}) + \dots , \quad (5.23)$$

where terms with less than 4 powers of logarithms are neglected. We now see that the integral of the leading-logarithmic term of  $\sigma^{(2)}(\hat{\rho})$  in  $\hat{\rho}$  has a large factor  $\approx 4!$  due to the integral of  $\log^4(1 - \hat{\rho})$ , while the integral of the full expression, eq. (5.22), gives

$$\int_0^1 d\hat{\rho} \sigma^{(2)}(\hat{\rho}) = \frac{1}{2} (2C\alpha_s)^2 \frac{\alpha_s^2}{m^2} \left( \int_0^1 dz \left[ \frac{\log(1-z)}{1-z} \right]_+ \right)^2 \int_0^1 d\hat{\rho} f^{(0)}(\hat{\rho}) = 0 , \quad (5.24)$$

since the integrals of the soft emission factors vanish with the  $+$  prescription. In general, we see that if we take generic moments of  $\sigma^{(k)}(\hat{\rho})$  (i.e.  $\int \hat{\rho}^m d\hat{\rho} \sigma^{(k)}(\hat{\rho})$ ), the leading-log expression grows like  $(2k)!$ , while the full expression grows only geometrically with  $k$ .

The criticism described so far applies to the calculations of soft-gluon effects in heavy-flavour production given in refs. [Laenen92, Laenen94] and [Berger95]. As one may expect, the large factorial terms give rise to large corrections to the cross section. Since the terms of the perturbative expansion grow strongly with the order, they also give large uncertainties. In refs. [Laenen92, Laenen94], the presence of large uncertainties is in fact recognized. In ref. [Berger95] it is claimed that the uncertainties are small. Even there, however, an unphysically large cutoff is needed in order to make sense out of the resummation formulae.

A second, more subtle problem with resummation prescriptions has to do with the presence of  $1/Q$  corrections that arise from infrared renormalons. It was shown in ref. [Beneke95] that soft-gluon resummation does not yield the correct renormalon structure of the Drell–Yan cross section. More precisely, it was shown that in a fully calculable model the soft-gluon approximation yields a  $1/Q$  correction, while in the exact result  $1/Q$  effects are absent. This result suggests the absence of  $1/Q$  corrections in Drell–Yan cross sections, an issue that is still much debated in the literature [Korchemsky95, Dokshitzer95, Akhoury95, Akhoury95a, Akhoury96, Beneke96, Korchemsky96]. We would like to remark, however, that even if  $1/Q$  corrections were present in Drell–Yan and heavy-flavour production, they would only be of the order of 1% for top production at the Tevatron, and also that the result of ref. [Beneke95] shows that the soft-gluon approximation cannot describe them adequately.

It is possible to formulate the resummation of soft gluons in such a way that the kinematic constraints are explicitly satisfied, and no factorial growth arises in the perturbative expansion. It is enough to formulate the resummation problem in the Mellin transform space<sup>13</sup>.

In ref. [Catani96a] a resummation prescription using the Mellin space formula is given. It is shown there that there are, with this prescription, no factorially growing terms in the resummed perturbative expansion. Yet, soft effects are consistently included. This prescription is called “Minimal Prescription” (MP hereafter), because it does not introduce large terms that are not justified by the soft-gluon approximation.

### 5.3 Phenomenological applications

As stated earlier, when using the MP approach, one finds negligible resummation effects in most experimental configurations of interest. In figs. 43, 44 and 45, we plot the quantities

$$\frac{\delta_{gg}}{\sigma_{\text{NLO}}^{(gg)}}, \quad \frac{\delta_{q\bar{q}}}{\sigma_{\text{NLO}}^{(q\bar{q})}}, \quad \frac{\delta_{gg} + \delta_{q\bar{q}}}{\sigma_{\text{NLO}}^{(gg)} + \sigma_{\text{NLO}}^{(q\bar{q})}}. \quad (5.25)$$

Here  $\delta$  is equal to the MP-resummed hadronic cross section in which the terms of order  $\alpha_s^2$  and  $\alpha_s^3$  have been subtracted, and  $\sigma_{\text{NLO}}$  is the full hadronic NLO cross section. Thus, these plots show how important the impact of resummation is beyond the already computed NLO terms. The results for  $b$  production at the Tevatron

---

<sup>13</sup>In fact, resummation formulae are usually derived in Mellin space.

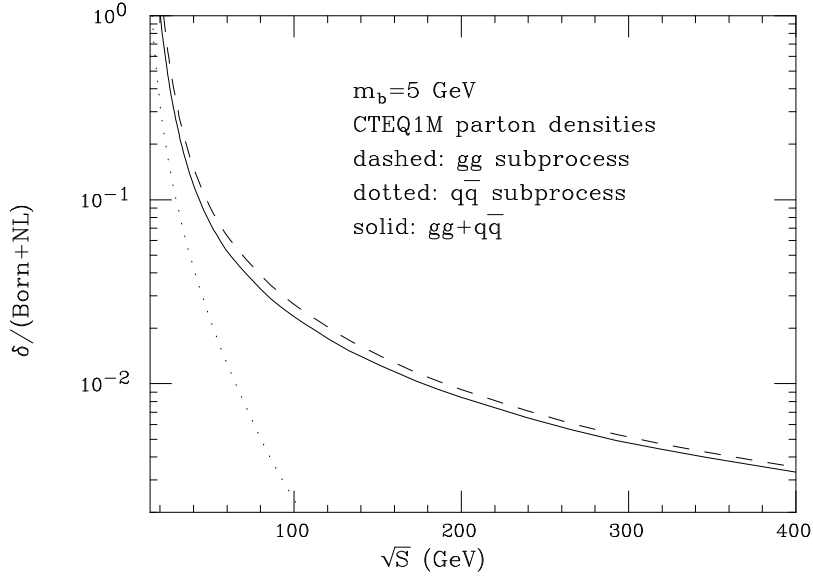


Figure 43: Contribution of gluon resummation at order  $\alpha_s^4$  and higher, relative to the NLO result, for the individual channels and for the total, for bottom production as a function of the CM energy in  $pp$  collisions.

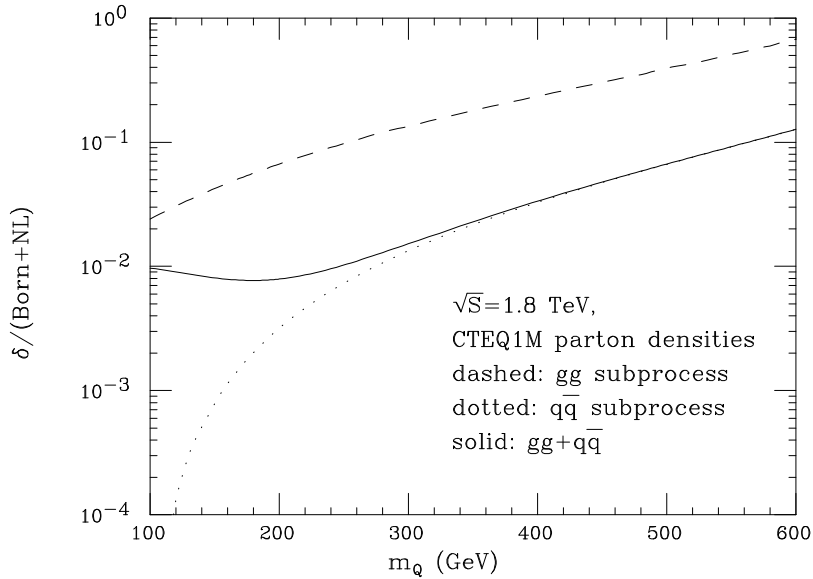


Figure 44: Contribution of gluon resummation at order  $\alpha_s^4$  and higher, relative to the NLO result, for the individual subprocesses and for the total, as a function of the quark mass in  $p\bar{p}$  collisions at 1.8 TeV.

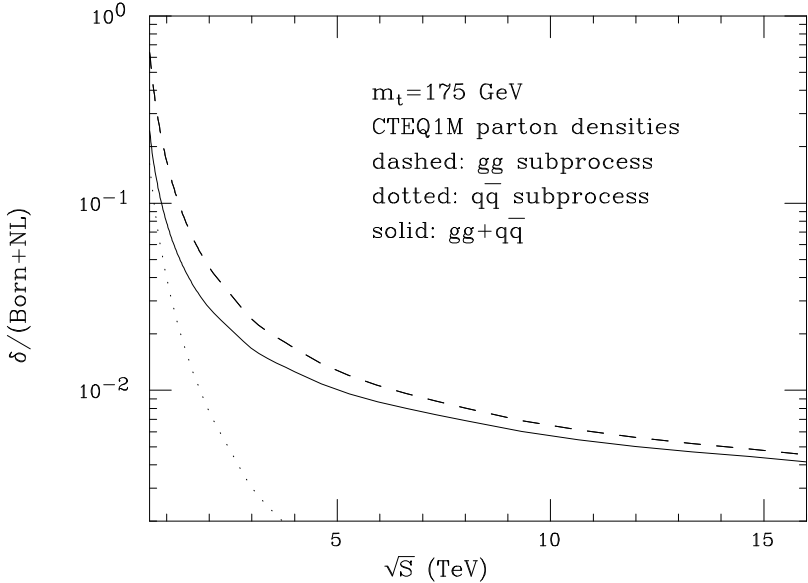


Figure 45: *Contribution of gluon resummation to the top cross section at order  $\alpha_s^4$  and higher, relative to the NLO result, for the individual channels and for the total, as a function of the CM energy in pp collisions.*

can easily be inferred from fig. 43, since the  $q\bar{q}$  component is negligible at Tevatron energies.

For top production (figs. 44 and 45), we see that in most configurations of practical interest, the contribution of resummation is very small, being of the order of 1% at the Tevatron. A complete review of top-quark production at the Tevatron, based upon these findings, has been given in ref. [Catani96]. We also observe that, for top production at the LHC, soft-gluon resummation effects are equally negligible. Of course, in this last case, there are other corrections, not included here, that may need to be considered. Typically, since the values of  $x$  involved are small in this configuration, one may have to worry about the resummation of small- $x$  logarithmic effects [Ellis90, Catani90, Catani91, Collins91].

We see from the figures that in most experimental configurations of interest these effects are fully negligible. One notable exception is  $b$  production at HERA-B, at  $\sqrt{S} = 39.2$  GeV, where we find a 12% increase in the cross section. This correction is however well below the uncertainty due to higher-order radiative effects. For example, from the NLO calculation with the MRSA' [Martin94] parton densities and  $m_b = 4.75$  GeV, we get  $\sigma_{b\bar{b}} = 10.5^{+8.2}_{-4.7}$  nb, a range obtained by varying the renormalization and factorization scales from  $m_b/2$  to  $2m_b$ . Thus the upper bound is 80% higher than the central value, to be compared with a 10% increase from the resummation effects. This result is much less dramatic than the results of ref. [Kidonakis95], obtained using the resummation prescription outlined in [Laenen92].

## 6 HEAVY-FLAVOUR PRODUCTION IN $e^+e^-$ COLLISIONS

### 6.1 Preliminaries

Heavy-flavour physics is a considerable part of the physics programme in  $e^+e^-$  collisions, both at LEP and the SLC. An entire chapter of this book is devoted to this topic [Kuhn97]. We shall limit ourselves here to some QCD aspects of the production dynamics. In particular we will discuss the most recent studies of the  $b$  fragmentation function, the quark-antiquark correlations, and the gluon-splitting production mechanism.

We will not discuss specific topics related to the LEP2 programme. We would like, however, to point out that LEP2 offers the possibility of studying heavy-flavour production in photon-photon collisions. Relevant NLO computations have been performed for both the  $\gamma\gamma$  [Drees93, Kraemer96] and the  $e\gamma$  cases [Laenen96]. Some phenomenological studies have already begun [Aurenche96]. A calculation of heavy-flavour production at high transverse momentum has also been presented [Cacciari96a].

### 6.2 Fragmentation function

Theoretical predictions for fragmentation functions rely essentially upon two ingredients: perturbation theory, and a model for non-perturbative fragmentation effects. A comprehensive discussion of these topics is given in ref. [Nason92]. Leading-order formulae have been available for a long time [Azimov82, Azimov84], while the computation of the NLO perturbative corrections is given in refs. [Mele90, Mele91]. Theoretical studies of the effects of non-perturbative physics are given in refs. [Colangelo92, Randall95, Nason96a]. Here we would like to call attention to the study of ref. [Colangelo92], where a definite prediction was made for the  $b$ -fragmentation function at LEP for various values of  $\Lambda_{\text{QCD}}$ . In fig. 46 we report the predictions of ref. [Colangelo92] together with the data of ref. [Buskulic95]. Observe that the same figures were reported in ref. [Nason92], together with some unpublished L3 data, and at that time the agreement with theory seemed quite poor. Interestingly enough, the position of the peak is well reproduced by the QCD calculation. In general, a value of  $\Lambda_{\text{QCD}}^{(5)}$  between 200 and 300 MeV gives an adequate fit of the data. In ref. [Alexander96] a more detailed fit was performed, using the calculation of ref. [Colangelo92]. The results are shown in fig. 47. There we can see that commonly used parametrizations fail to reproduce the slope of the fragmentation function, while the QCD result is quite consistent with the data. It also turns out that for the larger values of  $\Lambda$  the non-perturbative part of the initial condition is strongly peaked towards large values of  $x$ . This means that, if we can assume that  $\Lambda_{\text{QCD}}^{(5)} \geq 0.25$  GeV, the fragmentation function is largely perturbative, that is to say, is mostly made up of QCD evolution and soft-gluon emission effects [Mele91]. The results of LEP measurements of the fragmentation functions are important also in view of possible applications to collider physics. The problems that are encountered in large transverse momentum

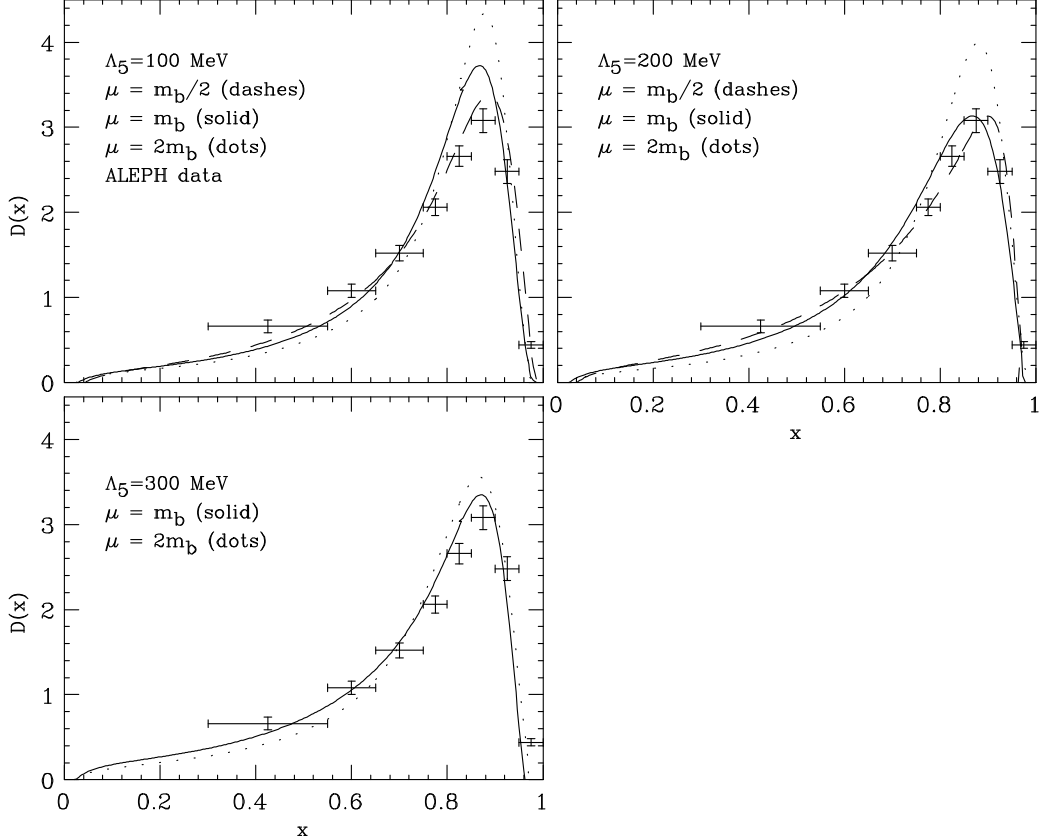


Figure 46: *Theoretical prediction for the  $b$  fragmentation functions at LEP together with ALEPH data. Only the statistical error is shown.*

heavy-flavour production at hadron colliders may be partially due to a lack of proper treatment of the fragmentation effects. The study of the fragmentation function has concentrated in the past on the determination of its second moment (i.e. the average momentum of the  $B$  meson), as measured in  $e^+e^-$  collisions. On the other hand, as pointed out in subsection 4.1,  $b$  production at hadron colliders is also sensitive to higher moments of the fragmentation function. Since the new data from LEP experiments are now also sensitive to higher moments, it would be interesting to perform a new computation of the heavy-flavour production cross section at large transverse momentum, using fragmentation functions that fit the LEP data adequately.

### 6.3 Heavy-quark production via gluon splitting

The importance of the measurement of  $\Gamma_b$  (the width of the  $Z^0$  into  $b\bar{b}$ ) has prompted several experimental and theoretical studies of  $b$ -production characteristics (see, for instance, [Kuhn97]). One important issue is to understand how often  $b\bar{b}$

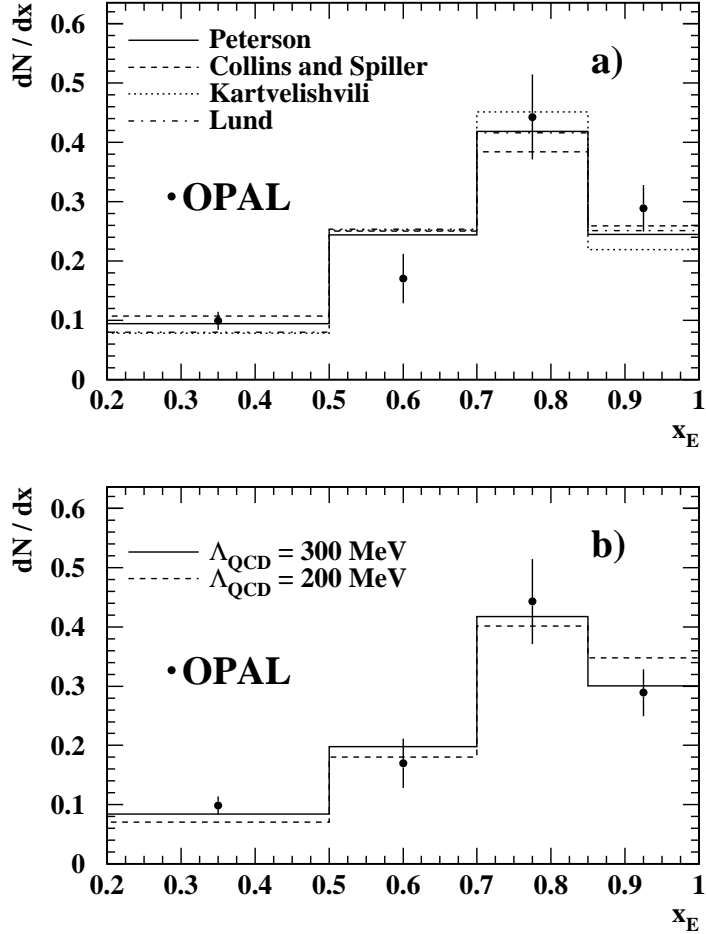


Figure 47: *OPAL results for the  $b$  fragmentation function at LEP.*

or  $c\bar{c}$  pairs are produced indirectly, via a gluon splitting mechanism. Several theoretical studies are available on this topic [Nason92, Mueller86, Mangano92a, Seymour95]. Experimental studies on charm production via gluon splitting have been presented in refs. [Akers95, Akers95a, Hansper96], and a first measurement of  $g \rightarrow b\bar{b}$  has been given in [Branchini96]. The reported values are given in table 5. In ref. [Seymour95] an explicit calculation of these quantities has been performed. Using these results<sup>14</sup> we computed the charm and bottom multiplicities for different values of the masses and of  $\Lambda_5^{\overline{\text{MS}}}$ . We report them in table 5. As can be seen, the averaged experimental result of  $2.38 \pm 0.48\%$  [Przysiezniak96] is consistent with the upper range of the theoretical prediction, preferring lower values of the quark mass, and larger values of  $\Lambda_5^{\overline{\text{MS}}}$ . A similar problem, although much more severe, was mentioned in subsection 4.3.2, in relation to charm jets in hadronic collisions.

As reported in ref. [Seymour95], Monte Carlo models are in qualitative agreement with these results, although the spread of the values they obtain is somewhat larger

<sup>14</sup>We thank M. Seymour for providing us with the relative FORTRAN code.

	$\bar{n}_{g \rightarrow c\bar{c}} \text{ (%)}$	$\bar{n}_{g \rightarrow b\bar{b}} \text{ (%)}$
[Akers95a]	$2.27 \pm 0.28 \pm 0.41$	
[Hansper96]	$2.65 \pm 0.74 \pm 0.51$	
[Branchini96]		$0.22 \pm 0.10 \pm 0.08$
[Seymour95]		
$\Lambda_5^{\overline{\text{MS}}} = 150 \text{ MeV}$	$1.35^{+0.48}_{-0.30}$	$0.20 \pm 0.02$
$\Lambda_5^{\overline{\text{MS}}} = 300 \text{ MeV}$	$1.85^{+0.69}_{-0.44}$	$0.26 \pm 0.03$

Table 5: *Fraction of events containing  $g \rightarrow c\bar{c}$  and  $g \rightarrow b\bar{b}$  subprocesses in  $Z$  decays, as measured by the various collaborations, compared with theoretical predictions. The central values for the theoretical predictions are obtained with  $m_c = 1.5$  and  $m_b = 4.75 \text{ GeV}$ , the upper limits with  $m_c = 1.2$  and  $m_b = 4.5 \text{ GeV}$ , and the lower limits with  $m_c = 1.8$  and  $m_b = 5 \text{ GeV}$ .*

than the theoretical error estimated by the direct calculation. In particular, one finds that while HERWIG [Marchesini92] and JETSET [Sjostrand87] agree quite well with the theoretical calculation, ARIADNE [Lonnblad92] is higher by roughly a factor of 2, and thus is in better agreement with data.

#### 6.4 Correlations

Correlations in the kinematical properties of the  $b$  and  $\bar{b}$  also affect the systematics of the measurement of  $\Gamma_b$ . The most important effect is the correlation in the momentum of the  $b$  and  $\bar{b}$  quark, since detection efficiency is often strongly momentum-dependent. In ref. [Nason96] an explicit leading-logarithmic calculation of the momentum correlation is given. The main result of ref. [Nason96] is the  $\mathcal{O}(\alpha_s)$  formula for the double-inclusive distribution

$$\begin{aligned}
 \frac{d\sigma}{dx_1 dx_2} = & D(x_1)D(x_2) + \frac{2\alpha_s}{3\pi} \int_0^1 dy_1 dy_2 \theta(y_1 + y_2 - 1) \frac{y_1^2 + y_2^2}{(1 - y_1)(1 - y_2)} \times \\
 & \left[ D\left(\frac{x_1}{y_1}\right) D\left(\frac{x_2}{y_2}\right) \frac{1}{y_1 y_2} \theta(y_1 - x_1) \theta(y_2 - x_2) - D(x_1)D\left(\frac{x_2}{y_2}\right) \frac{1}{y_2} \theta(y_2 - x_2) \right. \\
 & \left. - D\left(\frac{x_1}{y_1}\right) D(x_2) \frac{1}{y_1} \theta(y_1 - x_1) + D(x_1)D(x_2) \right], \tag{6.1}
 \end{aligned}$$

where  $D(x)$  is the total heavy-flavour fragmentation function, and  $x_1$  and  $x_2$  are the energy fractions of the two heavy flavoured hadrons ( $x = 2E/\sqrt{S}$ ). As an illustration,

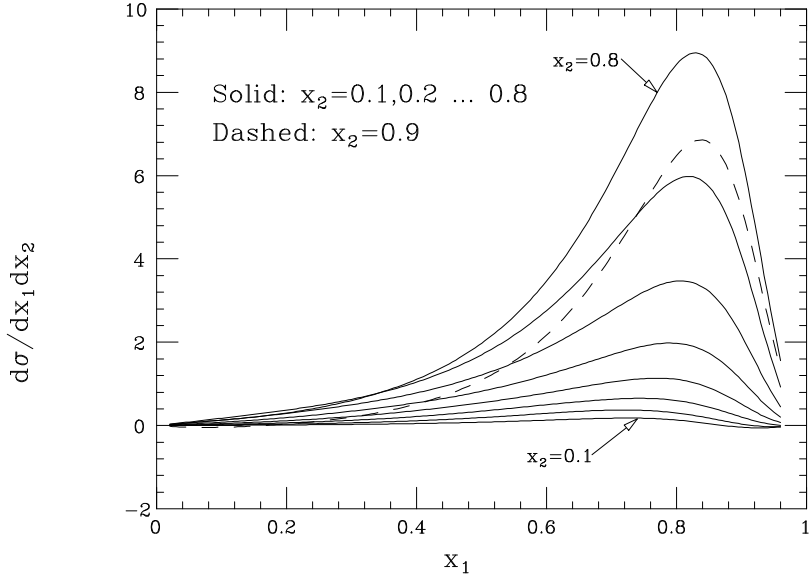


Figure 48: Double inclusive cross section  $d\sigma/dx_1 dx_2$ , plotted as a function of  $x_1$  for several values of  $x_2$ .

we plot in fig. 48 the double-inclusive cross section  $d\sigma/dx_1 dx_2$  as a function of  $x_1$  for several values of  $x_2$ . We use the Peterson parametrization given in eq. (2.9) with  $\epsilon = 0.04$ , which gives  $\langle x \rangle = 0.70$  and  $\alpha_s = 0.12$ . The positive momentum correlation is quite visible in fig. 48. As  $x_2$  increases, the peak of the distribution in  $x_1$  also moves towards larger values. A particularly interesting quantity is the average momentum correlation, defined as

$$r = \frac{\langle x_1 x_2 \rangle - \langle x \rangle^2}{\langle x \rangle^2}. \quad (6.2)$$

This quantity is independent of the fragmentation function, and has therefore an expansion in the strong coupling with finite coefficients, starting at order  $\alpha_s$ . In fact, one gets (in the limit  $m^2/S \rightarrow 0$ )

$$r = 0.1\alpha_s + \mathcal{O}(\alpha_s^2). \quad (6.3)$$

Since the correlation is so small, non-perturbative effects may be competitive with the perturbative ones. For example, if corrections of the order of  $\Lambda_{\text{QCD}}/\sqrt{S}$  were present, this would be the case at LEP energies. In ref. [Nason96a] it was shown that in the renormalon approach power corrections to correlations are suppressed at the level of  $\Lambda_{\text{QCD}}^2/S$  at least. This result, being based upon the renormalon approach, is not fully conclusive. It is however encouraging, since it suggests that the perturbative calculation should be very reliable at LEP energies.

## 7 CONCLUSIONS AND OUTLOOK

We collect here the main conclusions of the various sections, and present our outlook on future progress in the field.

The experimental results on total cross sections for charm production at fixed target are in good agreement with NLO QCD. In the case of hadroproduction the experimental accuracy is far superior to the theoretical accuracy, and might ultimately help in better pinning down the values of the theoretical parameters. For example, current data in pion- and proton-induced reactions strongly disfavour a charm mass value as large as 1.8 GeV. Similar conclusions could not be drawn from a study of the charm photoproduction data. This is because, although the general precision of the data is better than the overall theoretical uncertainty, data from different experiments have a large spread, not obviously compatible with the statistical and systematic uncertainties quoted by the single experiments. Within the large theoretical and experimental uncertainties, the agreement with theoretical expectations is nevertheless good, and consistent with a charm mass value of 1.5 GeV, and with parameters such as  $\Lambda_5^{\overline{\text{MS}}}$  and PDF sets favoured by the hadroproduction studies.

Bottom production in fixed-target experiments is affected by the low statistics available. Even within the statistical uncertainties, there are however conflicting results in the present data. The agreement with theory, afflicted by equally large uncertainties, is therefore at this time not particularly enlightening. These conflicts should be resolved by the current and next generation of high-sensitivity experiments (at FNAL and HERA-B).

While the theoretical description of the total production rates is expected to be insensitive to possible non-perturbative aspects of the production mechanisms, differential distributions for charmed hadrons produced in fixed-target experiments provide an important probe of these phenomena. The overall conclusions of the studies we presented can be summarized as follows. The inclusive  $p_T$  spectra predicted by NLO QCD for charm photoproduction are too hard to agree with the data; they show clear evidence of a non-perturbative fragmentation mechanism that slows down the charmed hadrons. If this fragmentation is then applied to charm hadroproduction, the spectra turn out to be far too soft. The apparent inconsistency can be solved by invoking the effect of an intrinsic non-perturbative  $k_T$  kick of the partons inside the hadron. This  $k_T$  kick makes the  $p_T$  spectrum harder, an effect that is stronger in hadroproduction than in photoproduction because of the presence of two hadrons instead of one in the initial state. The need for a substantial  $k_T$  kick, of the order of 0.7 to 1 GeV, is corroborated by the study of azimuthal correlations of charm pairs, both in photo- and in hadroproduction. There remain indications that a non-perturbative fragmentation slightly softer than the standard Peterson parametrization would provide a better agreement with data. Nevertheless the overall picture is that once these two main effects are accounted for, the qualitative and quantitative features of most of the available distributions are properly described by the theory, independently of the nature of the beam.

Additional non-perturbative effects, such as colour-drag from the beam, should be invoked to properly describe the  $x_F$  distribution at large  $x_F$  and  $D/\overline{D}$  asymmetries. The modelling of colour-drag effects contained in the available Monte Carlo programs can be properly tuned to provide an acceptable description of the data.

Heavy-quark photo- and electroproduction studies at HERA are still in an early stage, with much more statistics waiting to become available in the near future. The current data on charm total cross sections agree with the NLO QCD calculations for choices of parameters consistent with low-energy fixed-target results. However, the current HERA experimental accuracy and the spread of the low-energy photoproduction data are not sufficient as yet to improve our knowledge of the gluon densities of either the proton or the photon. Differential distributions in  $p_T$  and in rapidity have also been presented, and a general agreement with the theory was found. Some discrepancies, as found for example in the rapidity distributions, are not statistically compelling as yet.

Progress in the study of the gluon density of the proton will come when higher statistics, and in particular large samples of charm pairs, will be available. Improved efficiencies at large rapidity and higher statistics will likewise help the understanding of the gluon structure of the photon.

The study of bottom production at the Tevatron shows that there is good agreement between the shape of the  $b$ -quark  $p_T$  distribution predicted by NLO QCD and that observed in the data for central rapidities. A similar conclusion can be reached in the case of the shape of the azimuthal correlations between  $b$  quarks. Although the data rate is higher by a factor of approximately 2 relative to the default choice of theoretical parameters, acceptable choices of  $\Lambda_5^{\overline{\text{MS}}}$  and of renormalization and factorization scales bring the theory in perfect agreement with the data of UA1 and D0, and within 30% of the CDF measurements. It is encouraging that studies of higher-order logarithmic corrections favour the choice of low values for  $\mu_R$  and  $\mu_F$ . The CDF measurements at 630 and 1800 GeV indicate that theory correctly predicts the scaling of the differential  $b$ -quark  $p_T$  distribution between 630 and 1800 GeV, a fact that had often been questioned in the past and now finds strong support.

More theoretical studies should be devoted to the understanding of the non-perturbative fragmentation function for heavy quarks. We showed that the interpretation of the experimental data on the  $p_T$  spectrum depends very strongly on the assumed shape of the fragmentation function. Measurements of the  $b$ -quark content of high- $E_T$  jets, a quantity that is rather independent of the fragmentation properties of the  $b$  quark, indicate a good agreement between data and theory. This suggests that residual discrepancies in the comparison of theory and data for the  $p_T$  spectra, and possibly for the azimuthal correlations, could be resolved with a better understanding of the fragmentation phenomena.

No surprise has so far come up in the comparison of the data on top production with the predictions of NLO perturbative QCD. Given the claimed accuracy of the theoretical predictions, which in the case of the total cross section is of the order of 10%, only additional statistics will make these comparisons more compelling. We

remark here that, on the theoretical side, soft-gluon resummation effects have been found to be much less important than previously thought. Furthermore, the  $\alpha_s$  dependence of the top cross section is quite small, because of a compensation mechanism due to structure-function evolution effects. Thus, the theoretical error on the cross section is quite credible in this case. Detailed features of the structure of the final state in top production, such as studies of the jet activity, have so far been probed only indirectly in the context of the mass measurements. It is likely that a lot will be learned in the future from these more detailed analyses, and that significant progress will be made in their MC modelling.

Considerable progress has been made in the study of heavy-flavour production in  $e^+e^-$  annihilation. The measurement of the  $B$  fragmentation function at LEP has reached a remarkable level of accuracy. Some details of the production mechanism, particularly important for the determination of  $\Gamma_b$  have received special attention. Thus, the heavy-flavour production by the gluon-splitting mechanism has been studied both experimentally and theoretically, and analytical calculations of the correlations of the heavy-flavour pair have been performed. Besides their intrinsic value,  $e^+e^-$  studies could clarify several aspects of the production mechanism, which are important also at hadron colliders.

### **Acknowledgements**

We wish to thank J. Appel, D. Barberis, T. Carter, R. Eichler, C. Grab, C. Harris, D. Harris, K. Harrison, P. Koehn, E. Laenen, B. Ossulati, H. Przysiezniak, L. Rossi and M. Seymour for useful conversations, for information relative to experimental results, for suggestions, and for providing us with useful computer programs. Part of the material presented in this review is taken from work done by some of us in collaboration with S. Catani, G. Colangelo, C. Oleari and L. Trentadue.

## REFERENCES

[Abachi95] S. Abachi et al., D0 Coll., *Phys. Rev. Lett.* **74**(1995)2632, [hep-ex/9503003](#).

[Abachi95a] S. Abachi et al., D0 Coll., *Phys. Rev. Lett.* **74**(1995)3548.

[Abachi96] S. Abachi et al., D0 Coll., *Phys. Lett.* **B370**(1996)239.

[Abachi96a] S. Abachi et al., D0 Coll., submitted to the Int. Conf. on High Energy Physics, Warsaw, 1996, paper Pa05-023.

[Abachi96b] S. Abachi et al., D0 Coll., submitted to the Int. Conf. on High Energy Physics, Warsaw, 1996, paper Pa05-025.

[Abachi96d] S. Abachi et al., D0 Coll., Fermilab-Conf-96/258-E.

[Abe92] F. Abe et al., CDF Coll., *Phys. Rev. Lett.* **68**(1992)1104.

[Abe92a] F. Abe et al., CDF Coll., *Phys. Rev. Lett.* **68**(1992)3403.

[Abe92b] F. Abe et al., CDF Coll., *Phys. Rev. Lett.* **69**(1992)3704.

[Abe93] F. Abe et al., CDF Coll., *Phys. Rev. Lett.* **71**(1993)500.

[Abe93a] F. Abe et al., CDF Coll., *Phys. Rev. Lett.* **71**(1993)2396.

[Abe93b] F. Abe et al., CDF Coll., *Phys. Rev. Lett.* **71**(1993)2537.

[Abe94] F. Abe et al., CDF Coll., *Phys. Rev.* **D50**(1994)2966.

[Abe94a] F. Abe et al., CDF Coll., Fermilab-Pub-94/131-E.

[Abe95] F. Abe et al., CDF Coll., *Phys. Rev. Lett.* **74**(1995)2626, [hep-ex/9503002](#).

[Abe95a] F. Abe et al., CDF Coll., *Phys. Rev. Lett.* **75**(1995)1451, [hep-ex/9503013](#).

[Abe96] F. Abe et al., CDF Coll., *Phys. Rev. Lett.* **77**(1996)438, [hep-ex/9601008](#).

[Abe96a] F. Abe et al., CDF Coll., CDF/PHYS/BOTTOM/PUBLIC/3733, submitted to the Int. Conf. on High Energy Physics, Warsaw, 1996.

[Abe96b] F. Abe et al., CDF Coll., *Phys. Rev.* **D53**(1996)1051, [hep-ex/9508017](#).

[Abe96c] F. Abe et al., CDF Coll., *Phys. Rev.* **D54**(1996)6596, [hep-ex/9607003](#).

[Abe96d] F. Abe et al., CDF Coll., Fermilab-Pub-96/216-E, to appear in *Phys. Rev.* **D**.

[Abe96e] F. Abe et al., CDF Coll., *Phys. Rev. Lett.* **77**(1996)5005.

[Abe96f] F. Abe et al., CDF Coll., Fermilab-Pub-96/198-E.

[Abramowicz91] H. Abramowicz, K. Charchula and A. Levy, *Phys. Lett.* **269B**(1991)458.

[Adamovich87] M.I. Adamovich et al., Photon Emulsion Coll., *Phys. Lett.* **B187**(1987)437 and references therein.

[Adamovich92] M.I. Adamovich et al., WA82 Coll., *Nucl. Phys. (Proc. Suppl.)* **B27**(1992)212.

[Adamovich95] M.I. Adamovich et al., WA92 Coll., *Phys. Lett.* **B348**(1995)256.

[Adamovich96] M.I. Adamovich et al., WA92 Coll., preprint CERN-PPE/96-180, submitted to *Nucl. Phys. B*.

[Adamovich96a] M.I. Adamovich et al., WA92 Coll., *Phys. Lett.* **B385**(1996)487.

[Adloff96] C. Adloff et al., H1 Coll., DESY-96-138, *hep-ex/9607012*, to appear in *Z. Phys. C*.

[Aguilar85a] M. Aguilar-Benitez et al., LEBC-EHS Coll., *Phys. Lett.* **B161**(1985)400.

[Aguilar85b] M. Aguilar-Benitez et al., LEBC-EHS Coll., *Phys. Lett.* **B164**(1985)404.

[Aguilar88] M. Aguilar-Benitez et al., LEBC-EHS Coll., *Z. Phys. C* **40**(1988)321.

[Ahmed95] T. Ahmed et al., H1 Coll., *Nucl. Phys.* **B445**(1995)195, *hep-ex/9504004*.

[Aid96] S. Aid et al., H1 Coll., *Nucl. Phys.* **B472**(1996)32, *hep-ex/9604005*.

[Aitala96] E.M. Aitala et al., E791 Coll., *Phys. Lett.* **B371**(1996)157, *hep-ex/9601001*.

[Aitala96a] E.M. Aitala et al., E791 Coll., Fermilab-Pub-96-206-E, submitted to *Phys. Rev. Lett.*.

[Aivazis94] M.A.G. Aivazis, F.I. Olness and Wu-Ki Tung, *Phys. Rev.* **D50**(1994)3085, *hep-ph/9312318*.

[Aivazis94a] M.A.G. Aivazis, J.C. Collins, F.I. Olness and Wu-Ki Tung, *Phys. Rev.* **D50**(1994)3102, *hep-ph/9312319*.

[Akers95] R. Akers et al., OPAL Coll., *Z. Phys. C* **67**(1995)27.

[Akers95a] R. Akers et al., OPAL Coll., *Phys. Lett.* **B353**(1995)595.

[Akhouri95] R. Akhouri and V.I. Zakharov, *Phys. Lett.* **B357**(1995)646, *hep-ph/9504248*.

[Akhoury95a] R. Akhoury and V.I. Zakharov, *Phys. Rev. Lett.* **76**(1996)2238, [hep-ph/9512433](#).

[Akhoury96] R. Akhoury, L. Stodolsky and V.I. Zakharov, MPI-Ph/96-88, UM-TH-96-14, [hep-ph/9609368](#).

[Alam96] S. Alam, K. Hagiwara and S. Matsumoto, [hep-ph/9607466](#), to appear in *Phys. Rev. D*.

[Albajar91] C. Albajar et al., UA1 Coll., *Phys. Lett.* **B256**(1991)121, erratum *ibid.* **B262**(1991)497.

[Albajar94] C. Albajar et al., UA1 Coll., *Z. Phys. C* **61**(1994)41.

[Albajar96] C. Albajar et al., UA1 Coll., *Phys. Lett.* **B369**(1996)46.

[Alexander96] G. Alexander et al., OPAL Coll., *Phys. Lett.* **B369**(1996)163.

[Altarelli77] G. Altarelli and G. Parisi, *Nucl. Phys.* **B126**(1977)298.

[Alvarez92] M.P. Alvarez et al., NA14/2 Coll., *Phys. Lett.* **B278**(1992)385.

[Alvarez93] M.P. Alvarez et al., NA14/2 Coll., *Z. Phys. C* **60**(1993)53.

[Alvero95] L. Alvero and H. Contopanagos, *Nucl. Phys.* **B436**(1995)184, [hep-ph/9407293](#).

[Alves92] G.A. Alves et al., E769 Coll., *Phys. Rev. Lett.* **69**(1992)3147.

[Alves96] G.A. Alves et al., E769 Coll., *Phys. Rev. Lett.* **77**(1996)2388.

[Alves96a] G.A. Alves et al., E769 Coll., *Phys. Rev. Lett.* **77**(1996)2392.

[Amidei96] D. Amidei and R. Brock, eds., Report of the TeV2000 Study Group, Fermilab-Pub-96/082.

[Ammar88] R. Ammar et al., LEBC-MPS Coll., *Phys. Rev. Lett.* **61**(1988)2185.

[Anjos89] J.C. Anjos et al., E691 Coll., *Phys. Rev. Lett.* **62**(1989)513.

[Anjos90] J.C. Anjos et al., E691 Coll., *Phys. Rev. Lett.* **65**(1990)2503.

[Aoki88] S. Aoki et al., WA75 Coll., *Phys. Lett.* **B209**(1988)113.

[Aoki92] S. Aoki et al., WA75 Coll., *Progr. Theor. Phys.* **87**(1992)1305.

[Aoki92a] S. Aoki et al., WA75 Coll., *Progr. Theor. Phys.* **87**(1992)1315, erratum *ibid.* **88**(1992)621; *Phys. Lett.* **B209**(1988)113.

[Appel88] D. Appel, G. Sterman and P. Mackenzie, *Nucl. Phys.* **B309**(1988)259.

[Aurenche92] P. Aurenche et al., *Z. Phys.* **C56**(1992)589.

[Aurenche94] P. Aurenche, M. Fontannaz and J.P. Guillet, *Z. Phys.* **C64**(1994)621, [hep-ph/9406382](#).

[Aurenche96] P. Aurenche and G.A. Schuler (conveners) et al., “ $\gamma\gamma$  physics”, [hep-ph/9601317](#), in Physics at LEP2, eds. G. Altarelli, T. Sjöstrand and F. Zwirner, (CERN 96-01, Geneva, 1996), vol. 1, p. 291.

[Aversa89] F. Aversa, P. Chiappetta, M. Greco and J.P. Guillet, *Nucl. Phys.* **B327**(1989)105.

[Aversa90a] F. Aversa, P. Chiappetta, M. Greco and J.P. Guillet, *Phys. Rev. Lett.* **65**(1990)401.

[Azimov82] Ya.I. Azimov, Yu.L. Dokshitzer and V.A. Khoze, *Sov. J. Nucl. Phys.* **36**(1982)878.

[Azimov84] Ya.I. Azimov et al., *Sov. J. Nucl. Phys.* **40**(1984)498.

[Bailey96] B. Bailey, E.L. Berger and L.E. Gordon, *Phys. Rev.* **D54**(1996)1896, [hep-ph/9602373](#).

[Bardeen79] W.A. Bardeen and A.J. Buras, *Phys. Rev.* **D20**(1979)166.

[Bari91] G. Bari et al., *Nuovo Cimento* **104A**(1991)1787.

[Barlag88] S. Barlag et al., ACCMOR Coll., *Z. Phys.* **C39**(1988)451.

[Barlag91] S. Barlag et al., ACCMOR Coll., *Z. Phys.* **C49**(1991)555.

[Barlag91a] S. Barlag et al., ACCMOR Coll., *Phys. Lett.* **B257**(1991)519.

[Barnett96] Particle Data Group, R.M. Barnett et al., *Phys. Rev.* **D54**(1996)1.

[Basile81] M. Basile et al., *Nuovo Cimento* **65A**(1981)391.

[Baur93] U. Baur, F. Halzen, S. Keller, M.L. Mangano and K. Riesselmann, *Phys. Lett.* **B318**(1993)544, [hep-ph/9308370](#).

[Bawa89] A.C. Bawa and W.J. Stirling, *J. Phys.* **G15**(1989)1339.

[Beenakker89] W. Beenakker, H. Kuijf, W.L. van Neerven and J. Smith, *Phys. Rev.* **D40**(1989)54.

[Beenakker91] W. Beenakker, W. L. van Neerven, R. Meng, G. A. Schuler and J. Smith, *Nucl. Phys.* **B351**(1991)507.

[Beenakker94] W. Beenakker, A. Denner, W. Hollik, R. Mertig, T. Sack and D. Wackerlo, *Nucl. Phys.* **B411**(1994)343.

[Bellini94] G. Bellini, Proc. of Les Rencontres de Physique de la Vallée d'Aoste, La Thuile, 1994.

[Beneke95] M. Beneke and V.M. Braun, *Nucl. Phys.* **B454**(1995)253, [hep-ph/9506452](#).

[Beneke96] M. Beneke, SLAC-PUB-7277, [hep-ph/9609215](#), presented at the Int. Conf. on High Energy Physics, Warsaw, 1996.

[Berger95] E. Berger and H. Contopanagos, *Phys. Lett.* **B361**(1995)115, [hep-ph/9507363](#).

[Berger96] E. Berger and H. Contopanagos, *Phys. Rev.* **D54**(1996)3085, [hep-ph/9603326](#).

[Blazey96] G. Blazey, for the D0 Coll., presented at the Rencontres de Moriond on QCD and Hadronic Interactions, Les Arcs, 1996.

[Bordalo88] P. Bordalo et al., NA10 Coll., *Z. Phys.* **C39**(1988)7.

[Bordes95] G. Bordes and B. van Eijk, *Nucl. Phys.* **B435**(1995)23.

[Borzumati93] F. Borzumati and G.A. Schuler, *Z. Phys.* **C58**(1993)139.

[Botts93] J. Botts et al., *Phys. Lett.* **B304**(1993)159, [hep-ph/9303255](#).

[Branchini96] P. Branchini and E. Graziani, DELPHI Coll., Preprint DELPHI 96-112 CONF 39, talk given at the Int. Conf. on High Energy Physics, Warsaw, 1996.

[Brodsky80] S.J. Brodsky et al., *Phys. Lett.* **B93**(1980)451.

[Buchmueller91] W. Buchmüller and G. Ingelman, eds., Proc. Workshop on Physics at HERA, DESY, Hamburg, 1991.

[Budnev74] V.M. Budnev et al., *Phys. Rep.* **C15**(1974)181.

[Buskulic95] D. Buskulic et al., ALEPH Coll., *Phys. Lett.* **B357**(1995)699.

[Cacciari94] M. Cacciari and M. Greco, *Nucl. Phys.* **B421**(1994)530, [hep-ph/9311260](#).

[Cacciari96] M. Cacciari and M. Greco, *Z. Phys.* **C69**(1996)459, [hep-ph/9505419](#).

[Cacciari96a] M. Cacciari, M. Greco, B.A. Kniehl, M. Krämer, G. Kramer and M. Spira, *Nucl. Phys.* **B466**(1996)173, [hep-ph/9512246](#).

[Cacciari96b] M. Cacciari, M. Greco, S. Rolli and A. Tanzini, preprint DESY-96-146, [hep-ph/9608213](#).

[Campagnari96] C. Campagnari and M. Franklin, preprint UCSB-HEP-96-01, [hep-ex/9608003](#), to appear in *Rev. Mod. Phys.*

[Caner96] A. Caner, for the CDF Coll., Fermilab-Proc-96/208-E, presented at the 10th Rencontres de Physique de la Vallée d'Aoste, La Thuile, 1996.

[Carter96] T. Carter, for the E791 Coll., presented at the Workshop on Heavy Quarks at Fixed Target, St. Goar, Germany, 1996.

[Casalbuoni96] R. Casalbuoni et al., *Z. Phys.* **C69**(1996)519, [hep-ph/9505212](#).

[Catanesi89] M.G. Catanesi et al., WA78 Coll., *Phys. Lett.* **231B**(1989)328.

[Catani89] S. Catani and L. Trentadue, *Nucl. Phys.* **B327**(1989)323.

[Catani90] S. Catani, M. Ciafaloni and F. Hautmann, *Phys. Lett.* **B242**(1990)97.

[Catani91] S. Catani, M. Ciafaloni and F. Hautmann, *Nucl. Phys.* **B366**(1991)135.

[Catani96] S. Catani, M.L. Mangano, P. Nason and L. Trentadue, *Phys. Lett.* **B378**(1996)329, [hep-ph/9602208](#).

[Catani96a] S. Catani, M.L. Mangano, P. Nason and L. Trentadue, *Nucl. Phys.* **B478**(1996)273, [hep-ph/9604351](#).

[Chrin87] J. Chrin, *Z. Phys.* **C36**(1987)163.

[Colangelo92] G. Colangelo and P. Nason, *Phys. Lett.* **B285**(1992)167.

[Collins86] J.C. Collins and Wu-Ki Tung, *Nucl. Phys.* **B278**(1986)934.

[Collins89] For a review, see J.C. Collins, D.E. Soper and G. Sterman, in *Perturbative Quantum Chromodynamics*, ed. A.H. Mueller (World Scientific, Singapore, 1989) and references therein.

[Collins91] J. C. Collins and R. K. Ellis, *Nucl. Phys.* **B360**(1991)3.

[Combridge79] B.L. Combridge, *Nucl. Phys.* **B151**(1979)429.

[Contopanagos94] H. Contopanagos and G. Sterman, *Nucl. Phys.* **B419**(1994)77, [hep-ph/9310313](#).

[Contopanagos96] H. Contopanagos, E. Laenen and G. Sterman, ANL-HEP-25, [hep-ph/9604313](#).

[Cortese91] S. Cortese and R. Petronzio, *Phys. Lett.* **B253**(1991)494.

[Dawson85] S. Dawson, *Nucl. Phys.* **B284**(1985)449.

[Derrick95] M. Derrick et al., ZEUS Coll., *Phys. Lett.* **349B**(1995)225, [hep-ex/9502002](#).

[DeWitt79] R.J. DeWitt, L.M. Jones, J.D. Sullivan, D.E. Willen and H.D. Wyld, *Phys. Rev.* **D19**(1979)2046.

[Dokshitzer95] Yu.L. Dokshitzer, G. Marchesini and B.R. Webber, CERN-TH-95-281, [hep-ph/9512336](#).

[Drees93] M. Drees, M. Krämer, J. Zunft and P. Zerwas, *Phys. Lett.* **B306**(1993)371.

[Drees94] M. Drees and R.M. Godbole, *Phys. Rev.* **D50**(1994)3124, [hep-ph/9403229](#).

[Eichler96] R. Eichler and S. Frixione, [hep-ph/9609337](#), to appear in Proc. Workshop on Future Physics at HERA, eds. G. Ingelman, A. De Roeck and R. Klanner, DESY, Hamburg, 1996.

[Eichten94] E. Eichten and K. Lane, *Phys. Lett.* **B327**(1994)129, [hep-ph/9401236](#).

[Ellis79] R.K. Ellis, H. Georgi, M. Machacek, H.D. Politzer and G.G. Ross, *Nucl. Phys.* **B152**(1979)285.

[Ellis88] R. K. Ellis and Z. Kunszt, *Nucl. Phys.* **B303**(1988)653.

[Ellis89] R. K. Ellis and P. Nason, *Nucl. Phys.* **B312**(1989)551.

[Ellis89S] S. Ellis, Z. Kunszt and D. Soper, *Phys. Rev.* **D40**(1989)2188.

[Ellis90] R.K. Ellis and D.A. Ross, *Nucl. Phys.* **B345**(1990)79.

[Ellis90S] S. Ellis, Z. Kunszt and D. Soper, *Phys. Rev. Lett.* **64**(1990)2121.

[Ellis91] R.K. Ellis, *Phys. Lett.* **B259**(1991)492.

[Ellis92] R.K. Ellis and S.J. Parke, *Phys. Rev.* **D46**(1992)3785.

[Fadin90] V. Fadin, V. Khoze and T. Sjöstrand, *Z. Phys.* **C48**(1990)613.

[Fletcher89] R.S. Fletcher, F. Halzen and E. Zas, *Phys. Lett.* **B221**(1989)403.

[Frabetti93] P. Frabetti et al., E687 Coll., *Phys. Lett.* **B308**(1993)193.

[Frabetti96] P.L. Frabetti et al., E687 Coll., *Phys. Lett.* **B370**(1996)222.

[Frixione93] S. Frixione, M.L. Mangano, P. Nason and G. Ridolfi, *Phys. Lett.* **319B**(1993)339, [hep-ph/9310350](#).

[Frixione93a] S. Frixione, M.L. Mangano, P. Nason and G. Ridolfi, *Phys. Lett.* **B308**(1993)137, [hep-ph/9304289](#).

[Frixione94] S. Frixione, M.L. Mangano, P. Nason and G. Ridolfi, *Nucl. Phys.* **B431**(1994)453.

[Frixione94a] S. Frixione, M.L. Mangano, P. Nason and G. Ridolfi, *Nucl. Phys.* **B412**(1994)225, [hep-ph/9306337](#).

[Frixione95] S. Frixione, M.L. Mangano, P. Nason and G. Ridolfi, *Phys. Lett.* **B351**(1995)555, [hep-ph/9503213](#).

[Frixione95a] S. Frixione, P. Nason and G. Ridolfi, *Nucl. Phys.* **B454**(1995)3, [hep-ph/9506226](#).

[Frixione95b] S. Frixione, M.L. Mangano, P. Nason and G. Ridolfi, *Phys. Lett.* **B348**(1995)633, [hep-ph/9412348](#).

[Frixione96] S. Frixione and M.L. Mangano, preprint CERN-TH/96-85, ETH-TH/96-09, [hep-ph/9605270](#), to appear in *Nucl. Phys.* **B**.

[Frixione96a] S. Frixione, [hep-ph/9607333](#), to appear in Proc. XI Topical Workshop on  $p\bar{p}$  Collider Physics, Abano Terme, Italy, 1996.

[Frixione96b] S. Frixione and G. Ridolfi, *Phys. Lett.* **B383**(1996)227, [hep-ph/9605209](#).

[Galtieri96] A. Galtieri, for the CDF Coll., FERMILAB-CONF-96/146-E, presented at the XXXI Rencontres de Moriond on QCD and High Energy Hadronic Interactions, Les Arcs, France, 1996.

[Geiser92] A. Geiser, PhD thesis, RWTH Aachen, 1992, Aachen Report PITHA 92/31.

[Giele94] W.T. Giele, E.W.N. Glover and D.A. Kosower, *Phys. Rev. Lett.* **73**(1994)2019, [hep-ph/9403347](#).

[Giele96] W.T. Giele, S. Keller and E. Laenen, *Phys. Lett.* **B372**(1996)141, [hep-ph/9511449](#).

[Glover96] E.N. Glover, A.D. Martin, R.G. Roberts and W.J. Stirling, *Phys. Lett.* **B381**(1996)353, [hep-ph/9603327](#).

[Gluck88] M. Glück and E. Reya, *Z. Phys.* **C39**(1988)569.

[Gluck91] M. Glück, E. Reya and W. Vogelsang, *Nucl. Phys.* **B351**(1991)579.

[Gluck92] M. Glück, E. Reya and A. Vogt, *Phys. Rev.* **D45**(1992)3986.

[Gluck92a] M. Glück, E. Reya and A. Vogt, *Phys. Rev.* **D46**(1992)1973.

[Gordon92] L.E. Gordon and J.K. Storrow, *Z. Phys.* **C56**(1992)307.

[Gordon96] L.E. Gordon and J.K. Storrow, ANL-HEP-PR-96-33, MC-TH-96-16, [hep-ph/9607370](#).

[Grannis96] P. Grannis, presented at the Int. Conf. on High Energy Physics, Warsaw, 1996.

[Hagiwara95] K. Hagiwara, M. Tanaka, I. Watanabe and T. Izubuchi, *Phys. Rev.* **D51**(1995)3197, [hep-ph/9406252](#).

[Hansper96] G. Hansper, for the ALEPH Coll., submitted to the Int. Conf. on High Energy Physics, Warsaw, 1996, Pa05-065.

[Harlander95] R. Harlander, M. Jezabek and J.H. Kühn, *Acta Phys. Polon.* **27**(1996)1781, [hep-ph/9506292](#).

[Harris95] B.W. Harris and J. Smith, *Nucl. Phys.* **B452**(1995)109, [hep-ph/9503484](#).

[Harris95a] B.W. Harris and J. Smith, *Phys. Lett.* **B353**(1995)535, [hep-ph/9502312](#).

[Harris96] D. Harris, for the CCFR Coll., presented at the Int. Conf. on High Energy Physics, Warsaw, 1996, Pa03-031.

[Hill94] C.T. Hill and S.J. Parke, *Phys. Rev.* **D49**(1994)4454, [hep-ph/9312324](#).

[Holdom95] B. Holdom and M.V. Ramana, *Phys. Lett.* **B353**(1995)295, [hep-ph/9504403](#).

[Huston95] J. Huston et al., *Phys. Rev. Lett.* **77**(1996)444, [hep-ph/9511386](#).

[Huth91] J. Huth et al., Proc. Summer Study on High Energy Physics: Research Directions for the Decade, Snowmass, CO, 1990, ed. E. Berger (World Scientific, Singapore, 1991), p. 134.

[Ingelman96] G. Ingelman, A. De Roeck and R. Klanner, eds., Proc. Workshop on Future Physics at HERA, DESY, Hamburg, 1996.

[Jansen95] D.M. Jansen et al., E605 Coll., *Phys. Rev. Lett.* **74**(1995)3118.

[Jesik95] R. Jesik et al., E672-E706 Coll., *Phys. Rev. Lett.* **74**(1995)495.

[Kane96] G. Kane and S. Mrenna, *Phys. Rev. Lett.* **77**(1996)3502, [hep-ph/9605351](#).

[Kao93] C. Kao, G.A. Ladinsky and C.P. Yuan, FSU-HEP-930508, [hep-ph/9305270](#).

[Kaplan94] D.M. Kaplan and S. Kwan, eds., FERMILAB-CONF-94/190, C94/06/07.1, Proc. Workshop on the Future of High Sensitivity Charm Experiments: CHARM2000, Batavia, Ill. 1994.

[Kidonakis95] N. Kidonakis and J. Smith, ITP-SB-95-16, [hep-ph/9506253](#).

[Kidonakis96] N. Kidonakis and G. Sterman, ITP-SB-97-7, [hep-ph/9604234](#).

[Kim96] J. Kim, J. Lopez, D. Nanopoulos and R. Rangarajan, *Phys. Rev. D* **54**(1996)4364, [hep-ph/9605419](#).

[Kniehl95] B.A. Kniehl, M. Krämer, G. Kramer and M. Spira, *Phys. Lett. B* **356**(1995)539.

[Kniehl96] B. A. Kniehl, G. Kramer and M. Spira, CERN-TH/96-274, [hep-ph/9610267](#).

[Kodama91] K. Kodama et al., E653 Coll., *Phys. Lett. B* **263**(1991)573.

[Kodama91a] K. Kodama et al., E653 Coll., *Phys. Lett. B* **263**(1991)579.

[Kodama92] K. Kodama et al., E653 Coll., *Phys. Lett. B* **284**(1992)461.

[Kodama93] K. Kodama et al., E653 Coll., *Phys. Lett. B* **303**(1993)359.

[Koehn95] P. Koehn, for the CDF Coll., presented at the CTEQ Workshop on Collider Physics, Michigan State University, East Lansing, 1995.

[Korchemsky95] G.P. Korchemsky and G. Sterman, *Nucl. Phys. B* **437**(1995)415, [hep-ph/9411211](#).

[Korchemsky96] G.P. Korchemsky, talk given at the Int. Conf. on High Energy Physics, Warsaw, 1996.

[Kraemer96] M. Krämer and E. Laenen, *Phys. Lett. B* **371**(1996)303, [hep-ph/9511358](#).

[Kuhn97] J.H. Kühn and P.M. Zerwas, “Heavy flavours in  $e^+e^-$ ”, in this book.

[Kunszt84] Z. Kunszt, *Nucl. Phys. B* **247**(1984)339.

[Laenen92] E. Laenen, J. Smith and W.L. van Neerven, *Nucl. Phys. B* **369**(1992)543.

[Laenen92a] E. Laenen, S. Riemersma, J. Smith and W.L. van Neerven, *Phys. Lett. B* **291**(1992)325.

[Laenen93] E. Laenen, S. Riemersma, J. Smith and W.L. van Neerven, *Nucl. Phys. B* **392**(1993)162.

[Laenen93a] E. Laenen, S. Riemersma, J. Smith and W.L. van Neerven, *Nucl. Phys. B* **392**(1993)229.

[Laenen94] E. Laenen, J. Smith and W.L. van Neerven, *Phys. Lett. B* **321**(1994)254, [hep-ph/9310233](#).

[Laenen96] E. Laenen and S. Riemersma, *Phys. Lett.* **B376**(1996)169, [hep-ph/9602258](#).

[Laenen96a] E. Laenen et al., in Proc. Workshop on Future Physics at HERA, eds. G. Ingelman, A. De Roeck and R. Klanner, DESY, Hamburg, 1996.

[Lai96] H.L. Lai et al., MSUHEP-60426, CTEQ-604, [hep-ph/9606399](#).

[Lai97] H.L. Lai and W.K. Tung, MSU-HEP-61222, [hep-ph/9701256](#).

[Leitch94] M.J. Leitch et al., E789 Coll., *Phys. Rev. Lett.* **72**(1994)2542.

[Levin91] E. M. Levin, M. G. Ryskin and Yu. M. Shabelsky, *Phys. Lett.* **B260**(1991)429.

[Li95] C.S. Li et al., *Phys. Rev.* **D52**(1995)5014, erratum *ibid.* **53**(1996)4112.

[Li96] C.S. Li et al., [hep-ph/9606271](#).

[Llewellyn78] C.H. Llewellyn Smith, *Phys. Lett.* **B79**(1978)83.

[Lonnblad92] L. Lönnblad, *Comput. Phys. Commun.* **71**(1992)15.

[Mangano92] M.L. Mangano, P. Nason and G. Ridolfi, *Nucl. Phys.* **B373**(1992)295.

[Mangano92a] M.L. Mangano and P. Nason, *Phys. Lett.* **B285**(1992)160.

[Mangano93] M.L. Mangano, P. Nason and G. Ridolfi, *Nucl. Phys.* **B405**(1993)507.

[Mangano93a] M.L. Mangano, *Nucl. Phys.* **B405**(1993)536.

[Mangano94] M.L. Mangano, [hep-ph/9311378](#), Proc. IX Topical Workshop on Proton-Antiproton Collider Physics, eds. K. Kondo and S. Kim, (Universal Academy Press, Tokyo, 1994), p. 181.

[Marchesini88] G. Marchesini and B.R. Webber, *Nucl. Phys.* **B310**(1988)461.

[Marchesini92] G. Marchesini, B.R. Webber, G. Abbiendi, I.G. Knowles, M.H. Seymour and L. Stanco, *Comput. Phys. Commun.* **67**(1992)465.

[Martin94] A.D. Martin, R.G. Roberts and W.J. Stirling, *Phys. Rev.* **D50**(1994)6734, [hep-ph/9406315](#).

[Martin95] A.D. Martin, R.G. Roberts and W.J. Stirling, *Phys. Lett.* **B354**(1995)155, [hep-ph/9502336](#).

[Martin95a] A.D. Martin, R.G. Roberts and W.J. Stirling, *Phys. Lett.* **B356**(1995)89, [hep-ph/9506423](#).

[Martin96] A.D. Martin, R.G. Roberts, M.G. Ryskin and W.J. Stirling, DTP-96-102, [hep-ph/9612449](#).

[Mele90] B. Mele and P. Nason, *Phys. Lett.* **245B**(1990)635.

[Mele91] B. Mele and P. Nason, *Nucl. Phys.* **B361**(1991)626.

[Mueller85] A.H. Mueller and P. Nason, *Phys. Lett.* **157B**(1985)226.

[Mueller86] A.H. Mueller and P. Nason, *Nucl. Phys.* **B266**(1986)265.

[Narain96] M. Narain, for the D0 Coll., Fermilab-Conf-96-192-E, presented at the 10th Rencontres de Physique de la Vallée d'Aoste, La Thuile 1996.

[Nason88] P. Nason, S. Dawson and R. K. Ellis, *Nucl. Phys.* **B303**(1988)607.

[Nason89] P. Nason, S. Dawson and R. K. Ellis, *Nucl. Phys.* **B327**(1989)49, erratum *ibid.* **B335**(1990)260.

[Nason92] P. Nason, “Heavy quark production”, in *Heavy Flavours*, eds A.J. Buras and M. Lindner, Advanced Series on Directions in High Energy Physics, (World Scientific, Singapore, 1992).

[Nason96] P. Nason and C. Oleari, *Phys. Lett.* **B387**(1996)623, [hep-ph/9607347](#).

[Nason96a] P. Nason and B.R. Webber, preprint CERN-TH/96-290, [hep-ph/9612353](#).

[Olsen79] H.A. Olsen, *Phys. Rev.* **D19**(1979)100.

[Orr95] L.H. Orr, T. Stelzer and W.J. Stirling, *Phys. Rev.* **D52**(1995)124, [hep-ph/9412294](#).

[Orr95a] L.H. Orr, T. Stelzer and W.J. Stirling, *Phys. Lett.* **B354**(1995)442, [hep-ph/9505282](#).

[Paige86] F. Paige and S.D. Protopopescu, Brookhaven report BNL-38034 (1986).

[Peterson83] C. Peterson, D. Schlatter, I. Schmitt and P. Zerwas, *Phys. Rev.* **D27**(1983)105.

[Przysiezniak96] H. Przysiezniak, talk given at the XXXI Rencontres de Moriond on QCD and High Energy Hadronic Interactions, Les Arcs, 1996.

[Randall95] L. Randall and N. Rius, *Nucl. Phys.* **B441**(1995)167, [hep-ph/9405217](#).

[Riemersma92] S. Riemersma, J. Smith and W.L. van Neerven, *Phys. Lett.* **282B**(1992)171.

[Scalise96] R.J. Scalise, F.I. Olness and W.-K. Tung, SMU-HEP-96-08.

[Schmelling96] M. Schmelling, [hep-ex/9701002](#), Plenary talk given at the Int. Conf. on High Energy Physics, Warsaw, 1996.

[Schuler93] G.A. Schuler and T. Sjöstrand, *Phys. Lett.* **B300**(1993)169.

[Schuler93a] G.A. Schuler and T. Sjöstrand, *Nucl. Phys.* **B407**(1993)539.

[Seligman97] W.G. Seligman et al., CCFR Coll., NEVIS-REPORT-292, Jan 1997, Submitted to *Phys. Rev. Lett.*, [hep-ex/9701017](#).

[Seymour95] M.H. Seymour, *Nucl. Phys.* **B436**(1995)163.

[Sinervo96] P. Sinervo, FERMILAB-CONF-96/223-E, Lectures presented at 23rd Annual SLAC Summer Institute on Particle Physics, SLAC, Stanford, 1995.

[Sjostrand87] T. Sjöstrand and M. Bengtsson, *Comput. Phys. Commun.* **43**(1987)367.

[Smith92] J. Smith and W.L. van Neerven, *Nucl. Phys.* **B374**(1992)36.

[Sommerfeld39] A. Sommerfeld, *Atombau und Spektrallinien*, (Vieweg, Braunschweig, 1939), Bd. 2.

[Spiegel96] L. Spiegel for the E771 Coll., Proceedings of the Workshop on Heavy Quarks at Fixed Target, St. Goar, Germany, 1996.

[Stange93] A. Stange and S. Willenbrock, *Phys. Rev.* **D48**(1993)2054, [hep-ph/9302291](#).

[Stange94] A. Stange, W. Marciano and S. Willenbrock, *Phys. Rev.* **D49**(1994)1354, [hep-ph/9309294](#).

[Stange94a] A. Stange, W. Marciano and S. Willenbrock, *Phys. Rev.* **D50**(1994)4491, [hep-ph/9404247](#).

[Stelzer95] T. Stelzer and S. Willenbrock, *Phys. Lett.* **B357**(1995)125, [hep-ph/9505433](#).

[Sterman87] G. Sterman, *Nucl. Phys.* **B281**(1987)310.

[Stratmann95] M. Stratmann and W. Vogelsang, *Phys. Rev.* **D52**(1995)1535.

[Stratmann96] M. Stratmann and W. Vogelsang, DO-TH-96/10, RAL-TR-96-033, [hep-ph/9605330](#).

[Sullivan96] Z. Sullivan, [hep-ph/9611302](#).

[Sutton92] P.J. Sutton, A.D. Martin, R.G. Roberts and W.J. Stirling, *Phys. Rev.* **D45**(1992)2349.

[Tavernier87] S.P.K. Tavernier, *Rep. Progr. Phys.* **50**(1987)1439.

[Uematsu82] T. Uematsu and I.F. Walsh, *Nucl. Phys.* **B199**(1982)93.

[Vogelsang91] W. Vogelsang, in Proc. Workshop on Physics at HERA, eds. W. Buchmüller and G. Ingelman, DESY, Hamburg, 1991, Vol. 1.

[Weizsaecker34] C.F. Weizsäcker, *Z. Phys.* **88**(1934)612.

[Willenbrock86] S. Willenbrock and D.A. Dicus, *Phys. Rev.* **D34**(1986)155.

[Williams34] E.J. Williams, *Phys. Rev.* **45**(1934)729.

[Witten77] E. Witten, *Nucl. Phys.* **B120**(1977)189.

[Yuan90] C.P. Yuan, *Phys. Rev.* **D41**(1990)42.

[Zeus96] ZEUS Coll., submitted to the Int. Conf. on High Energy Physics, Warsaw, 1996, Pa02-031.

[Zeus96a] ZEUS Coll., submitted to the Int. Conf. on High Energy Physics, Warsaw, 1996, Pa05-051.